

**Collection, Processing, and Characterization of *Galleria mellonella* Silk**

by

Mary Joanne Glasper

A thesis submitted in partial fulfillment of the requirements for the degree of

Master of Science

in

Textiles and Clothing

Department of Human Ecology

University of Alberta

© Mary Glasper, 2019

## Abstract

This study investigates a potential new source of silk fibre, *Galleria mellonella* Linnaeus (Lepidoptera: Pyralidae), commonly known as the greater wax moth. The larvae of this moth are a major pest of stored or unattended beehive brood combs. The larvae produce large quantities of strong, elastic silk in the construction of tunnels to protect themselves from bees in this environment. The unique mechanical properties of *Galleria* silk, combined with the large quantities produced by the larvae, make it a natural fibre worth investigating for textile end-uses. This research focuses specifically on the collection, processing, and characterization of *Galleria* silk and serves as an important foundation for the future utilization of this fibre. A method to collect clean cocoons free from frass and debris was developed, and those cocoons were used to assess how effective conventional degumming methods were in removing the sericin coating from *Galleria* silk. A novel method was developed for collecting naturally spun silk threads directly from the insect, so that the samples were handled as minimally as possible and the results would more closely represent the properties of *Galleria* silk as extruded by the insect. The results from the tensile tests were compared and contrasted to other studies where mechanical properties of *Galleria* silk was tested; the results were similarly compared to known values of other lepidopteran and spider silks, and to other man-made materials such as high tenacity textile fibres and steel. This study found that *Galleria* can be reared in such a way as to collect cocoons free from contamination for degumming and use. The most effective degumming method used in this study, as determined by a combination of quantitative and qualitative evaluation, was boiling the silk in a combined solution of  $\text{Na}_2\text{CO}_3$  and sodium lauryl sulfate. Tensile specimens were collected as the insect deposited a single fibre while walking. This approach limited the amount of handling that could alter the silk's mechanical properties prior to testing. *Galleria* silk has unique mechanical properties for lepidopteran silk and is more comparable to the properties of commonly studied spider silks. This silk could be a viable alternative to synthetic or transgenically produced spider silks currently being researched and utilized.

## Preface

This thesis is an original work by Mary Glasper. No part of this thesis has been previously published.

The acrylic holder used in the collection of the tensile test specimens was designed and constructed by Dr. Andrew Keddie and the staff of the Biological Sciences machine shop at the University of Alberta.

The geometric model used to estimate the cross-sectional area of the silk fibres was co-developed with Dr. John Nychka.

Some of the preliminary research conducted for this thesis was done in collaboration with two undergraduate students at the University of Alberta.

- The initial tensile strength silk collection protocol using the acrylic holder was developed by Rachel Maki as part of her BIOL 298 (Understanding Biological Research) term project, co-supervised with Dr. Andrew Keddie.
- Preliminary silk degumming work, including determination of degumming volume and chemical concentrations, was done in collaboration with Leah Goettler, a Chemical Engineering student, as part of her Dean's Research Award from the Faculty of Engineering.

## **Dedication**

This thesis is dedicated to the wonderful role models and mentors I've had over the years, both personal and professional. Thank you for supporting me, pushing me to be my best, and inspiring me to stay curious and follow my own path, however odd or unconventional it may seem.

## Acknowledgements

I would like to sincerely thank the following people and organizations, without whom much of this work would not have been possible:

- Dr. Jane Batcheller, for being my primary supervisor, and for giving me the freedom to pursue the projects I was most passionate about. Thank you for your steadfast encouragement, support, and mentorship, and for providing opportunities for me to grow as a textile researcher and educator;
- Dr. John Nychka, for agreeing to work with a biologist-turned-textile-scientist who had no background in engineering. I cannot imagine what this experience would have been like without being a part of your research group, or without your mentorship, curiosity, seemingly endless knowledge of all things materials-related, and sense of humour;
- Dr. Andrew Keddie, for providing the inspiration for this research, having great discussions which helped direct my thinking, and for allowing me access to use your lab and *Galleria* colony as needed;
- The AATCC Foundation for awarding me a Student Research Support Grant, which enabled the purchase of research materials and SEM time;
- The Government of Alberta, the Faculty of Graduate Studies and Research, the Graduate Students' Association, and the Department of Human Ecology, for awarding scholarships to support my graduate education and experience;
- Leah Goettler and Rachel Maki for their assistance with developing the degumming and silk collection methods, and Robin Chen for maintaining the *Galleria* colony used for this research;

- The staff at The Royal Alberta Museum, specifically Dr. Tyler Cobb, Michelle Mark, Dr. Matthias Buck, and Darcie Thauvette for allowing me to use their imaging system, and their time teaching me to use it;
- Nathan Gerein of the Earth and Atmospheric Sciences SEM Lab, and Arlene Oatway of the Biological Sciences Advanced Microscopy Facility, for their assistance with obtaining SEM images of my samples;
- Stephen Paskaluk of the Protective Clothing and Equipment Research facility, for helping me with setup and troubleshooting of the tensile testing equipment;
- The MATI group, specifically Jonathan Backs, Nicole Furtak, Kalan Kucera, Kevin Hodder, Scott Pavelich, and Terry Runyon. Our weekly meetings were a huge highlight of my degree, and I learned so much from all of you;
- My fellow Human Ecology graduate students, specifically Robyn Stobbs, Mohammed Abdul-Bari, Mariko Wakefield, and Nicole Furtak. We're a small group with a lot of heart! Robyn, thank you for everything.
- The Sunday night games group and Carley Okamura for helping me keep my sanity;
- My mother, Jean, for making sure I was fed properly, and for helping me develop ideas and experimental plans, and my sister, Catherine, for cheering me on and keeping my spirits up;
- Last but not least, my loving partner, Ronan, who kept me grounded through all of the long days I worked towards the end of this degree, and made sure I was fed, slept properly, and always had a warm cup of tea to keep me going.

## Table of Contents

1	Introduction .....	1
1.1	Statement of Problem.....	1
1.2	Research questions.....	2
1.3	Justification.....	3
1.4	Scope.....	4
1.5	Contributions.....	4
2	Literature Review .....	5
2.1	The silk fibre.....	5
2.1.1	History & use .....	7
2.1.2	Types of silk.....	8
2.2	Silk structure .....	13
2.2.1	Primary & secondary protein structure.....	13
2.2.2	Spider silk structure .....	19
2.2.3	Lepidopteran silk structure .....	19
2.3	Commercial production .....	24
2.3.1	Rearing and collection .....	24
2.3.2	Commercial processing.....	25
2.4	Research collection processes.....	27

2.4.1	Sampling from cocoons .....	28
2.4.2	Forced silking.....	28
2.5	Processing.....	30
2.5.1	Degumming.....	30
2.5.2	Evaluation of degumming effectiveness.....	32
2.6	Fibre characterization.....	33
2.6.1	Qualitative.....	33
2.6.2	Quantitative.....	34
2.7	Conclusion .....	42
3	Methods.....	43
3.1	Silk collection .....	43
3.1.1	Rearing Conditions .....	43
3.1.2	Cocoon collection .....	44
3.1.3	Tensile Specimens .....	48
3.2	Degumming.....	51
3.2.1	Degumming processes .....	52
3.2.2	Evaluation of effectiveness .....	54
3.3	Fibre Characterization.....	56
3.3.1	Appearance and morphology .....	56
3.3.2	Cross-section and diameter .....	57

3.3.3	Tensile properties.....	61
3.4	Data Analysis.....	64
3.4.1	Degumming.....	64
3.4.2	Tensile tests.....	64
4	Results & Discussion.....	65
4.1	Silk Collection.....	65
4.1.1	Cocoon collection.....	65
4.1.2	Tensile specimen collection.....	70
4.2	Imaging.....	71
4.2.1	Photography.....	71
4.2.2	Optical microscopy.....	74
4.2.3	Scanning electron microscopy.....	75
4.3	Degumming.....	80
4.3.1	Quantitative evaluation.....	80
4.3.2	Qualitative evaluation.....	82
4.3.3	Comparative evaluations.....	88
4.4	Tensile tests.....	92
4.4.1	Diameter and cross-sectional area.....	92
4.4.2	Tensile properties.....	93
5	Conclusions and Future Work.....	110

5.1 Summary.....	110
5.2 Conclusions.....	110
5.3 Future work.....	112
References.....	114
Appendix A: Diet Recipe.....	131
Appendix B: Degumming Experiments & Statistical Analysis.....	132
Appendix C: Diameter & Cross-Sectional Area.....	136
Appendix D: Tensile Data & Statistical Analysis.....	140

## List of Tables

		Page
Table 2.1	Summary chart of the amino acid content, H-fibroin size and structure, and other metrics used to describe the structure of <i>Bombyx</i> , <i>Antheraea</i> , and <i>Galleria</i> silks.	20
Table 2.2	Tensile Strength Calculations, adapted from ASTM D4848 (1998), and Collier & Epps, (1999)	36
Table 2.3	Mechanical properties of select silks, adapted from Denny (1980).	39
Table 3.1	A visual matrix of the small vs. large jars, and fine vs. coarse mesh.	48
Table 3.2	Dependent, independent, and controlled variables of the degumming experiments.	52
Table 3.3	Experimental conditions of each degumming treatment.	53
Table 4.1	Replication and average weight change results for each degumming treatment.	81
Table 4.2	Photographs of each replication of each treatment after staining.	90
Table 4.3	Comparison of all degumming methods. Top row: before staining; second row: after staining; third row: optical microscope; fourth row: secondary electron SEM.	91
Table 4.4	Average diameter measurements and cross-sectional area calculations for each insect.	92
Table 4.5	Average tensile properties of <i>Galleria</i> silk.	98
Table 4.6	Average tensile properties of <i>Galleria</i> silk compared to results from other studies.	102
Table 4.7	Average tensile properties of <i>Galleria</i> silk from the present study compared to silks collected from other lepidopterans and spiders (separated by a line).	105
Table 4.8	Average tensile properties of <i>Galleria</i> silk from the present study compared to silks collected from other lepidopterans and spiders (separated by a line), with proline content.	108
Table 4.9	Average tensile properties of <i>Galleria</i> silk from the present study compared to the mechanical properties of other man-made materials.	109

## List of Figures

		Page
Figure 2.1	Right silk gland of the last instar larva of <i>Galleria mellonella</i> . The labels describe the following regions of the silk gland: PSG = posterior silk gland, where silk fibroin is secreted; MSG = middle silk gland, where sericins are produced; ASG = anterior silk gland, where the liquid silk dope polymerizes into a solid filament coated with sericin. Magnification not specified.	6
Figure 2.2	<i>G. mellonella</i> egg (a), larva (b), pupae with/without cocoon (c), and adults (d).	11
Figure 2.3	Crystalline and amorphous regions of silk fibroin.	14
Figure 2.4	Amino acid structures. (a) is the basic amino acid structure, (b) is glycine, the simplest amino acid, (c) is alanine, and (d) is serine.	14
Figure 2.5	Sample primary structure of fibroin, composed of glycine, alanine, and serine.	15
Figure 2.6	basic $\beta$ -sheet protein structure (left), and a basic $\alpha$ -helix protein structure (right).	17
Figure 2.7	Antiparallel and parallel $\beta$ -pleated sheets.	17
Figure 2.8	Twenty-one day old <i>Bombyx mori</i> larvae feeding on mulberry leaves in a commercial sericulture operation.	25
Figure 2.9	Engineering stress-strain curve showing Young's modulus of elasticity (E), stress and strain at elastic limit ( $\sigma_e$ , $\epsilon_e$ ), ultimate tensile strength (UTS), strain at break ( $\epsilon_f$ ), and toughness (grey area under curve).	37
Figure 2.10	Generalized stress-strain curves for select $\beta$ -sheet silks tested in water at ambient temperature. A = <i>Anaphe moloneyi</i> (Notodontidae), B = <i>Bombyx mori</i> , C = <i>Antheraea mylitta</i> (Saturniidae), and D = <i>Galleria mellonella</i> .	41
Figure 3.1	The main <i>Galleria</i> colony housed in mason jars.	44
Figure 3.2	A late (6-7th) instar <i>Galleria</i> larva, typical of what was used for the experiments in this study.	45
Figure 3.3	The empty cocoon (left) after the pupa (centre) and final larval exuvium (right) have been removed.	45
Figure 3.4	Cocoons formed against the glass of the mason jar (left), and the crushed insect (right) as a result of attempting to remove the cocoon from the glass with forceps.	46
Figure 3.5	The white nylon mesh (left) and the black window screen mesh (right).	47
Figure 3.6	The acrylic holder with removable component and their dimensions.	49

Figure 3.7	The acrylic holder with a tensile paper tab inside. The black tab shown was an early prototype; white dashed lines show an approximation of the final dimensions of the paper tab.	49
Figure 3.8	The acrylic holder with mounted paper tab and <i>Galleria</i> larva walking along the channel.	51
Figure 3.9	The silk samples mounted on SEM stubs prior to sputter coating. Outside of the cocoon (left), inside of the cocoon (centre), and feeding tunnel silk (right).	57
Figure 3.10	The piece of cocoon mounted on-end using copper conductive tape.	58
Figure 3.11	An image of baves in cross-section, as outlined in yellow on the left image. The freeform selection tool was used to measure the cross-sectional area (left), and the line tool was used to measure the diameter (right).	59
Figure 3.12	A plot of diameter vs. cross-sectional area measurements, with the geometric model shown in red (right).	59
Figure 3.13	The prepared silk sample mounted on the stub prior to applying the sputter coat. The silk's location is to the left of the red bracket (the single white strand extending vertically).	60
Figure 3.14	An example of a bave diameter measurement (vertical yellow line) being taken with ImageJ software. The medial line is observable as the horizontal white- and dark-shaded region in the centre of the strand.	61
Figure 3.15	A schematic of the paper tab used for the tensile tests.	62
Figure 3.16	The tensile test set-up showing the paper tab held in the clamps of the tensile tester with the sides cut, ready to be tested.	63
Figure 4.1	Cocoons formed by the insects within the diet (left, indicated with black arrows); cocoons covered with frass and diet (right).	65
Figure 4.2	A cocoon formed on fine mesh with frass and debris (left); cocoons, a pupa (indicated with an arrow), and feeding tunnel silk formed on coarse mesh with noticeably less frass and debris (right).	66
Figure 4.3	The mesh flush with the sides of the small jar (left), and the mesh not flush with the sides of the large jar (right) due to the narrowing at the mouth of the jar.	67
Figure 4.4	The insects moving between the mesh and side of jar after being added (left); cocoons formed up against the glass as a result (right).	68
Figure 4.5	The mesh sewn together with polyester thread (left); the thread chewed through, with a cocoon formed against the glass in the background (right).	69
Figure 4.6	The mesh sewn together with craft wire(left); the insects contained within the mesh shortly after being transferred to the pupation jar (right).	69

Figure 4.7	A bave with what appears to be a flattened sheet of sericin beneath it (see arrow).	71
Figure 4.8	A photograph of a <i>Galleria</i> cocoon, with the dimpled appearance, loose silk fibres on the outside, and the eclosion opening on the end (indicated with an arrow).	73
Figure 4.9	A photograph of <i>Galleria</i> feeding tunnel silk, as collected from the main colony.	73
Figure 4.10	Images of cocoon silk (left) with the red arrow indicating a bave, and feeding tunnel silk (right) when viewed with an optical microscope at high magnification.	74
Figure 4.11	Images of the inside surface of a cocoon viewed under SEM at three different levels of magnification.	76
Figure 4.12	Image of the outside of a cocoon viewed under SEM, with a small portion of the underlying cocoon visible (indicated by an arrow).	76
Figure 4.13	Images of the feeding tunnel silk viewed under SEM at three different levels of magnification; the bottom image shows several silk strands adhered together (see arrow).	78
Figure 4.14	Images of the cocoon in cross-section viewed under SEM at two different levels of magnification (all images: inside = top, outside = bottom). The outlines of the individual brins can be seen (indicated by brackets and arrows) embedded in the sericin adhesive.	79
Figure 4.15	Images of a <i>B. mori</i> cocoon shown from the outside (top), and in cross-section (bottom). Note the fibres seen individually in cross-section, as opposed to being embedded in a sericin layer as seen in Figure 4.41.	80
Figure 4.16	The average weight loss of each condition. Error bars represent standard deviation; n=3 for all conditions.	81
Figure 4.17	A sample taken from the control group before staining (top left), after staining (top right), a stained sample under the optical microscope (bottom left), and under secondary electron SEM (bottom right).	83
Figure 4.18	A sample taken from the water only group before staining (top left), after staining (top right), a stained sample viewed under the optical microscope (bottom left), and under secondary electron SEM (bottom right).	84
Figure 4.19	A sample taken from the Na <sub>2</sub> CO <sub>3</sub> only group before staining (top left), after staining (top right), a stained sample viewed under the optical microscope (middle left), and under secondary electron SEM (thick sheet of sericin: middle right, and separating brins: bottom).	85

Figure 4.20	A sample taken from the SLS only group before staining (top left), after staining (top right), a stained sample viewed under the optical microscope (bottom left), and under secondary electron SEM (bottom right).	86
Figure 4.21	A sample taken from the Na <sub>2</sub> CO <sub>3</sub> + SLS group before staining (top left), after staining (top right), a stained sample viewed under the optical microscope (bottom left), and under secondary electron SEM (bottom right).	87
Figure 4.22	The average diameter measurement for each insect. Error bars represent standard deviation; G1 n=3, G2 n=5, G3 n=4, G4 n=6, G5 n=7, G6 n=3.	93
Figure 4.23	UTS for each insect: Force-extension curves in mN and mm (left); stress-strain in MPa and mm/mm (right). G1 n=3, G2 n=5, G3 n=4, G4 n=6, G5 n=7, G6 n=3.	94
Figure 4.24	Tensile strength curves for each insect: Engineering stress-strain in MPa and mm/mm. All curves have been scaled to fit their area and are to be compared for shape only. G1 n=3, G2 n=5, G3 n=4, G4 n=6, G5 n=7, G6 n=3.	95
Figure 4.25	Representative engineering stress-strain curves from three different insects, with a closer view of the linear region of elastic deformation inset upper left; these are the portions of the curves from which Young's Elastic Modulus was calculated.	96
Figure 4.26	The average Young's modulus of elasticity for each insect. Error bars represent standard deviation; G1 n=3, G2 n=5, G3 n=4, G4 n=6, G5 n=7, G6 n=3.	97
Figure 4.27	The average ultimate tensile strength (UTS) for each insect in MPa. Error bars represent standard deviation; G1 n=3, G2 n=5, G3 n=4, G4 n=6, G5 n=7, G6 n=3.	99
Figure 4.28	The toughness for each insect in MJ/m <sup>3</sup> . Error bars represent standard deviation; G1 n=3, G2 n=5, G3 n=4, G4 n=6, G5 n=7, G6 n=3.	100
Figure 4.29	The generalized stress-strain curve of <i>Galleria</i> silk (Hepburn et al., 1979, fig. 1) superimposed upon the tensile curves from Figure 4.25.	103
Figure 4.30	The <i>A. pernyi</i> stress-strain curves presented by Fu et al. (2011) in black, superimposed upon the tensile curves from Figure 4.25.	106

# 1 Introduction

Silk, a natural protein fibre produced by many different organisms, is both an ancient and modern material. What was once used as the fibre of choice for emperors and royalty, then later as a technical fibre for parachutes and rifle sights, is being explored more heavily as a promising biomedical textile and is being reproduced synthetically for fashion and technical applications.

*Galleria mellonella*, the Greater Wax Moth, is a prolific producer of silk. While it is a well-known model organism used in insect and mammalian pathology research, it has not yet been investigated as a source of textile fibre. The body of research surrounding *Galleria* silk is limited; some foundational work on its protein structure and mechanical properties has been done (Fedič, Žurovec, & Sehnal, 2003; Warwicker, 1960; Žurovec & Sehnal, 2002), but the majority of lepidopteran silk research has been conducted using the silk of *Bombyx mori*, the domesticated silkworm, from which the majority of the world's silk products are made. Other prominent silk producing organisms include several moths of the family Saturniidae, which produce tussah (tasar) and eri silk, and several spiders of the family Araneidae, the orb-weavers. Due to the limited availability of research material on *Galleria* silk, this thesis relies upon the body of work surrounding *B. mori* silk, and to a lesser extent, that of *Antheraea pernyi*. Certain assumptions have been made surrounding basic similarities between silks produced by moths, and that the research done on *B. mori* and *A. pernyi* silks may be applicable to *Galleria* silk.

## 1.1 Statement of Problem

Silk is widely recognized as a luxury fibre used in fine, high-fashion clothing, but it is also used extensively in the medical field for tissue engineering applications due to its biocompatibility with the human body. This preliminary study investigates a potential new source of silk fibre,

*Galleria mellonella* (Lepidoptera: Pyralidae), commonly known as the greater wax moth. The larvae of this moth are a major pest of stored or unattended beehive brood combs. The larvae produce large quantities of strong, elastic silk in the construction of tunnels to protect themselves from bees in this environment. The unique mechanical properties of *Galleria* silk, combined with the large quantities produced by the larvae, make it a natural fibre worth investigating for textile end-uses. This research focuses specifically on the collection, processing, and characterization of *Galleria* silk and serves as an important foundation for the future utilization of this fibre.

The purpose of this research is to investigate the potential use of *Galleria mellonella* silk as a textile fibre by:

- a) identifying a useful method to rear the insects,
- b) developing a method to collect the silk in its naturally produced state,
- c) comparing degumming methods for the silk to be used in textiles,
- d) evaluating cocoon morphology and structure,
- e) measuring the tensile properties of collected silk fibres, and
- f) comparing and contrasting mechanical characteristics of this silk to results published in other *Galleria* and invertebrate studies and selected man-made materials.

## **1.2 Research questions**

Can *Galleria* silk be collected, processed, and characterized to provide a foundation for its future use as a textile fibre? To do this the following must be addressed:

1. Can the insects be reared so that the silk collected is free from dirt and debris?
2. Can the sericin coating on the silk be removed from the cocoon silk using conventional degumming methods?

3. How do select fibre properties of *Galleria* silk compare to other silk fibres used in textile research and industry?

### 1.3 Justification

A large amount of current silk research is dedicated to the synthetic or transgenic production of spider dragline silk. Spider silk has impressive mechanical properties but cannot be collected conventionally as spiders do not construct silk structures like cocoons, where large quantities of fibre can easily be collected. Additionally, due to their predatory and sometimes cannibalistic nature, spiders are difficult to rear in the densities required for large-scale production. In contrast, *Galleria* larvae are very easily reared in captivity, can survive on a variety of diets (Jindra & Sehnal, 1989), producing large quantities of silk which is both strong and elastic (Sehnal & Akai, 1990). As a popular lab organism, its silk was included in foundational studies about silk protein structure (Marsh, Corey, & Pauling, 1955a; Warwicker, 1960), but its mechanical properties were not investigated until the late 1970s (Hepburn, Chandler, & Davidoff, 1979). A group of researchers took great interest in the protein structure of *Galleria* silk in the 1990s and early 2000s, sequencing its protein structure and doing some mechanical tests of their own (Fedič et al., 2003; Žurovec, Kodrík, Yang, Sehnal, & Scheller, 1998; Žurovec, Vašková, Kodrík, Sehnal, & Kumaran, 1995; Žurovec & Sehnal, 2002). The above studies on the mechanical properties of *Galleria* silk showed a lepidopteran silk with great toughness (Hepburn et al., 1979), and claims were made that the silk was closer in protein structure to spider silks than to that produced by other silkworms (Žurovec & Sehnal, 2002).

What has not yet been done, however, is to look at the mechanical properties of the silk in greater detail (the studies above reported generalized results of only a few properties), how this

silk may be collected and processed as a textile fibre, and how its properties compare to other lepidopteran and spider silks, and textile fibres.

#### **1.4 Scope**

This study is limited to studying the silk from one colony of insects housed in the Insectary at the University of Alberta's Department of Biological Sciences; comparisons will not be drawn among *Galleria* colonies. The degumming experiments were carried out on cocoon silk only, not on feeding tunnel silk, and while suitable degumming methods were found, they were not optimized. The tensile tests were carried out on silk fibres as they were laid down by the insect; experiments were not done with samples taken from feeding tunnel or cocoon silk, nor were they done with silk samples force-reeled from the insect.

#### **1.5 Contributions**

From the results of this study, others wanting to study *Galleria* silk will be able to utilize the collection methods developed for both cocoons and tensile specimens, the degumming procedures identified as most effective, and the data produced by the tensile testing as a foundation for any future work performed on this silk fibre, allowing researchers to make decisions about how and where this fibre may be used.

## 2 Literature Review

*Galleria mellonella*, the Greater Wax Moth, is a well-known organism to those who work in insect and mammalian pathology research, but not to those in textiles. While a small body of research exists on the silk produced by this species, it has not yet been investigated as a source of textile fibre. Due to the limited availability of research material on *Galleria* silk, this thesis relies upon the body of work surrounding both cultivated and wild silk produced by other silkworm species. Certain assumptions have been made surrounding basic similarities between silks produced by moths, and that the research done on these silks, particularly on processing and characterization, may be applicable to *Galleria* silk.

In the following review, the structure and composition of silk is discussed, and relevant studies done with *Galleria* silk are included. An overview of how different types of silk are collected and processed, both industrially and in research settings, and the methods used to characterize fibres are presented.

### 2.1 The silk fibre

Silk, the only natural fibre which is spun, can be defined as “an externally spun fibrous protein secretion formed into fibers, usually resulting in material structures such as cocoons or webs” (Matsumoto et al., 2007, p. 383). It is a protein-based polymer (polypeptide) produced by many types of arthropods, but has become most specialized in spiders and many lepidopteran larvae (caterpillars) (Žurovec & Sehnal, 2002). Silk spinning occurs in the larval and adult forms of many insect orders such as Trichoptera (caddisflies), Siphonaptera (fleas), Diptera (flies), Hymenoptera (ants, bees and wasps), and Lepidoptera (butterflies and moths) (Sehnal & Sutherland, 2008). Lepidopteran silk is a dual-protein consisting of a fibroin core surrounded by

sericin, an adhesive gum; two separate fibres, called brins, are secreted from each labial gland, and are adhered together into a single thread, or bave, as it exits through a spinneret on the insect's "lower lip" or labium (Asakura et al., 2007; Ganga, 2003; Needles, 1981). Silkworms spin their silk by moving their head in a figure-eight motion, pulling the viscous silk from the spinneret and stretching it to achieve the correct molecular orientation (Magoshi, Magoshi, & Nakamura, 1993).



*Figure 2.1* Right silk gland of the last instar larva of *Galleria mellonella*. The labels describe the following regions of the silk gland: PSG = posterior silk gland, where silk fibroin is secreted; MSG = middle silk gland, where sericins are produced; ASG = anterior silk gland, where the liquid silk dope polymerizes into a solid filament coated with sericin. Reprinted with permission from Springer Nature (Sehnal, 2011, fig. 11.1). Magnification not specified.

The labial glands, originally for the production of saliva, consist of a fibroin-producing posterior region and sericin-producing middle region (see Figure 2.1) (Sehnal, 2011; Žurovec & Sehnal, 2002). The silk core normally consists of three different proteins: heavy-chain fibroin (H-

fibroin), light chain fibroin (L-fibroin), and P25 glycoprotein. H-fibroin comprises the bulk of the silk fibre, and determines the structure and physical properties of the silk (Žurovec & Sehnal, 2002). Fibroins provide the structural basis of cocoon silks for a variety of pupating insects (Lucas, Shaw, & Smith, 1960), and for silks with other functions such as shelter, structural support, reproduction, and thermal insulation (Craig, 2003; Denny, 1980).

### **2.1.1 History & use**

Silk, produced by domestic silkworms, has been used in the creation of textiles for almost 5,000 years (Matsumoto et al., 2007). Sericulture was first developed in ancient China around 2650 BC, where the wild silkworm *Bombyx mandarina* was domesticated and renamed *Bombyx mori*, the silkworm used today for commercial silk production (Sehnal, 2011). Sericulture spread both east and west from China, reaching its height of economic importance during the 19<sup>th</sup> and early 20<sup>th</sup> centuries (Sehnal, 2011). Silk was highly valued during this “silk road” period, and was by weight, considered to be as valuable as gold (Matsumoto et al., 2007). It was used extensively for parachute material during World War II (Ganga, 2003); with the discovery of nylon at that time, global silk production declined but has begun to rise again in recent years (Sehnal, 2011). Silk has been traditionally used for fine, high-fashion clothing and accessories such as blouses, formal dresses, lingerie, suits, ties, and kimonos; indoors, silk is used for upholstery, wall coverings, rugs, and beddings (Babu, 2012; Rheinberg, 1991). *Bombyx* silk has a long history in medicine, having been used as a suture material for centuries before synthetic materials became available (Babu, 2012; Matsumoto et al., 2007; Sehnal, 2011). More recently, silk has been used both *in vitro* and *in vivo* as a biomaterial for tissue engineering applications, tissue scaffolding, and is used in ocular, neural, and cardiovascular surgeries due to its biocompatibility and slow degradation in the human body (Babu, 2012; Sehnal, 2011).

A lot of waste silk is created during the manufacturing process (e.g., from breakages, deflossing, unreelable cocoons). One use for this waste is to produce silk fibre-reinforced composites from epoxy and other biodegradable polymeric resins; another use for silk reeling and weaving waste is to produce non-woven materials by air-laying and bonding, or needle punching, which could be used for technical and medical textiles (Babu, 2012).

### **2.1.2 Types of silk**

Collectively, insects produce many different kinds of silk and silk proteins, but each individual can only produce one kind; spiders on the other hand, may individually produce up to nine different types of silks, each of which may be composed of more than one kind of protein (Craig, 2003).

#### **2.1.2.1 Spider silk**

The use of spider silk has been extensively researched, but has not yet become widely commercially viable due to the challenges of mass-rearing, collection, and synthetic reproduction (Vollrath, Porter, & Holland, 2011). The dragline silk from the golden silk orb weaver, *Nephila clavipes*, is one of the most well-characterized spider silks (Matsumoto et al., 2007). Unlike silkworms, spiders have not been domesticated for silk production due to their predatory and sometimes cannibalistic nature; they do not produce cocoons like silkworms do, instead spinning webs comprised of small quantities of several different types of silk, each of which are not reelable as single, continuous fibres. Spider fibroin proteins, also called spidroins (Eisoldt, Smith, & Scheibel, 2011), are produced in the opisthosomal (abdominal) glands, which produce silks such as cylindrical (egg sacs), aciniform (prey wrapping), major and minor ampullate (dragline), flagelliform (prey capture), and others; each of these silks differ in their protein structure (Craig, 2003). Some spider silks are incredibly fine, with diameters as small as 10  $\mu\text{m}$

(Matsumoto et al., 2007), and unlike lepidopteran silks, do not have a sericin coating (Craig, 2003). An additional feature of some spider silks is that they can supercontract up to 50% of their original length when exposed to water or high humidity (Work, 1981), which is seen to a much lesser extent in some lepidopteran silks (Fu, Porter, Chen, Vollrath, & Shao, 2011).

The desirable mechanical properties of spider silk, combined with the difficulties in rearing them at a commercial scale, have led researchers to develop synthetic alternatives. Everything from transgenic goats (Jones et al., 2015), silkworms (Wen et al., 2009; Xu et al., 2018), yeast (Bolt Threads, n.d.), and bacteria (Fahnestock & Irwin, 1997) have been modified to excrete spider silk proteins. Other researchers have gone the route of synthetic, biomimetic production (Andersson et al., 2017; Holland, Vollrath, Ryan, & Mykhaylyk, 2012); while these are all important advancements in silk research, they are not the focus of this study and will not be discussed in greater detail.

#### **2.1.2.2 Lepidopteran silk**

The majority of silk produced in the world comes from the mulberry silkworm *Bombyx mori* (Bombycidae), which feeds exclusively on the leaves of the mulberry plant (Babu, 2013), and may eat up to 30 g of mulberry leaves to produce just 2 g of silk (Rheinberg, 1991). These silkworms are completely domesticated and reared indoors. *B. mori* silk contains two fibroin filaments, 5-10  $\mu\text{m}$  in diameter each, which together form a bave 10-25  $\mu\text{m}$  in diameter (Matsumoto et al., 2007). Degummed mulberry silk is triangular in cross-section, and has a smooth surface (Nayak, Padhye, & Fergusson, 2012).

Eri silk, also known as endi or errandi, is produced by the domesticated silkworm *Philosamia ricini* (Saturniidae), which feeds mainly on castor leaves in Assam and elsewhere in northern India (Babu, 2013; Rheinberg, 1991). Eri silk may be white or brick red. Unlike other silk

varieties, the larva constructs a hole in the cocoon from which the adult emerges after pupation. This means the cocoons are unreelable and only staple-length fibres may be collected from the open-ended cocoons.

Muga silk is golden yellow in colour, and comes from the semi-domesticated silkworm *Antheraea assamensis* (Saturniidae) (Babu, 2013; Ganga, 2003). It is specific to the Assam region of India where they feed on the leaves of som and sualu plants (Rheinberg, 1991).

Tasar (Indian), or tussah (Chinese) silk, is a coarse, copper-coloured silk from the silkworm *Antheraea mylitta* (Saturniidae), which feed on asan, arjun, or Chinese oak trees in tropical India (Babu, 2013; Rheinberg, 1991). The silk has less lustre than mulberry silk and is used primarily for interior and upholstery fabrics. Oak tussah silk is a finer variety produced by *Antheraea proylei* (Saturniidae), which feed on oak trees found in the sub-Himalayan belt, or more temperate area of India. China is the main producer of oak tussah in the world, which comes from *Antheraea pernyi* (Saturniidae) (Babu, 2013). Tussah silks are fatter, coarser, and more ribbon-like, with fine striations along the fibre length, and are crescent- or wedge-shaped in cross-section (Nayak et al., 2012). They also contain less sericin than *B. mori* silk, approximately 13-14% compared to 20-25% (Mahall, 1993).

Anaphe silk, found in central and southern Africa, comes from wild silkworms in the genus *Anaphe*, which create communal nests of cocoons for pupation; as a result the cocoons cannot be reeled, but the silk is desirable because of its softness compared to other wild silks (Rheinberg, 1991).

*G. mellonella* (Pyralidae), the greater wax moth, is nocturnal, and is a major pest of stored or unattended beehive brood combs (Powell, 2009). Wax moths consume brood comb (wax

structures in which the bees' eggs are laid and the larvae or brood develop), but they are not known to harm the bees or spread disease. The life cycle of *Galleria* (see Figure 2.2) is entirely dependent on temperature and availability of food. A female moth will lay a large number of eggs (300-1000) on an unattended comb, which hatch, and larvae consume the comb. In this species, the production of silk is not only for cocoons. From the second instar moult onward, larvae produce large quantities of silk to construct silk feeding tubes which protect them against detection and killing by the bees (Žurovec & Sehnal, 2002). Once the larvae have reached the seventh and final instar, they can leave their feeding tube and descend on a silk thread in search of a pupation site. Under ideal conditions (28-30°C), the larval stage lasts 20 days, the pupal stage lasts 8 days, and the adults live for approximately three weeks (Somerville, 2007).

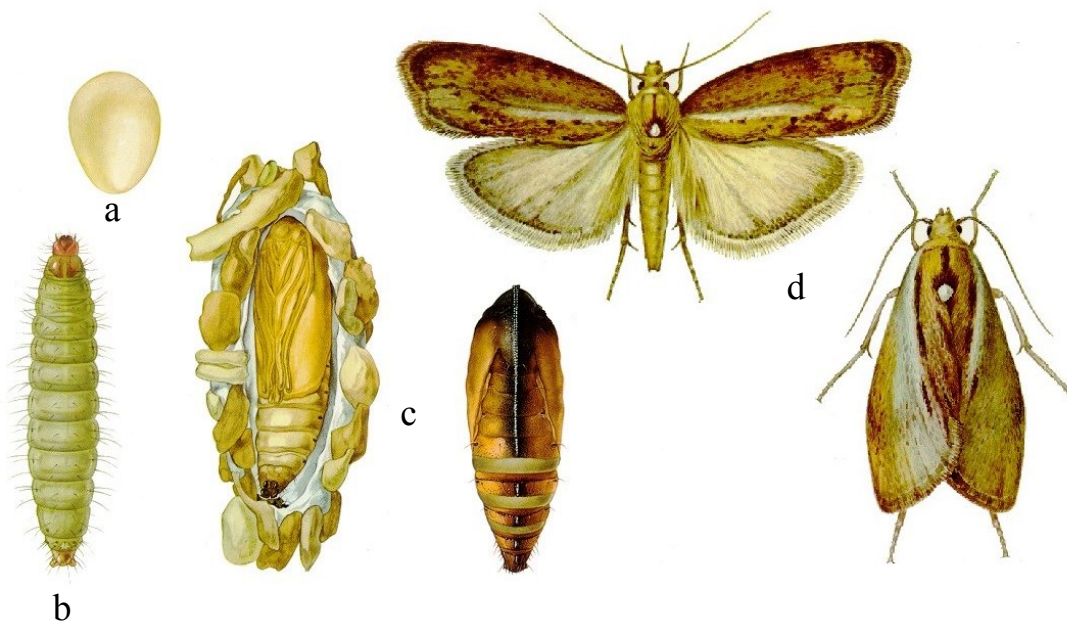


Figure 2.2 *G. mellonella* egg (a), larva (b), pupae with/without cocoon (c), and adults (d).  
(Adapted from: [http://agspsrv34.agric.wa.gov.au/ento/pestweb/Query1\\_1.idc?ID=904795699](http://agspsrv34.agric.wa.gov.au/ento/pestweb/Query1_1.idc?ID=904795699)).

The environment in which *G. mellonella* lives requires the continuous production of silk that is both strong and elastic (Žurovec & Sehnal, 2002). The fact that it continually produces silk as a larva differentiates *Galleria* from many other lepidopterans, including *Bombyx* and *Antheraea* silkworms, for whom silk production is mostly restricted to cocoon construction (Žurovec et al., 1998). In *B. mori*, for example, the silk glands can be up to 40% of the insect's body weight in the last instar, whereas in *Galleria* they are just 12% of the insect's body weight; *Galleria* larvae can still produce >30 mg of silk during the final larval stage, however, reserving <10 mg for cocoon production (Sehnal & Akai, 1990).

*Galleria* is a species already well-known to researchers, as it is a popular model organism for the study of medically-significant pathogens (Mukherjee, Domann, & Hain, 2011). This is because *Galleria* can be reared at 37°C, which is the ideal mammalian physiological temperature, and is essential for the (re)production of human viruses and pathogens. Many studies have been conducted on captive rearing techniques (Bronskill, 1961; Marston, Campbell, & Boldt, 1975) and artificial diet recipes, to keep rearing as successful and cost-effective as possible (Dadd, 1964, 1966; Eischen & Dietz, 1990; Good, Morrison, & Mankiewicz, 1953; Haydak, 1936; Roy, 1937; Sehnal, 1966). These studies highlighted the versatility of rearing *Galleria* larvae, who have been described as being “capable of converting even diverse foods to their biomass with remarkably similar efficacy” (Jindra & Sehnal, 1989, p. 722). This ability to eat a diverse range of foods saw *Galleria* in the spotlight in early 2017, making headlines for their ability to eat and digest polyethylene bags (Bombelli, Howe, & Bertocchini, 2017). Finally, *Galleria* silk could be a viable biomedical textile in the future, as it has been found to possess inherent antibacterial and antifungal properties (Nirmala, Kodrik, Žurovec, & Sehnal, 2001).

## **2.2 Silk structure**

Silks, which are protein polymers (fibroins) of amino acid residues, are essential to the life of many different organisms (Liljas et al., 2009). Proteins are extremely plastic, and can be globular or fibrous, stiff or elastic. Silks are a type of fibrous protein, along with others found in nature such as keratins, collagens, and elastins (Matsumoto et al., 2007). There are three types of fibrous proteins: the first are globular proteins which aggregate in a linear or helical manner; the second are very long polypeptide chains with alpha ( $\alpha$ ) helical secondary structure (such as keratin); and the third are protein aggregates which form long, parallel or anti-parallel beta ( $\beta$ ) sheets (Liljas et al., 2009). Silks fall under the latter two categories and are discussed in greater detail in this section.

### **2.2.1 Primary & secondary protein structure**

Like other polymeric textile fibres, silk contains both crystalline and amorphous regions (Pérez-Rigueiro, Viney, Llorca, & Elices, 2000a). In the crystalline regions, extended protein chains (primary structures) fold into thin, flat structures called lamellae, or sheets (secondary structures) (see Figure 2.3); the amorphous regions are composed of primary protein structures which do not contribute to lamellae formation (Pérez-Rigueiro et al., 2000a). The composition of these primary and secondary structures are discussed in this section.

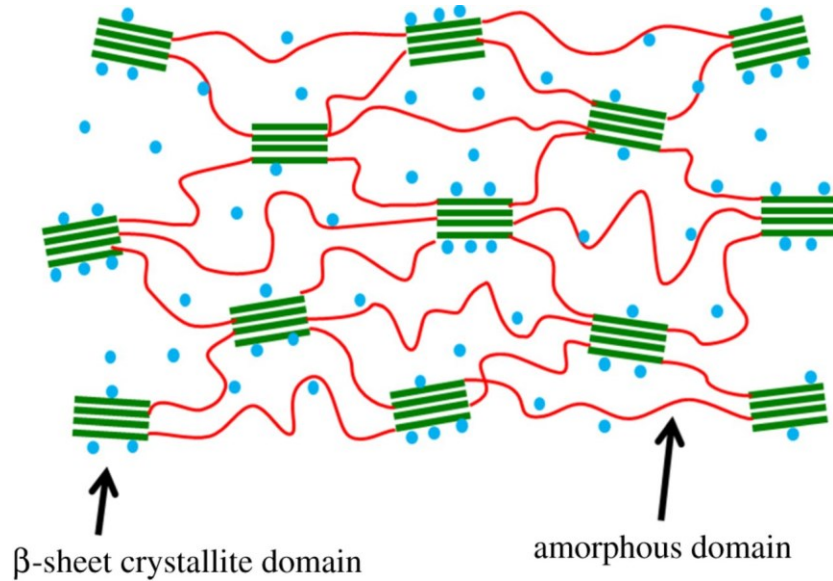


Figure 2.3 Crystalline and amorphous regions of silk fibroin.

Reprinted with permission from Royal Society (Cheng et al., 2014, fig. 1).

### 2.2.1.1 Primary protein structure

The basic building blocks or primary structure of all proteins are amino acids, which are comprised of a central carbon atom (C) bound to a hydrogen atom (H), an amine group (NH<sub>2</sub>), carboxyl group (COOH), and a side chain (R) (see Figure 2.4), which are linked together by peptide bonds (Liljas et al., 2009).

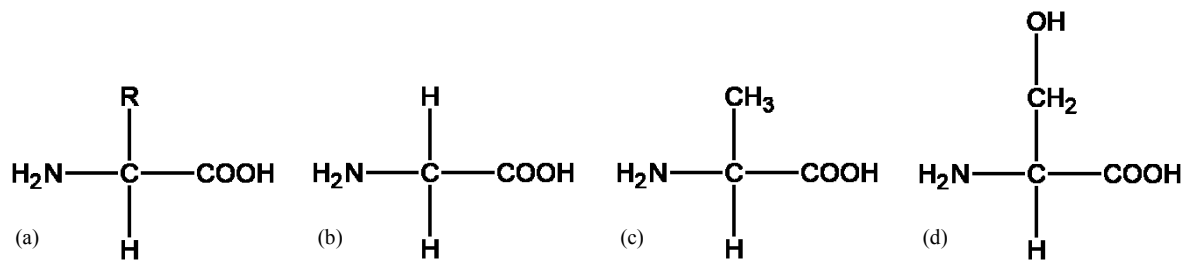


Figure 2.4 Amino acid structures. (a) is the basic amino acid structure, (b) is glycine, the simplest amino acid, (c) is alanine, and (d) is serine.

Amino acids are identified by their side chains (residues), which may be categorized as nonpolar, charged polar, uncharged polar, and no side chain (Liljas et al., 2009). These residues, and how they interact with each other based on their size, shape, charge, H-bonding capacity, and chemical reactivity, give proteins their unique properties (Craig, 2003; Liljas et al., 2009). There are twenty different amino acids from which all proteins are assembled, but only three make up the majority of silk proteins: glycine, alanine, and serine (Craig, 2003); the proportions of these amino acids differ between silk produced by different insect species.

The amino acid composition of insect fibroins has been the subject of study since the 1950s and '60s. At that time, many different types of silk from moths, wasps, and spiders were analyzed using dinitrophenyl (DNP) and ion-exchange chromatography to determine their amino acid compositions (Lucas & Rudall, 1968; Lucas et al., 1960). It was found that the three “simplest” amino acids, glycine, alanine, and serine, together comprised between 42.6 and 94.6% of fibroin protein (see Figure 2.5). Sulphur-containing amino acids such as cysteine and methionine were detected in very small amounts, and were thought to be potentially important to the secondary structure of fibroin (Lucas & Rudall, 1968).

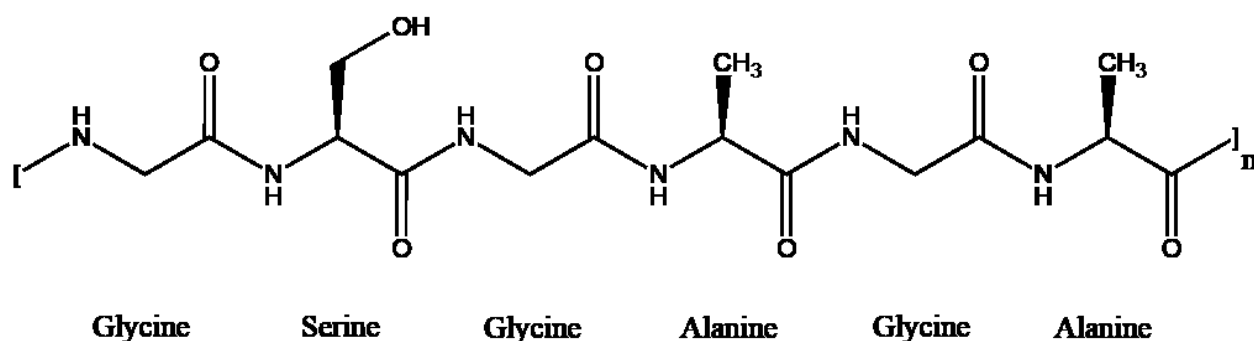


Figure 2.5 Sample primary structure of fibroin, composed of glycine, alanine, and serine.

The highly repetitive amino acid sequences in silk allow for the identification of shorter consensus sequences, which in turn, help researchers identify corresponding gene sequences (Matsumoto et al., 2007). This sequence analysis can shed light on the molecular evolution of a certain protein, and how it is similar or dissimilar to proteins produced by other homologous organisms (those evolving from a common ancestor) (Liljas et al., 2009). There is a wide variation in the amino acid compositions of different silks, all with the seemingly similar function of protecting the insect during pupation in Lepidoptera (Lucas et al., 1960).

### **2.2.1.2 Secondary protein structure**

When a long chain of amino acids adopt the same conformation, the protein's secondary structure is formed (Liljas et al., 2009). These secondary structures are either  $\alpha$ -helices or  $\beta$ -sheets (see Figure 2.6).  $\alpha$ -helices are formed when a carbonyl (C=O) oxygen interacts with the amine (NH) hydrogen of the following turn.  $\beta$ -sheets are formed when the C=O and NH groups of extended chains, or  $\beta$ -strands, interact with neighbouring strands;  $\beta$ -sheets can be parallel, antiparallel, or mixed (see Figure 2.7), with the polymer chain axis parallel to the fibre axis (Liljas et al., 2009; Matsumoto et al., 2007). Antiparallel sheets have hydrogen bonds perpendicular to the chain axis, between a carbonyl of one chain, and an amine of another.  $\beta$ -sheets containing poly-alanine repeats are symmetrical, whereas  $\beta$ -sheets comprised of glycine-alanine repeats are asymmetrical, with one surface projecting alanine residues and the other projecting glycine residues (Matsumoto et al., 2007).  $\beta$ -sheets are not flat but have a right-hand twist; the degree of twist depends on the chemical composition of the sheet.

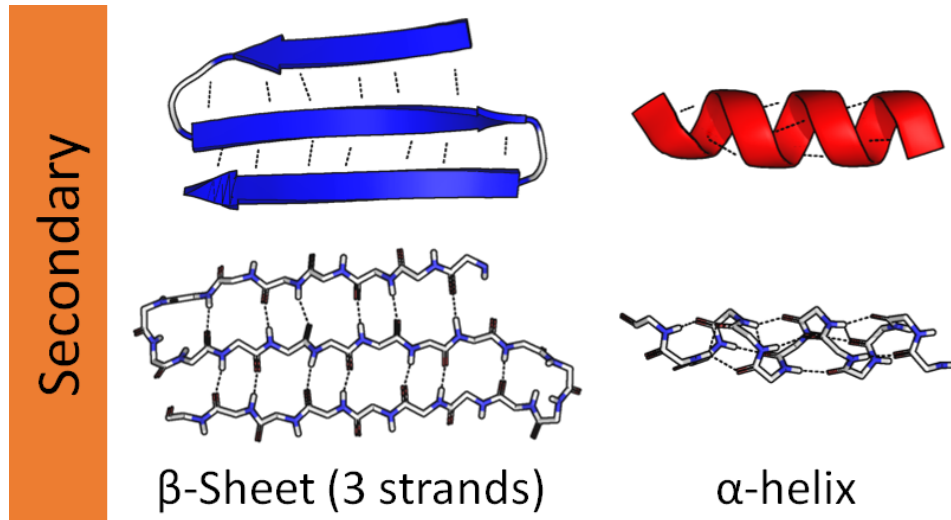


Figure 2.6 A basic  $\beta$ -sheet protein structure (left), and a basic  $\alpha$ -helix protein structure (right).

Figure by Thomas Shafee, distributed under a CC BY-SA 4.0 license.

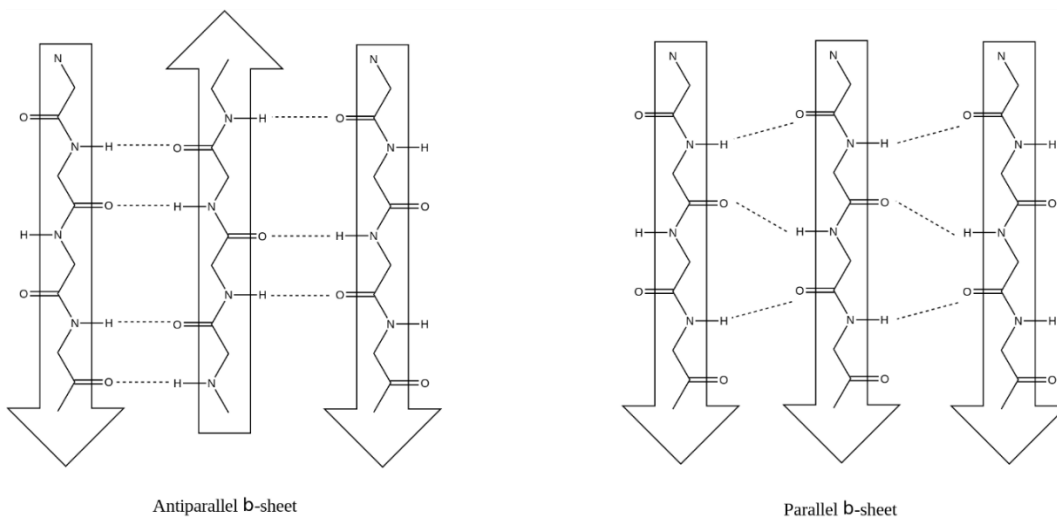


Figure 2.7 Antiparallel and parallel  $\beta$ -pleated sheets. Figure by Mysterioso, distributed under a CC BY-SA 3.0 license.

Most silkworm and spider silks have an antiparallel  $\beta$ -pleated crystalline structure (Marsh, Corey, & Pauling, 1955b; Rudall, 1962); they are semicrystalline, with 30–50% crystallinity in spider silks, 62–65% in *Bombyx mori* cocoon silk, and 50–63% in Tussah/wild silkworm cocoons (Matsumoto et al., 2007).

A subcategory of the parallel  $\beta$ -sheet is the cross- $\beta$  sheet; in this configuration, the polymer chain axis is perpendicular to the fibre axis (Geddes, Parker, Atkins, & Beighton, 1968), which when stretched, assumes a parallel- $\beta$  structure (Craig, 2003).

$\alpha$ -helical fibroins have a lower glycine content, but higher amounts of acidic residues, such as glutamic acid (Rudall & Kenchington, 1971). It has been noted that  $\alpha$ -helical fibroins are often used in combination with other materials or silks, which could mean that  $\alpha$ -helical silks lack certain mechanical properties that other silks might have (Craig, 2003). This difference could be explained by the presence of stabilizing hydrogen bonds between polypeptide chains in  $\beta$ -pleated protein structures, as opposed to the within-chain hydrogen bonds of  $\alpha$ -helical protein structures (Craig, 2003; Matsumoto et al., 2007).

In the early days of silk research, parallel and antiparallel “chain rippled sheets” in silk fibroin were described (Pauling & Corey, 1953), and the parallel- $\beta$  structure of Tussah silk (*Antheraea pernyi*) was identified using x-ray diffraction (Marsh et al., 1955b). Examples of other secondary structures were soon found in insect fibroins, however, such as  $\alpha$ -helical honey bee silk and cross  $\beta$ -sheet lacewing silk (Rudall, 1962). Thirty years later, Takahashi (1993) expanded upon the work of these early scholars, presenting the case for antipolar antiparallel  $\beta$ -sheets, as opposed to polar antiparallel  $\beta$ -sheets, as a means to explain the greater diversity of silk molecular structures being observed.

From the soluble protein in a silk gland to the finished fibre, many silks undergo a range of different secondary structures during production. The formation of these structures, their orientation, and their size, all have a direct impact on the mechanical properties of the silk fibre (Matsumoto et al., 2007); like all textile fibres, the crystalline areas of the polymer provide strength and brittleness, while the amorphous regions allow for moisture penetration (which acts

as a plasticizer for silk, as discussed in section 2.6.2.2), elasticity, and flexibility (Collier & Epps, 1999).

### **2.2.2 Spider silk structure**

The amino acid contents of the parallel- $\beta$  silks taken from the cylindrical, ampullate, and flagelliform glands of a female garden spider, *Araneus diadematus*, were found to be primarily glycine, serine and alanine (Andersen, 1970). The adhesive piriform (also called pyriform) and aggregate silks, in contrast, were found to be composed primarily of hydrophilic, basic amino acids, lysine in particular (Andersen, 1970). More recent genetic sequencing has shown that, similar to silkworm moths, *A. diadematus* silks contain crystalline domains comprised of both poly-alanine and poly-glycine-alanine repeating motifs (Guerette, Ginzinger, Weber, & Gosline, 1996). The silk of the golden silk orb-weaver, *Nephila clavipes*, has been found to be composed of two different protein subunits, named Spidroin 1 (approximately 275 kDa) and Spidroin 2, both of which are in the antiparallel  $\beta$ -sheet conformation (Hinman & Lewis, 1992). *N. clavipes* silk has similar crystalline poly-alanine blocks, but are separated by glycine-rich amorphous regions (Guerette et al., 1996). In general, spider fibroins all have in common the tightly packed poly-alanine  $\beta$ -sheets, larger poly-glycine-alanine crystalline regions, and proline-containing ‘elasticity modules,’ all surrounded by non-repeating amorphous domains (Eisoldt et al., 2011).

### **2.2.3 Lepidopteran silk structure**

Of the four different orders which produce  $\beta$ -structured silks (Lepidoptera, Trichoptera, Hymenoptera and Embiidina), those produced by lepidopteran larvae (caterpillars) are among the most derived, or highly evolved (Craig, 2003). Table 2.1 below summarizes the properties discussed in the following sections.

Table 2.1 Summary chart of the amino acid content, H-fibroin size and structure, and other metrics used to describe the structure of *Bombyx*, *Antheraea*, and *Galleria* silks.

Insect	Amino Acid Content (various, see text)	H-fibroin molecular weight (Žurovec & Sehnal, 2002)	Secondary Protein Structure (Žurovec & Sehnal, 2002)	$E_{wet}/E_{dry}$ Ratio (Hepburn, et al., 1979)	Interplanar Spacing (Warwicker, 1960)
<i>Bombyx</i>	High glycine content	391 kDa	H- and L-fibroin heterodimers	0.64	Group 1 (9.3 Å)
<i>Antheraea</i>	High alanine content	197 – 250 kDa	H-fibroin homodimers	0.32	Group 3a (10.6 Å)
<i>Galleria</i>	High glycine content; also contains leucine, isoleucine, and valine (bulky side groups)	500 kDa	“exceptionally homogenous” H-fibroin structure	0.18	Group 3b (10.6 Å)

### 2.2.3.1 Silk moths

While both components of lepidopteran silk (fibroin and sericin) are proteins, they are structurally very different. Fibroin is predominantly composed of glycine, alanine, and serine, which form the building blocks of three major polypeptides: heavy-chain fibroin (H-fibroin), light-chain fibroin (L-fibroin), and P25 glycoprotein (Tanaka & Mizuno, 2001; Tanaka, Mori, & Mizuno, 1993). Each are categorized by their molecular weights, which for *B. mori* silk, are 350 kDa (kilodaltons), 25 kDa, and 30 kDa, respectively (Tanaka & Mizuno, 2001; Tanaka et al., 1993). The H-fibroin and L-fibroin are linked by disulfide bonds, and six of these heterodimers, together with one molecule of P25, form an elementary fibroin unit (Inoue et al., 2000). *B. mori* fibroin is characterized by dense molecule packing (large crystalline regions), and a high glycine content (Marsh et al., 1955a; Warwicker, 1960). The dense molecular packing of H-fibroin is due

to the alternation of glycine with larger residues (serine and tyrosine) in an approximate 3:2:1 ratio (Matsumoto et al., 2007; Pérez-Rigueiro et al., 2000a), allowing for smaller side-chain spacing (Lucas & Rudall, 1968). The glycine, alanine, and serine motifs in fibroin form the crystalline  $\beta$ -sheet areas of the protein, which contribute to the strength and stiffness of the fibre (Marsh et al., 1955a); the larger serine and tyrosine residues can cause random orientation of the H-fibroin molecules, giving the fibre flexibility (Denny, 1980).

By contrast, sericin is composed of at least 15 different polypeptides, 20 to 220 kDa, each containing glycine, alanine and serine as well, but with a large proportion of threonine, aspartic acid, and glutamic acid also (Gulrajani, 1992; Sprague, 1975). Sericin is largely amorphous with some  $\beta$ -structures and acts as an adhesive to bind the silk threads together during cocoon formation (Komatsu, 1981, as cited by Gulrajani, 1992; Perez-Rigueiro, Elices, Llorca, & Viney, 2001). Some researchers have separated sericin into four different fractions (sericin I, II, III, and IV), each with their own amino acid compositions and physical properties, based on how soluble they are in hot water (Komatsu, 1985, as cited by Gulrajani, 1992).

The silk produced by moths of the family Saturniidae always has a higher alanine content than glycine (Lucas et al., 1960), and consists solely of polymerized H-fibroin homodimers (Tamura and Kubota, 1989; Tanaka and Mizuno, 2001). These homodimers are made up of elements containing poly-alanine blocks (PAB) and non-poly-alanine blocks (NPAB) (Sezutsu & Yukuhiro, 2000). Warwicker (1960) classified *A. pernyi* as a group 3a silk, due to its high alanine content and crystalline regions “flanked” by amorphous regions. The H-fibroin of *A. pernyi* is largely composed of alanine, glycine, and serine, which together account for 81% of the amino acid content (Sezutsu & Yukuhiro, 2000). The PAB sequences are nearly identical to those of *Bombyx* H-fibroin, which suggests that the differences in the amino acid compositions

could be due to the glycine-rich NPAB sequences, and that variations between different fibroins may be due to these sequences (Sezutsu & Yukuhiro, 2000). The silk of the Eri silkworm, *Samia cynthia ricini*, is similar to *A. pernyi* in that it contains glycine-rich NPABs, but differs where at least one is actually glycine-poor (Sezutsu & Yukuhiro, 2014).

### 2.2.3.2 *Galleria* silk

Microscopic observations show that like other lepidopteran silks, *Galleria* silk is comprised of two threads or brins, paired together by sericin to form a bave (Fedič et al., 2003). However *Galleria* silk is different from other lepidopteran silks, with its “exceptionally homogenous” H-fibroin structure.

Initially, a partial (deduced) sequence of *Galleria* H-fibroin found that it was rich in glycine, serine, and alanine, but did not reveal any regular poly-alanine repeats (Žurovec, Sehnal, Scheller, & Kumaran, 1992). Researchers then sequenced all silk proteins of *Galleria*, finding high proportions of glycine (31.6%), alanine (23.8%), and serine (18.1%) (Žurovec & Sehnal, 2002), which differs from the alanine-rich amino acid composition of Tussah silks (Marsh et al., 1955b).

Physical fibre properties are influenced by the amino acid sequences of the H-fibroin, which is predominantly comprised of repeating units (Fedič et al., 2003); in *B. mori* silk, these repeats are predominantly GAGAGS motifs (Suzuki & Brown, 1972), and in *Antheraea* silk, the repeats are alanine-based (Sezutsu & Yukuhiro, 2000). Based on x-ray diffraction data, one would assume that the structure would be similar to that of *Antheraea* (Lucas & Rudall, 1968; Warwicker, 1960), but gene sequencing determined a more complex structure (Žurovec & Sehnal, 2002). About 95% of the gene produced 10-12 hierarchically arranged assemblies comprised of regular

repeat lengths and amino acids with bulky side chains, which contrasted with the relative variability of *Bombyx* and *Antheraea* H-fibroins.

When the secondary structure of *Galleria* silk was first studied (Lucas et al., 1960; Warwicker, 1960), it was categorized as a group 3 parallel- $\beta$  sheet structure (based on its inter-sheet distance of 10.6 Å) similar to that observed in Tussah silk (Marsh et al., 1955b). It was noted, however, that since *Galleria* silk (among others) had a much higher glycine content than alanine, it couldn't be the same structure as Tussah silk; this led to the conclusion that while the x-ray diffraction results gave an indication of the protein structure, it did not correlate with the amino acid composition (Lucas et al., 1960). Portions of the polypeptide chains with long amino acid residues were found in the amorphous regions, while the areas with shorter amino acid residues were found in the crystalline regions (Lucas et al., 1960; Warwicker, 1960). Hepburn, Chandler, and Davidoff (1979) first used this information to try to approximate the degree of crystallinity for *Galleria* fibroin by calculating its short-side-chain/long-side-chain (SC/LC) ratio, where a higher number would theoretically mean a higher crystallinity; *Galleria*'s SC/LC ratio was 3.0 (*Antheraea* was 3.9 and *Bombyx* was 6.6), but this method of estimation did not hold true against other silks in their study. Instead, borrowing upon research done on cotton fibres, they estimated the degree of crystallinity by calculating the wet and dry modulus ratio of the silk fibres, where 1 = completely crystalline and 0 = completely amorphous. *Galleria*'s  $E_{wet}/E_{dry}$  ratio was 0.18, *Antheraea* was 0.32, and *Bombyx* was 0.64. This method agrees with the estimated crystallinity of *Bombyx* described above, but not with that of tussah silk (*Antheraea*); therefore, one could say that the crystallinity of *Galleria* silk could be approximately 18%, but more research is needed in this area to either confirm or refute this estimate.

The H-fibroin gene in *Galleria* is homologous to those of other lepidopterans, but the protein is much larger at approximately 500 kDa (kilodaltons), *B. mori* H-fibroins are 391 kDa (Žurovec & Sehnal, 2002), *A. pernyi* (tussah silk) are 216 kDa (Sezutsu & Yukuhiro, 2000), *A. mylitta* (tasar silk) are 197 kDa (Datta, Ghosh, & C. Kundu, 2001), *A. yamamai* (Japanese tussah) are 250 kDa, and *Philosamia cynthia ricini* (eri silk) are 230 kDa (Tamura & Kubota, 1989).

While H-fibroin of *B. mori* contains repeated crystalline regions periodically interrupted by randomly-oriented “boundary sequences” giving the fibre flexibility, over 95% of the H-fibroin of *Galleria* contains numerous, short crystalline regions separated by short peptide strands similar to those proposed for spider dragline silks (Žurovec & Sehnal, 2002). Despite this difference in structure, *Galleria* silk has a similar tensile strength to *Bombyx* and *Antheraea* silks; it has been proposed that this finding could be due to larger repeat units in the latter two genera overlapping and interacting, as opposed to the “precision of repeat matching” in *Galleria* silk (Fedič et al., 2003, p. 35255). It has also been hypothesized that the combined requirement of strength (cocoon durability) and elasticity (silk feeding tubes) has probably driven the evolution of the silk in *Galleria* (Žurovec & Sehnal, 2002). The high proportion of large, nutrient-rich amino acids found in *Galleria* H-fibroin could also be related to the behaviour of caterpillars which spin protective tubes continuously, while consuming the other end; this could be a means of long-term nutrient storage for amino acids which are otherwise scarce in the insect’s diet (Fedič et al., 2003).

## **2.3 Commercial production**

### **2.3.1 Rearing and collection**

In commercial sericulture operations, *Bombyx mori* larvae are raised in captivity on foliage from the egg to pupal stage (see Figure 2.8). Mulberry leaves are first laid out in large, open-air trays,

and the eggs are distributed over the leaves; when they hatch, the caterpillars are only 2 mm long, but grow up to 30 mm long in about four to five weeks (Rheinberg, 1991). When the insects are ready to pupate, they are given straw frames upon which to build their cocoons; it takes eight days for the cocoon to be formed, and another three to four days for the insect within to become a pupa. If the silkworms are reared in very close conditions, sometimes a dual, or dupion cocoon is formed where two insects and their cocoons are attached together (Rheinberg, 1991). When the cocoons are fully formed and the insects have become pupae, they are collected and taken to a silk factory to be processed, which is described in more detail in the next section.



*Figure 2.8* Twenty-one day old *Bombyx mori* larvae feeding on mulberry leaves in a commercial sericulture operation. Photograph by Armin Kübelbeck, distributed under a CC-BY-SA license, Wikimedia Commons.

### **2.3.2 Commercial processing**

While many different insects produce silk, that which is produced by the mulberry silkworm, *B. mori*, is used most often in the commercial silk industry (Babu, 2013). Once the cocoon has been produced by the silkworm, it goes through many steps before it becomes the finished product

(Ganga, 2003). These steps include stifling, drying, deflossing and riddling, cooking and boiling, reeling or spinning, throwing, and weaving.

### **2.3.2.1 Preparation**

First, the pupae must be killed inside of their cocoons (stifling); to avoid soiling the cocoons, the pupae must be both stifled and dried so that decomposition does not occur. Cocoon drying must be done very carefully so that the quality of the silk is not adversely affected. Various methods of stifling and drying include sun-drying (cocoons are directly exposed to the sun for two-to-three days), steam-stifling (quick and uniform, but must be dried for long-term storage), and hot-air conditioning (simultaneous stifling and drying can denature silk proteins). After the stifling and drying steps, the tangled silk on the outer surface of the cocoon must be removed (deflossing) and the cocoons sorted by size (riddling). To reel effectively, the sericin must be softened uniformly by cooking and boiling the cocoons in hot water. Once the sericin has been softened, the cocoons are brushed so that the end of the silk filament can be found for reeling (Ganga, 2003).

### **2.3.2.2 Reeling**

Reeling, the process of unwinding the single silk filament (bave) from the cocoon, can be done in two ways: floating or top-reeling, and sunken reeling (Ganga, 2003). In top-reeling, the cocoons float on the surface of the hot water, so that only the outer layers of the cocoon are softened and the inner layers soften as reeling occurs. During sunken reeling, the cocoon cavity fills with water, allowing the cocoon to sink into the reeling water. This process allows for more uniform softening and makes the reeling process easier and with fewer defects. As they are reeled, the filaments from multiple cocoons are passed through a thread guide, become bound together with sericin, and produce a thread of desired thickness; 4-7 cocoons produce 14 denier (15.5 dtex)

yarns (Ganga, 2003), while 7-8 cocoons produce 20 denier (22.2 dtex) yarns (Rheinberg, 1991).

To ensure that the baves are firmly attached to one another, the thread is pulled under tension through a croissure (crossing, or temporary twisting together of the thread), then is finally wound onto a reel (Ganga, 2003). After reeling, the silk then goes on to the throwing and weaving process (Babu, 2013).

### **2.3.2.3 Weaving**

The reeled silk must be soaked in a mixture of soap, oil, water and borax before weaving to soften the sericin and lubricate the threads (Babu, 2013). The silk is then wound onto a bobbin, and two or more bobbins are then doubled and twisted together to create plied yarns (a process called throwing). Warping may then commence, and the weft is wound onto a pirn. Silk weaving is largely carried out on handlooms in many countries but can be done with modern powered looms. Different types of silk fabrics produced with these filament yarns include charmeuse, crepe de chine, georgette, and habutai (Babu, 2013).

An average of 35% by weight of raw silk waste is produced from cocoons, reeling waste, and thread waste (Babu, 2013). This waste can be utilized in different ways but is normally used for spun silk production by combing, spreading, drafting, drawing, roving, and spinning the staple-length silk fibres. Uses for these spun yarns include lining, hosiery, mufflers, pile fabrics, and blended fabrics (Babu, 2013).

## **2.4 Research collection processes**

Most researchers do not have access to large scale silk processing facilities, or want to develop new ways of collecting silk samples which would better aid in answering their research questions, particularly for the purposes of tensile testing. While it is likely impossible to avoid

inadvertently changing the mechanical properties of a silk fibre under artificial rearing and collection conditions, special care must be taken to minimize this.

#### **2.4.1 Sampling from cocoons**

The closest research sampling technique to reeling cocoon silk is to boil the cocoons in water to soften the sericin (or to partially degum the cocoons) and collect the loosened fibres manually with tweezers (Pérez-Rigueiro, Viney, Llorca, & Elices, 2000b). While researchers take care to not stretch the fibres permanently during the sampling process, one can imagine that must be difficult when the elastic limit of the fibre is reached at approximately 0.05 N.

Another popular method of sampling silk for tensile tests is simply to test pieces of the cocoon itself, though it has been shown correlate poorly to the tensile properties of individual silk fibres and is used instead as a way to measure the structural integrity of the cocoon (Borujeni, Najar, & Dolatabadi, 2017; Chen, Porter, & Vollrath, 2012a). The poor correlation between cocoon and fibre tensile properties is likely due to the random, unaligned orientation of the fibres in the cocoon structure; it would also likely be quite difficult to estimate the cross-sectional area of a piece of cocoon for converting to stress-strain curves.

#### **2.4.2 Forced silking**

Forced silking for the purposes of mechanical testing seems to have originated in spider silk research (Zemlin, 1968), and was made more humane by anaesthetizing the spider with carbon dioxide (Work, 1976). It was found at that time that the forcibly-silked fibres had lower tensile strength (average 48g/tex, 26% elongation) and less consistent results than the same silks sampled from webs of the same species (average 80 g/tex, 35% elongation); the morphologies of the fibres were noticeably different, with the silked fibres smooth and rod-like, and the web-sampled spiders rough and lacking cross-sectional uniformity (Work, 1976). The force required

for a spider to spool silk while freefalling accounts for approximately 2% of the silk fibre's tensile strength, while force-silking can create stresses over 50% of the fibre's tensile strength; this large force could cause a drawing-out effect in the silk, which would significantly impact the orientation of the polymer structures and potentially its mechanical properties in turn (Ortlepp & Gosline, 2004; Pérez-Rigueiro, Elices, Plaza, Real, & Guinea, 2006).

Similar work has been done with *Bombyx* silkworms, as a way to address the irregularities of silks sampled from cocoons (Perez-Rigueiro et al., 2001). This irregularity could be due to the presence of sericin, silk damage due to the degumming process, or a combination of both factors. The authors of this article do appear to have a slight misunderstanding about the cocoon reeling and degumming process, however, stating that degumming occurs during the reeling process, when this is not usually the case. Samples force-silked from the same silkworm had similar force-displacement curves, and samples from different silkworms had qualitatively (and sometimes quantitatively) similar curves. The researchers stated that the presence of sericin (hence, non-degummed samples), hindered their ability to accurately measure the cross-sectional area, and as such, the results were less consistent when converted to stress-strain curves. Additional problems with inconsistencies could also be because the cross-sectional areas were measured after testing (where plastic deformation has undoubtedly occurred) and calculated using the assumption that the cross-section was circular (baves are figure-eight- or oval-shaped in cross section). The average tensile strength of the samples was  $416 \pm 2$  MPa (Perez-Rigueiro et al., 2001), but since the average cross-sectional area was not clearly stated, it is hard to discern how this would compare to the average tenacity of reeled *B. mori* silks.

Only two studies in the literature have tested the mechanical properties of *Galleria* silk; one collected the tensile specimens by hand-drawing silk from the insect, though the exact method

was not described in detail (Hepburn et al., 1979), and one where the silk fibres were collected by sliding a larva down a glass slide tilted at 30° and collecting the resulting silk (Fedič et al., 2003). It is possible that the samples force-silked from the *Galleria* larvae are exhibiting the same reduced tensile strength as seen in forced spider silking, but there have been no studies done to-date to explore this problem.

## **2.5 Processing**

### **2.5.1 Degumming**

The process of degumming, or removing the sericin from the fibroin component of the silk, can be done either before or after weaving, depending on the type of silk used, fibre length (staple or filament), or type of fabric being woven (Humphries, 2009); having some sericin present during weaving can help protect the yarns against abrasion, but all sericin must be removed before dyeing (Rheinberg, 1991). At its simplest, the degumming process involves submerging silk in boiling water, usually including a salt or detergent to increase efficiency (Lucas, Shaw, & Smith, 1955); the mode of action is the hydrolytic cleavage of sericin peptide bonds and solubilization or dispersion in water (Gulrajani, 1992). For *Bombyx mori* silk, the amount of sericin present on the silk can be between 17–38% by weight. In this section, three main processes are discussed: water-only degumming, enzymatic degumming, and the use of “soap and soda” solutions.

#### **2.5.1.1 Water-only**

The most straightforward method of degumming is to simply submerge the silk in boiling water until the sericin has been removed. This process is commonly used in tensile experiments where individual fibres need to be degummed and the use of chemicals which might deteriorate the silk is to be avoided (Pérez-Rigueiro, Viney, Llorca, & Elices, 1998).

Another method of water-only degumming is to do it under pressure in an autoclave, but this option is generally not used commercially (Gulrajani, 1992). When done carefully, autoclaving can be very effective, removing about 96% of the sericin; care must be taken to not raise the temperature too high, however, as this can be detrimental to the silk (Knott, Freddi, & Belly, 1983).

### **2.5.1.2 Enzymatic**

Enzymatic degumming, which is a more biological option, is reported to be more gentle on the silk than conventional methods (Gulrajani, 1992). One such proteolytic enzyme is papain, which is extracted from the latex of papaya fruit. Its degumming action on *B. mori* silk seems to be comparable to conventional alkaline/soap (“soap & soda”) treatments, but the silk dyes more evenly and shows less damage (fibrillation) when viewed at high magnification (Nakpathom, Somboon, & Narumol, 2009). Additionally, woven fabric degummed with papain showed a reduction in strength of 18.55% and 14.20% (warp and weft, respectively), whereas the soap and soda method reduced the tensile strength of the same fabric by 27.95% and 26.37% (Chakraborty, Mahato, Rajak, & Ghosh, 2014). Commercial options are also available to use, and require lower temperatures and shorter dwell times than conventional methods (Anghileri, Freddi, Mossotti, & Innocenti, 2007).

### **2.5.1.3 Soap & soda**

The degumming of silk in soap solutions is a well-established process and has been used for more than 200 years (Walters & Hougen, 1934, as cited by Gulrajani, 1992). Olive oil or Marseilles soap has been most often used, more due to tradition than superior effectiveness (Gulrajani, 1992). 20-30% of the weight of material is generally used, with a degumming time of 90-120 minutes. It is recommended that alkalis such as sodium silicate, sodium carbonate,

sodium phosphate, or sodium hydroxide, up to 0.18% free in solution (mass or volume not specified), be added to the bath to maintain the pH at an effective level of 9.5-10.5, and to improve degumming efficiency; sodium carbonate is the most preferred alkali (Hall, 1935, as cited by Gulrajani, 1992). It is not recommended to use alkali alone, as it can leave the silk yellowish, thin, and harsh-feeling. While the process is often referred to as “boiling off”, it is advisable to keep the degumming temperature just below boiling at 90°C to maintain dyeability and handfeel (Gulrajani, 1992).

## **2.5.2 Evaluation of degumming effectiveness**

It is common to use a combination of qualitative and quantitative methods to assess the effectiveness of a degumming treatment, making use of microscopy, stains, solubility tests, and measures of weight loss.

### **2.5.2.1 Qualitative/Visual**

When viewing silk samples under the microscope, the sericin coating is visible as cracked, split, and irregularly attached to the silk strands; degummed silk appears long and smooth, and the individual filaments are separated (Mahall, 1993). Pauly reagent, which is normally used to detect chemical damage on silk, dyes sericin an orange-red colour. This dye can be used to detect the presence of sericin, but because it also dyes the silk that orange-red colour if it has been chemically damaged, this stain could cause some confusion. Another stain that can be used is Neocarmin W, but it too can be unreliable. The most reliable results are achieved by using Sirius Red (C.I. Direct Red 80); the silk is dyed in a 1% mass/volume solution for one minute then rinsed thoroughly. Another method suggested is to boil the silk in a 0.5% mass/volume solution of CI Direct Red 80 for 1 minute, then rinse (Knott et al., 1983). After staining, the sericin will

be stained red, and the silk will remain undyed (Mahall, 1993); in the event of incomplete degumming, the silk will be pale pink in colour (Nakpathom et al., 2009).

### **2.5.2.2 Quantitative**

The most common method of evaluating degumming effectiveness is by weighing the silk before and after the treatment, and calculating the percentage of weight loss; for *Bombyx mori* silk, a 20-25% weight reduction is generally expected after degumming (Mahall, 1993). Another method involving weight loss percentages is to dissolve the fibroin of the degummed sample with ninhydrin (Fan, 2005), trypsin (Knott et al., 1983) or with Cuoxam (Koch, 1972, as cited by Mahall, 1993), and weigh the remaining sericin.

Additional, more modern methods include amino acid composition analysis and fluorescence spectroscopy, where quick, accurate readings are needed; this assessment is especially important when the silk is being used for a biomedical device, as any residual sericin could trigger an inflammatory response in a patient (Wray et al., 2011).

## **2.6 Fibre characterization**

### **2.6.1 Qualitative**

Fibres may be identified using optical and/or electron microscopy, both longitudinally and in cross-section (AATCC Test Method 20, 2013). When using optical microscopy to study longitudinal features, a small quantity of fibres are placed on a glass slide, separated, mounted with immersion fluid (usually mineral oil), and covered with a cover slip (AATCC Test Method 20, 2013). When using electron microscopy, a number of different techniques can be utilized. Scanning electron microscopy (SEM) is used to examine surface details at medium-high magnifications, and has a larger depth of field than is possible when using optical microscopy

(Hearle & Morton, 2008). Transmission electron microscopy (TEM) requires the use of extremely thin specimens, and as such, is best used when working with replicas made from the fibre in question. TEM is used to study internal details, can examine fibre remnants after degradation, and can perform electron diffraction to view the fibre's crystal lattice structure in that area. Atomic force microscopy (AFM) allows for the observation of surface topography and can measure nano-mechanical properties such as stiffness and elastic modulus. Nuclear magnetic resonance (NMR) can be used to determine the crystalline/non-crystalline ratio of the material being analyzed (Hearle & Morton, 2008).

## **2.6.2 Quantitative**

### **2.6.2.1 Diameter & cross-sectional area**

It is apparent that challenges in measuring the stress or specific stress of a fibre can be caused by inaccurate cross-sectional measurements. There are three main ways cross-sectional area can be measured: calculating an average using SEM, calculating the linear density, or by Fraunhofer laser diffraction. After observing the cross-section of a fibre via SEM, formulas may be employed to calculate the cross-sectional area of a fibre depending on its shape (Hearle & Morton, 2008); if the fibre is circular, the calculation is straightforward. If the fibre is not circular, another approach is to measure the diameter at from two perspectives,  $0^\circ$  and  $50^\circ$  for example, and use the difference between those two measurements to estimate the result (Perez-Rigueiro et al., 2001). Still another would be to measure the diameter of a bave, divide that in half, and use it to calculate the cross-sectional areas of the two brins attached together, making the assumption that the brins are circular in cross-section (Fedič et al., 2003).

Cross-sectional area is proportional to linear density; one may be calculated from the other so long as the fibre density is known, though it has been acknowledged that the linear density of a

single strand of silk can vary from 1.0-1.75 dtex along its length (Hearle & Morton, 2008). This inconsistency can cause high variability in tensile testing of silk fibres, because the average cross-sectional area calculated for a quantity of fibre may not be representative of the point of failure of each individual fibre sample (Dunaway, Thiel, & Viney, 1995). To address this variability, laser diffraction can be used to non-destructively measure fibre cross-sectional areas on the test specimens themselves, at or near the point of failure (Dunaway, Thiel, Srinivasan, & Viney, 1995; Dunaway, Thiel, & Viney, 1995). Laser diffraction can only be used on near-circular fibres, however, meaning that it is not an appropriate technique to measure the irregularly attached brins of silkworm baves (Dunaway, Thiel, & Viney, 1995). This limitation hasn't stopped researchers from using it to measure silkworm baves (Reed, Bianchini, & Viney, 2012), however, so perhaps more investigations are needed to determine whether it can be used effectively on insect silks. Apart from calculating linear density, the above methods are not very accurate, given that silk fibres are not circular in cross-section, but are instead triangular or wedge-shaped.

#### **2.6.2.2 Tensile Strength**

Silk is strong, due to its crystalline,  $\beta$ -sheet protein structure; it loses strength when wet, due to the hydrolyzation of the inter-sheet hydrogen bonds (Gohl & Vilensky, 1983). While natural material properties vary within an organism and between organisms and species, silk has been shown to store more elastic energy per unit weight or volume, than man-made steel springs (Ashby, Gibson, Wegst, & Olive, 1995), and a higher elongation to failure than high performance fibres such as Kevlar® (Matsumoto et al., 2007; Pérez-Rigueiro et al., 1998). Generally, silkworm silks have slightly lower tensile strength than spider silks, but many more silks have yet to be characterized (Matsumoto et al., 2007).

Many tensile tests are presented in the form of force-elongation curves or stress-strain curves. Force refers to the absolute force applied to the test specimen, and elongation refers to the amount of stretch; stress (engineering stress) refers to the force applied relative to the original cross-sectional area of the specimen, while strain (engineering strain) is the extension of the specimen relative to its initial length (Collier & Epps, 1999). As discussed in the previous section, determining the cross-sectional area of fibres and yarns can be quite difficult, as they are often irregularly shaped; as a result, in textile testing, specific stress is often used, which describes tensile strength relative to linear density (Collier & Epps, 1999). The formulas for these parameters are summarized in Table 2.2; fibre and yarn strengths are normally reported as stress for the purposes of comparing different materials (Collier & Epps, 1999).

*Table 2.2: Tensile Strength Calculations, adapted from ASTM D4848 (1998), and Collier & Epps, (1999)*

Property	Formula	Unit
Stress (Engineering Stress)	$Stress = \frac{Force}{Area}$	MPa (N/mm <sup>2</sup> )
Specific stress	$Specific\ stress = \frac{Force}{Mass/Length} = \frac{Force}{Linear\ density}$	N/tex
Strain (Engineering Strain)	$Strain = \frac{Initial\ Length - Final\ Length}{Initial\ Length} = \frac{Extension}{Initial\ Length}$	mm/mm or %

Force-elongation and stress-strain curves (example of the latter in Figure 2.9) can be very informative about a material's tensile properties, with the five predominant types of measurements from stress-strain curves outlined below (Collier & Epps, 1999):

1. Young's modulus of elasticity (E): The initial linear (straight) portion of the curve, which shows the initial, elastic (recoverable) resistance to the force;
2. Yield point (P( $\sigma_e$ ,  $\epsilon_e$ )): Where the curve changes from a straight line, which indicates the region of plastic (unrecoverable) deformation;
3. Ultimate tensile strength (UTS): Where the specimen breaks, and resistance drops to zero. This point indicates the breaking strength of the material;
4. Toughness, or work of rupture ( $J/m^3$ ): The area under the curve, which shows the total amount of energy required to break the material;
5. Strain to failure ( $\epsilon_f$ ): the total strain exhibited by the material up to the point of failure (the sum of the elastic and plastic strain to failure).

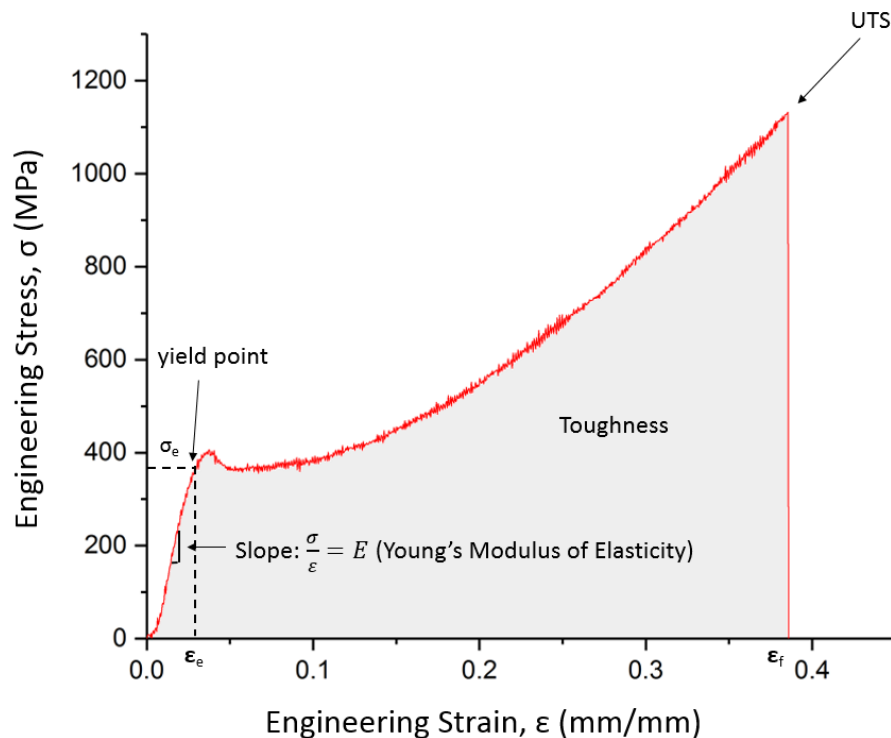


Figure 2.9 Engineering stress-strain curve showing Young's modulus of elasticity (E), stress and strain at elastic limit ( $\sigma_e$ ,  $\epsilon_e$ ), ultimate tensile strength (UTS), strain at break ( $\epsilon_f$ ), and toughness (grey area under curve).

Ideally, the capacity of the testing equipment should be appropriate for the material, and because the extension rate can affect the results (Hudspeth, Nie, Chen, & Lewis, 2012; Mortimer, Drodge, Siviour, & Holland, 2012), a standard  $20 \pm 3$  second time-to-break is recommended (Collier & Epps, 1999). It is helpful to test both wet and dry specimens because water can affect the strength of silk by acting as a plasticizer, penetrating amorphous regions and disrupting hydrogen bonds (Fu, Porter, & Shao, 2009; Pérez-Rigueiro, Elices, Llorca, & Viney, 2002; Yazawa, Ishida, Masunaga, Hikima, & Numata, 2016). It has been shown that increasing the relative humidity to 100% decreases the variability of results significantly, and produces similarly-shaped stress-strain curves between single fibres and yarns of the same material (Ahumada, Cocca, Gentile, Martuscelli, & D'Orazio, 2004).

While a number of studies have been done on the amino acid content and protein structures of *Galleria* silk (Grzelak, Couble, Garel, Kludkiewicz, & Alrouz, 1988; Lucas et al., 1960; Warwicker, 1960; Yang, Teng, Žurovec, Scheller, & Sehnal, 1998; Žurovec et al., 1998, 1992, 1995; Žurovec & Sehnal, 2002), only two studies, to this author's knowledge, have been done on its tensile properties (Fedič et al., 2003; Hepburn et al., 1979). In one study, the silk fibres were collected by sliding a larva down a glass slide tilted at  $30^\circ$  and collecting the resulting silk (Fedič et al., 2003). Fibres several centimetres in length (exact length was not specified) were taped between a weight and a string; the weight was placed on a laboratory balance, and the string was drawn over a pulley at  $37 \mu\text{m}/\text{sec}$  ( $0.037 \text{ mm}/\text{sec}$ ). The force readings were obtained by recording the reduction of the original weight, and the test was stopped after the fibre was broken. Force-extension curves were converted to stress-strain curves using the cross-sectional area of the fibre,  $22.9 \pm 5.5 \mu\text{m}^2$ , as calculated using SEM.

In the other study, silk samples were force-silked (manually drawn) from *Galleria* larvae, and individual fibres were tested on an extensometer fitted with a force transducer (Hepburn et al., 1979). The researchers used a gauge length of 1 mm and an extension rate of 0.0106 mm/sec (no time-to-break was given), which corresponded to a strain rate of 1%/sec. “Dry” tests were conducted in the standard testing conditions of 20°C and 65% relative humidity (RH); “wet” tests were conducted in distilled water at ambient temperature, presumably similarly to the procedures described in ASTM Test Method D3822 (2014), though the method did not exist at the time. Force-extension curves were converted to stress-strain curves using the average cross-sectional area of the fibre,  $1.57 \times 10^{-5} \text{ mm}^2$  ( $15.7 \mu\text{m}^2$ ), as measured using SEM.

*Galleria* silk appears to have different mechanical properties than other  $\beta$ -sheet cocoon silks produced by *A. pernyi* and *B. mori*, and  $\beta$ -sheet dragline (spider) silks from *A. diadematus* and *N. clavipes*, as summarized in Table 2.3.

Table 2.3 Mechanical properties of select silks, adapted from Denny (1980).

Species	Tensile Strength MPa	Extensibility (%)	Reference
<i>Galleria mellonella</i>	750	70 – 101	(Hepburn et al., 1979)*
<i>Galleria mellonella</i>	110	–	(Fedič et al., 2003)*
<i>Bombyx mori</i>	200 – 290	18 – 23	(Perez-Rigueiro et al., 2001)*
<i>Antheraea pernyi</i>	444 – 649	34 – 63	(Fu et al., 2011)*
<i>Araneus diadematus</i>	1080	28	(Madsen, Shao, & Vollrath, 1999)*
<i>Nephila clavipes</i>	1000	20	(Swanson, Blackledge, Beltrán, & Hayashi, 2006)*

\*force-silked

The authors of the more recent *Galleria* tensile paper (Fedič et al., 2003) acknowledge that their results were 6.8-fold lower than that of Hepburn et al. (1979). The suggestion they offer as to

why their results were so different is because of the test method; it is certainly not a common way to run tensile tests, and the results reported were incomplete. As a result, the rest of this section focuses on the other test results summarized in the table above.

While the tensile strength of *Galleria* silk is less than that of *A. diadematus*, and only marginally greater than that of *B. mori*, its extensibility is very high, which means that based on these results, *Galleria* silk has a high toughness. This high toughness could be due to *Galleria*'s unique protein structure of short crystalline regions separated by short peptide strands, as discussed in section 2.2.3.2. Based on the presence of a viscous component in both the dry and wet tests, it is likely that the peptide strands (amorphous regions) are contributing to the viscoelastic deformation of the silk, as represented by non-linearity in the stress-strain curves; this is especially apparent in the wet curves (see Figure 2.10), where the viscous effects are more pronounced in the presence of water (Hepburn et al., 1979).

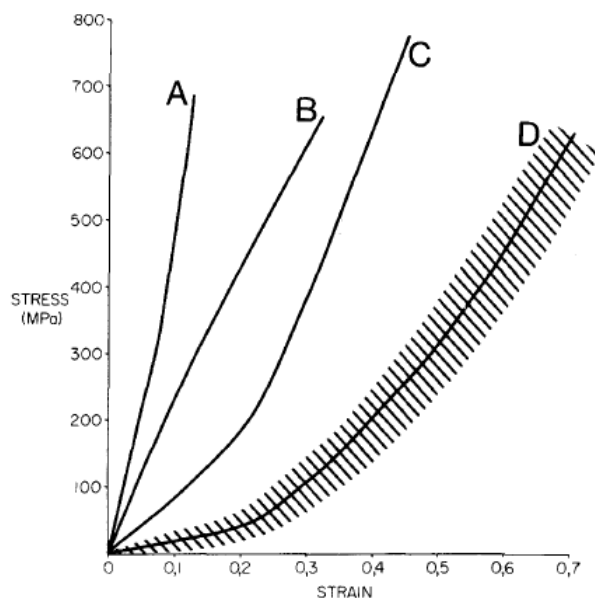


Figure 2.10 Generalized stress-strain curves for select  $\beta$ -sheet silks tested in water at ambient temperature. A = *Anaphe moloneyi* (Notodontidae), B = *Bombyx mori*, C = *Antheraea mylitta* (Saturniidae), and D = *Galleria mellonella*. Reprinted with permission from Elsevier (Hepburn et al., 1979, fig. 1).

Additionally, when exposed to solvents with a high affinity for H-bonds such as urea, lithium thiocyanate, and formamide, the effects on the  $\beta$ -sheet structure of *Galleria* silk are negligible, and do not differ significantly from the results obtained using water (Hepburn et al., 1979).

While the effects are more pronounced on an  $\alpha$ -helical silk and a cross- $\beta$  silk, it is not clear as to whether this result is due to parallel- $\beta$  protein structures in general, or if it is unique to the silk of *G. mellonella*.

The existing body of literature surrounding the tensile properties of *Galleria* silk is sparse and incomplete. Further work is needed to determine if the results from Hepburn et al. are typical for *Galleria* silk, or if the results from Fedič et al. are accurate.

## 2.7 Conclusion

Since the silk industry began nearly 5,000 years ago, silk has been used as a fine garment fabric, for parachutes in WWII, as sutures before synthetic filaments were available, and more recently, as a material of interest in advanced biomedical research studies. Traditionally produced silks such as mulberry, tussah, and eri, are still widely used today, but a range of silks produced by other insects and spiders are being researched due to their unique mechanical properties. Spider dragline silks, for example, are prized for their tensile strength; however, spiders are difficult to rear in captivity for mass production due to their predatory nature. *G. mellonella*, while largely considered a pest, is reared easily in captivity, and has silk that is both strong and elastic due to the selective pressures of its environment, the beehive.

This review has provided an overview of the protein structures of various silks, and how the unique molecular architecture of *G. mellonella* silk affects its mechanical properties. While some work has been done on this silk, these interesting properties certainly warrant closer and more detailed investigation. Future areas of work are numerous, but if this fibre has the potential to contribute to biomedical textile research, the first areas of study should set a foundation for its future use as a textile fibre. This work should include proper rearing and collection techniques, effective degumming procedures, and a more detailed view at other fibre characteristics such as colour, morphology, and mechanical properties.

### 3 Methods

The purpose of this research was to determine effective rearing, collection, and processing conditions for *Galleria* silk, and to test the tensile properties of the silk fibres as extruded by the insect. This research was divided into three parts:

1. Investigation into how silk could be collected for both degumming experiments and tensile tests;
2. Determining if degumming of *Galleria* silk could be performed using conventional methods; and
3. Measuring the tensile properties of *Galleria* silk as extruded by the insect, for the purposes of comparing it to silk produced by other insects and spiders, and other textile fibres.

#### 3.1 Silk collection

Cocoons collected for the degumming experiments were to be as clean and free from frass (insect excreta) and debris as possible. For the tensile experiments, a novel collection method was developed to test single silk baves without force-silking the insect. For each experiment, 6-7<sup>th</sup> instar larvae, approximately 2-3 cm in length, were selected from the main colony for silk collection.

##### 3.1.1 Rearing Conditions

*Galleria mellonella* larvae were reared in the Department of Biological Sciences at the University of Alberta. The larvae were reared in a growth chamber in total darkness at 33°C and were fed an artificial *ad libitum* diet comprised of glycerol, yeast, wheatgerm, honey, beeswax, and water (see Appendix A for diet recipe). Each cohort within the main *Galleria* colony was

housed separately in 650 mL mason jars with metal mesh-lined lids; approximately 200-300 insects were kept per jar (see Figure 3.1). Diet was added to each jar on an as-needed basis, typically three times per week.



Figure 3.1 The main *Galleria* colony housed in mason jars.

### 3.1.2 Cocoon collection

In the main *Galleria* colony, several hundred insects are housed together in a single mason jar. In this environment, the cocoons, feeding tunnel silk, frass, food, and other debris are entangled and difficult to separate. To determine which rearing conditions were best suited for the collection of clean cocoons with minimal amounts of debris, several experiments were conducted. In each experiment, a predetermined number of larvae (see Figure 3.2) were selected from the main colony and placed into another jar. The jar was placed back into the growth chamber for at least five days until the cocoons had darkened, indicating pupation. The cocoons were then collected, cut open with fine scissors, and the pupae with final larval exuvium (shed exoskeleton) removed. The pupae were then euthanized humanely by freezing (see Figure 3.3).



*Figure 3.2* A late (6-7<sup>th</sup>) instar *Galleria* larva, typical of what was used for the experiments in this study.



*Figure 3.3* The empty cocoon (left) after the pupa (centre) and final larval exuvium (right) have been removed.

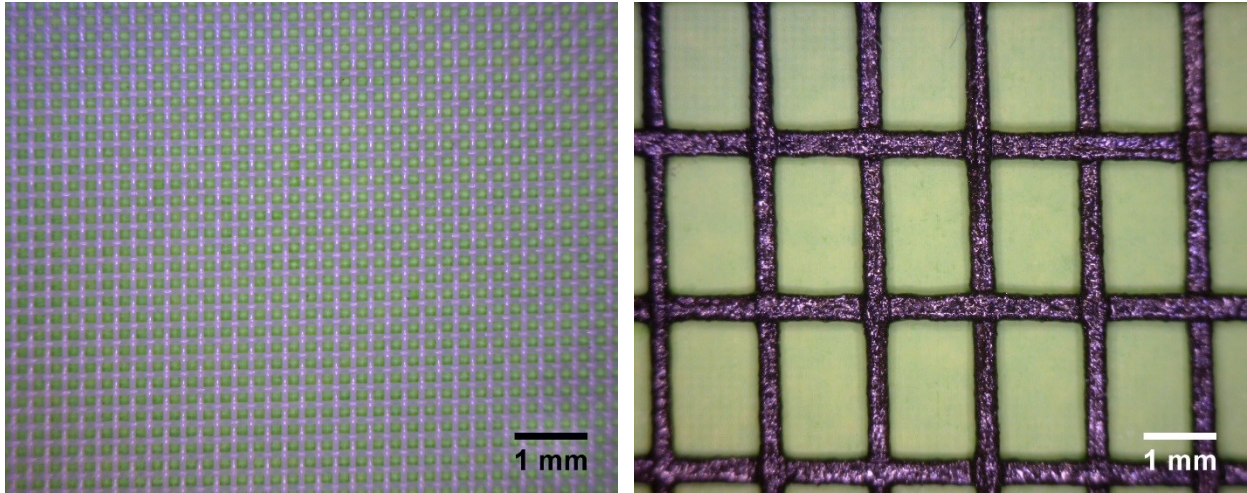
Preliminary experiments showed that when the insects were simply placed into an empty mason jar, the insects tended to construct their cocoons against the glass; this occurrence made the cocoons difficult to remove without inadvertently crushing the insect (Bronskill, 1961), contaminating the cocoons with fat body and haemolymph, and rendering them unusable for degumming experiments (see Figure 3.4). Some researchers use cut plastic straws to handle individual insects more easily, however this is used more when the insect itself needs to be isolated, as opposed to its cocoon (Eischen & Dietz, 1990). Cocoons which were attached to the mesh lid, however, were easily removed clean and intact.



*Figure 3.4* Cocoons formed against the glass of the mason jar (left), and the crushed insect (right) as a result of attempting to remove the cocoon from the glass with forceps.

Initial experiments were conducted to determine whether a small quantity of diet should be included with the larvae so that they might naturally feed to satiation before pupating, instead of artificially forcing pupation due to a lack of food source. Subsequent experiments tested two parameters: the effect of both jar size and mesh size on cocoon production and collection (see Table 3.1). To determine if the volume of the jar used affected the quality of cocoons produced (i.e., separate, clean cocoons instead of several cocoons grouped together due to lack of space), two sizes of mason jar were tested: 250 mL and 530 mL. To determine if the weave density of the mesh used to line the jars had an effect on the quality of cocoons collected, two different

mesh constructions were tested (see Figure 3.5): a white nylon mesh (44 x 44 yarns/cm) and a black window screen mesh (14 x 10 yarns/cm). In each experiment, ten 6-7<sup>th</sup> instar larvae were placed into each jar.



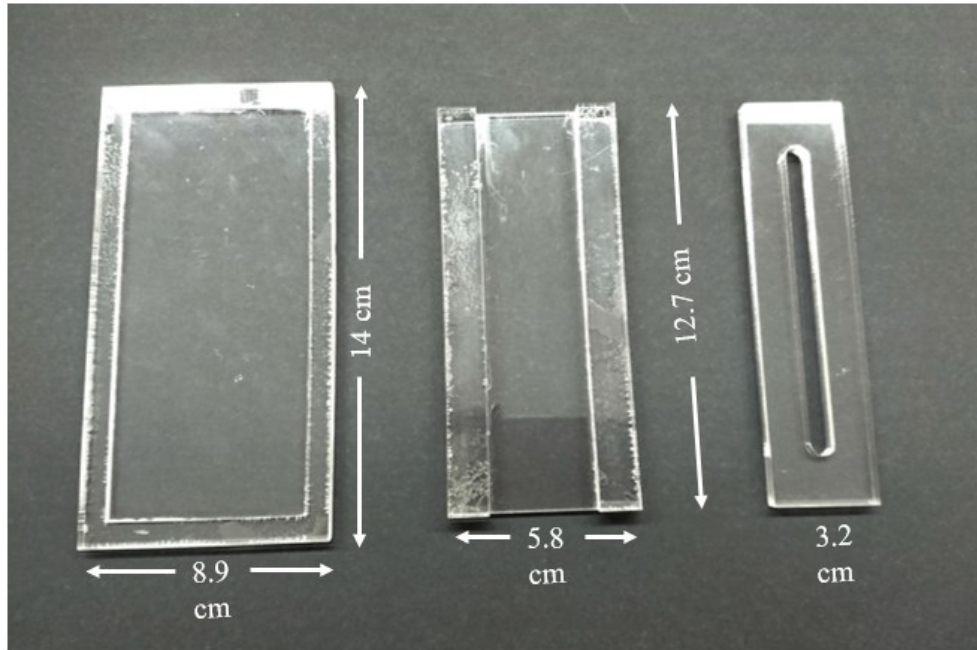
*Figure 3.5* The white nylon mesh (left) and the black window screen mesh (right).

Table 3.1 A visual matrix of the small vs. large jars, and fine vs. coarse mesh.

	Fine mesh (44 x 44 yarns/cm)	Coarse mesh (14 x 10 yarns/cm)
250 mL jar		
530 mL jar		

### 3.1.3 Tensile Specimens

For the collection of tensile test specimens without force-silking the insects, a novel collection method was developed. This method was designed to take advantage of *Galleria*'s tendency to lay a single strand (bave) of silk down as it walks. A clear acrylic holder was designed to hold a paper tab for mounting the fibre and to guide the insect to crawl across the centre of the tab, laying the silk strand down as it walked (see Figures 3.7 and 3.8). The acrylic holder measured 12.7 x 5.8 cm, with a 12.7 x 3.2 cm removable component containing a 0.7cm wide and 0.5 cm deep channel in the centre, with a 14 x 8.9 cm lid (see Figure 3.6).



*Figure 3.6* The acrylic holder with removable component and their dimensions.

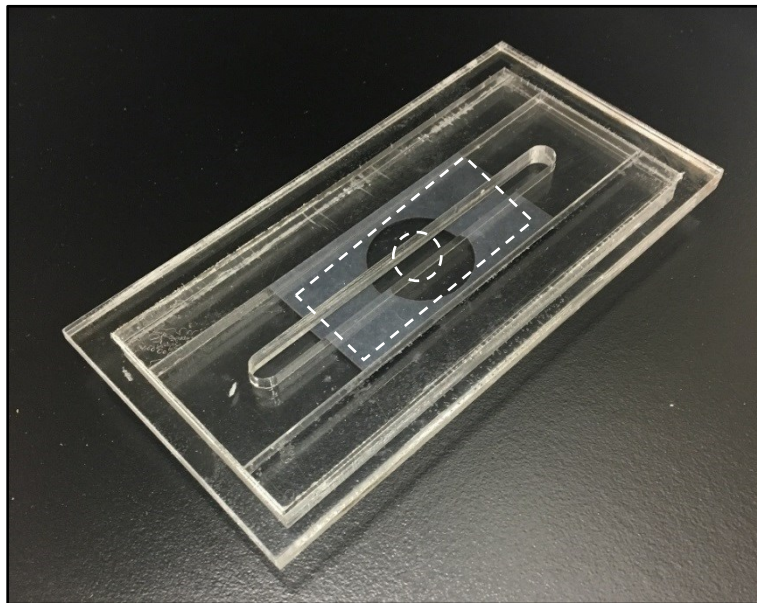


*Figure 3.7* The acrylic holder with a tensile paper tab inside. The black tab shown was an early prototype; white dashed lines show an approximation of the final dimensions of the paper tab.

The paper tab, made from black poster paper for contrast, was first centred and taped to the bottom piece of the holder; the second piece of the holder containing the channel was then placed on top of the paper tab. This assembly, along with the lid of the holder, was placed in a Ziploc® bag, and placed in a water bath at 33°C (Lab-Line Instruments, Inc.) for approximately two minutes to warm the holder. In between collections, the *Galleria* larvae were kept in a petri dish within an unsealed Ziploc bag in the water bath to keep them warm. The holder was then removed, and the insect was placed at one end of the channel and was encouraged to walk across the paper tab by physical stimulus of the insect's posterior end with forceps, if necessary. Once the insect had finished walking across the card, it was carefully removed from the acrylic holder. The channel piece was removed, and the tab was observed for the presence of silk using a Leica WILD M3C dissecting microscope; if present, the silk strand was taped to the card on either end. Finally, small dots of cyanoacrylate adhesive (Adhaero) were carefully placed over the silk strand on each side of the opening in the centre of the tab, adhering the silk to the card more securely and ensuring the accuracy of the gauge length for tensile testing. The prepared tabs were kept in a tray with a cover left ajar for air circulation and allowed to dry for 3-5 hours before being conditioned prior to testing. Tensile specimens were collected from a total of six insects, labelled G1 to G6. From each insect, an extra two or three specimens were collected, reserved, and prepared to be viewed under SEM so that the diameter of the bave could be measured for tensile analysis.



Figure 3.8 The acrylic holder with mounted paper tab and *Galleria* larva walking along the channel.

### 3.2 Degumming

A between-subjects, nonrandomized control group, posttest-only experimental design (Leedy & Ormrod, 2009) was used to determine differences between conventional degumming conditions and their effectiveness at removing the sericin from *Galleria* silk cocoons. The dependent, independent, and controlled variables of the degumming experiments are listed in Table 3.2.

Laboratory experiments were used to measure the following dependent variables:

1. Weight change after the degumming treatment;
2. Visual appearance after staining the cocoons with a sericin-reactive dye, and
3. The visual appearance of the silk under high magnification using scanning electron microscopy (SEM).

The independent variables were the different degumming solutions. The controlled variables were the amount of silk used for each experiment, the degumming procedure, and the staining procedure.

Table 3.2 Dependent, independent, and controlled variables of the degumming experiments.

Variable	Type of Variable	Description
Weight change	Dependent	Comparison of the weight before and after degumming treatment
Visual appearance, stain	Dependent	Appearance of post-degumming treatment cocoons when stained with a sericin-reactive dye
Visual appearance, SEM	Dependent	Appearance of post-degumming treatment cocoons when viewed under high magnification with a scanning electron microscope (SEM)
Degumming solution	Independent	The different solutions used for the degumming treatments: water, sodium carbonate (Na <sub>2</sub> CO <sub>3</sub> ), sodium lauryl sulfate (SLS), and Na <sub>2</sub> CO <sub>3</sub> + SLS.
Quantity of silk	Controlled	Each experiment used 50±1 mg of silk.
Degumming procedure	Controlled	Boiled for 30 min, rinsed, vacuum extracted 5 min, air dried overnight, conditioned at 20 ±2°C and 65 ±2% RH, and weighed.
Staining procedure	Controlled	Prepared solution added to silk, agitated 1 min, rinsed three times and put into the ultrasonic cleaner for 1 min. Blotted, dried overnight.

### 3.2.1 Degumming processes

The cocoons were collected as described in section 3.1.2, grouped according to the insect cohort they were acquired, and placed in a standard textile conditioning atmosphere of 20 ±2°C and 65 ±2% relative humidity (RH) for a minimum of 24 hours prior to each experiment (CGSB Test Method CAN/CGSB-4.2 No. 2, 1988). The cocoons for every degumming experiment were conveniently sampled; cocoons were taken from each cohort group in the order they were

collected, until a sufficient mass had been reached for the experiment. Some experiments had cocoons from just one cohort, while others had cocoons from two or three different cohorts, depending on the number of cocoons available.

The degumming methods were carried out in five different conditions: 1) control (rinse only), 2) water only, 3) 0.2 g/L sodium carbonate ( $\text{Na}_2\text{CO}_3$ ) solution, 4) 10 g/L sodium lauryl sulfate (SLS) solution (Orvus® WA Paste), and 5) a combination 0.2 g/L  $\text{Na}_2\text{CO}_3$  and 10 g/L SLS solution (see Table 3.3). In each condition (not including the control), the silk was boiled for 30 minutes in 100 mL of solution (in a 150 mL Pyrex® beaker) on a Corning PC-35 hot plate and covered with a watch glass. After boiling, the silk was filtered out of the solution by pouring into an 83 mm Büchner funnel with 70 mm P4 filter paper (Fisher Scientific), was rinsed with 100 mL of room temperature (approximately 22°C) reverse osmosis (RO) water and was vacuum extracted for an additional five minutes after the solution had filtered through completely. The treated silk with the filter paper was then transferred to a petri dish with the lid slightly ajar, and allowed to air dry in a fume hood overnight before being returned to a standard textile conditioning atmosphere (CGSB Test Method CAN/CGSB-4.2 No. 2, 1988).

Table 3.3 Experimental conditions of each degumming treatment.

Treatment	Quantity of silk	Solution concentration	Degumming time	Rinse	Extraction
Control	50 mg	n/a	n/a	100 mL room temperature RO water	5 minutes vacuum extraction
Water					
$\text{Na}_2\text{CO}_3$		0.2 g/L	30 minutes		
SLS		10 g/L			
$\text{Na}_2\text{CO}_3$ + SLS		0.2 g/L + 10 g/L			

### 3.2.2 Evaluation of effectiveness

The effectiveness of each degumming procedure was determined using both quantitative and qualitative methods. Quantitatively, the cocoons were weighed on a four-point scientific balance (Denver Instrument M-310) before and after the degumming treatment; the silk was weighed independently prior to the treatment and was weighed together with the filter paper after the treatment. The weight of the conditioned, pre-treatment filter paper was then subtracted from the total post-treatment weight to determine the weight of the degummed silk. The percent weight change was calculated using Eq. 3.1, where a negative result would indicate weight loss, and a positive result would indicate weight gain (AT: after-treatment weight; BT: before-treatment weight).

$$\% \text{ weight change} = \left( \frac{AT - BT}{BT} \right) * 100 \quad (3.1)$$

Qualitatively, the effectiveness of each degumming treatment was visually assessed using optical and scanning electron microscopy. After determining the degummed weight of the silk, it was separated from the filter paper and placed into approximately 20 mL of RO water for five minutes to pre-wet the silk for easier dyeing. Pre-wet silk was removed from the water, blotted with a Kimwipe®, and placed into a 50 mL Pyrex® beaker. Initial staining experiments were done by boiling the cocoons for one minute in a 0.5% mass/volume solution of C.I. Direct Red 80 (Knott et al., 1983), but this step was found to have a moderate degumming action on the silk which would interfere with degumming evaluation (see Appendix B). Instead, five to seven drops of a prepared 1% solution of C.I. Direct Red 80 or Sirius Red dye (Sigma-Aldrich) were dropped onto the silk, and a glass stirring rod was used to agitate the silk and dye for one minute (Mahall, 1993). Following the dyeing process, approximately 40 mL of RO water was added to

the dyeing beaker; the silk was stirred for one minute, before being transferred to a 150 mL beaker containing 120 mL of RO water. The silk was stirred for another minute before transferring to another beaker containing 120 mL of water. This final rinse bath was then transferred to an ultrasonic cleaner (LED) for one minute to remove the remaining traces of dye. After the rinsing process, the silk was removed from the rinse bath, blotted, and left to dry overnight in the same way as the degumming experiments.

After staining, each quantity of silk was photographed separately using a Canon PowerShot SD1400 IS digital camera. Additionally, stained samples from the first replication and unstained samples from the second replication were photographed at high magnification using a BK PLUS Lab System macro and micro-imaging system (Dun, Inc.) with Zerene image stacking software. The Canon EOS 6D DSLR camera was equipped with a Canon MPE 65mm 1-5X micro-photography lens ( $f/5.6$  at 1.5x zoom). Representative portions of the stained samples were then prepared for optical and scanning electron microscopy. To prepare for optical microscopy, the silk fibres were placed onto a glass slide with one drop of liquid paraffin mountant oil and covered with a glass coverslip (all from Fisher Scientific); images were taken at 100x and 400x magnification using an Olympus CX31 optical microscope. For both photography and optical microscopy, the extent of degumming was determined by the presence and intensity of the red dye; if the sericin-staining red dye was still visible, that was indicative of incomplete degumming (Mahall, 1993). To prepare for SEM, silk fibres were placed on 12 mm metal stubs (Ted Pella, Inc.) with carbon conductive spectro tabs (Canemco-Marivac) and were given a gold sputter coat (Nanotek SEMprep 2); images were taken at 500x and 1000x magnification using a Zeiss Sigma 300 VP-FESEM microscope. The extent of degumming was determined by the appearance of the

silk fibres – whether they were in brin or bave form – and whether sericin was present, and in what relative quantity.

### **3.3 Fibre Characterization**

As *Galleria* silk has not been used as a textile fibre before, characteristics such as the fibre's morphology, diameter, cross-sectional shape, and its tensile properties must be well understood when considering appropriate processing conditions and end-uses. Collecting this information also serves as a useful tool when comparing these properties to other silks produced by spiders and other lepidopterans, as such data is often reported in the literature, and is required to determine limitations for fibre processing, conversion, and end-use applications (ASTM Test Method D3822, 2014).

#### **3.3.1 Appearance and morphology**

Analyzing a fibre's shape and size using microscopy is often used as the first step towards identification (AATCC Test Method 20, 2013; Nayak et al., 2012). Initial attempts to view *Galleria* silk fibres under the magnification normally used for textile fibres (40-400x) proved to be insufficient to view the fibres in enough detail, even after staining with Textile Identification Stain #1 (Test Fabrics, Inc.) to improve contrast. Subsequent visual analysis was performed by SEM, using the same equipment as described in section 3.2.2. The longitudinal appearance and morphology of both cocoon and feeding tunnel silks was viewed; pieces of silk were cut from a cocoon and placed so that both the inside and the outside could be viewed, and a sample of feeding tunnel silk was taken from the jar containing the same cohort (see Figure 3.9).

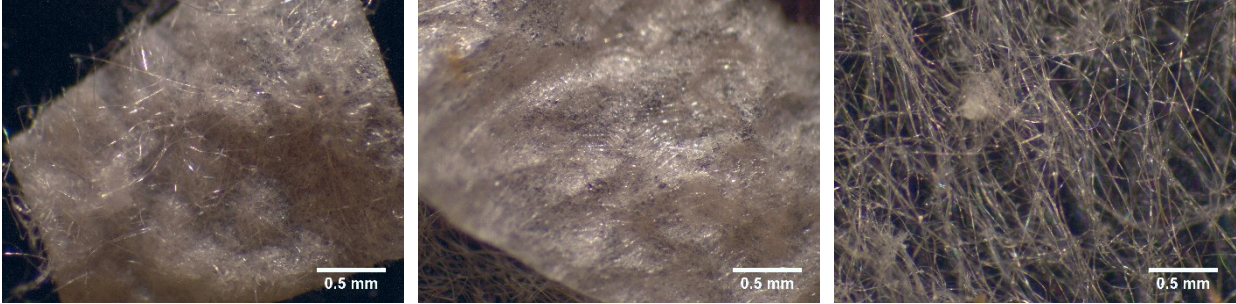


*Figure 3.9* The silk samples mounted on SEM stubs prior to sputter coating. Outside of the cocoon (left), inside of the cocoon (centre), and feeding tunnel silk (right).

The samples were viewed over a range of magnifications, from 100x up to 1000x, and qualitative observations were recorded regarding the fibres' appearance and morphologies. Cross-sectional shape, area, and diameter measurements were taken as described in the next section.

### **3.3.2 Cross-section and diameter**

In order to accurately convert measured force-extension curves to engineering stress-strain curves, a formula was developed to estimate the cross-sectional area of a silk bave based on its diameter—this approach was a new innovation over assumptions of simple geometry found in the literature. A piece of cocoon was cut with a scalpel and #10 blade, mounted on 12 mm metal stub (Ted Pella, Inc.) on-end with double-coated ½” copper conductive tape (Canemco-Marivac, see Figure 3.10), and was given a gold sputter coat (Nanotek SEMprep 2); images were taken at 6000x magnification using a Zeiss Sigma 300 VP-FESEM microscope.

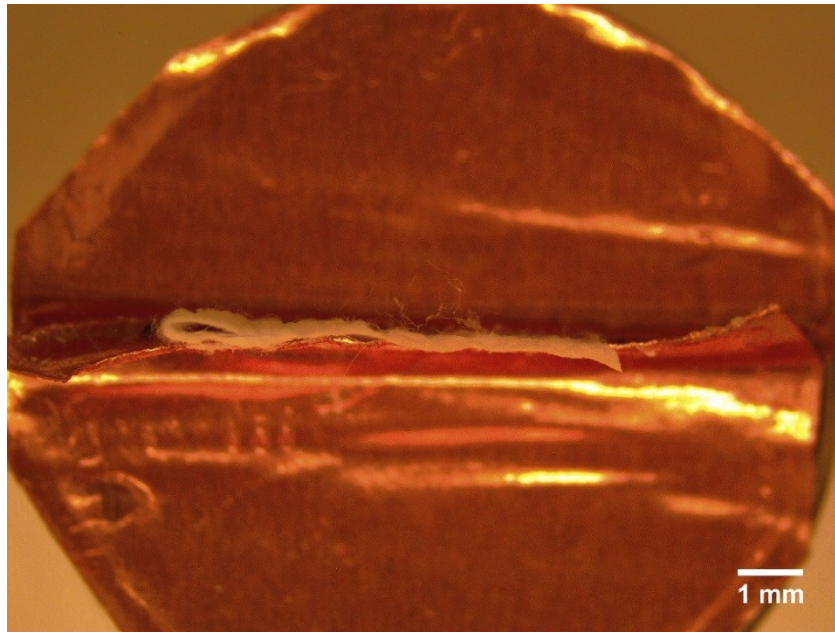


*Figure 3.10* The piece of cocoon mounted on-end using copper conductive tape.

The cross-sectional areas and diameters of all visible baves cut perpendicular to the fibre axis were measured using the ImageJ processing program (National Institutes of Health), and plotted against each other (n=14). It is understood that the observed cross-sections were unlikely to have been exactly perpendicular to the fibre's longitudinal axis, and as a result, some underestimation of the fibre diameters may have occurred (see Figure 3.11).

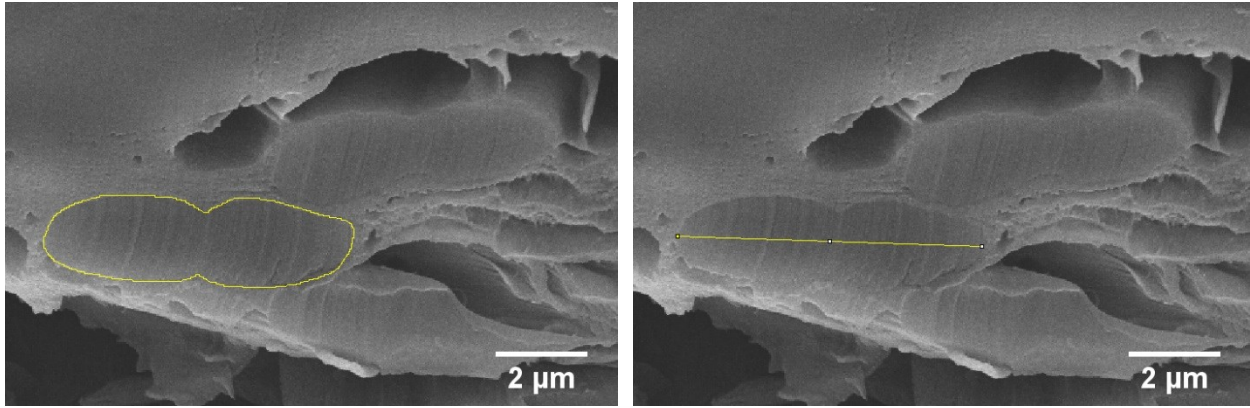


*Figure 3.11* An image of baves in cross-section, as outlined in yellow on the left image. The freeform selection tool was used to measure the cross-sectional area (left), and the line tool was used to measure the diameter (right).

With these data, a geometric model (based on the elliptical shape of the brins) was developed to generate a cross-sectional area formula, where  $A$  = the calculated cross-sectional area ( $\mu\text{m}^2$ ), and  $d$  = the measured diameter of the bave ( $\mu\text{m}$ ) (see Figure 3.12; details of the model development are in Appendix C):

$$A = 0.251327d^2 \quad (3.2)$$

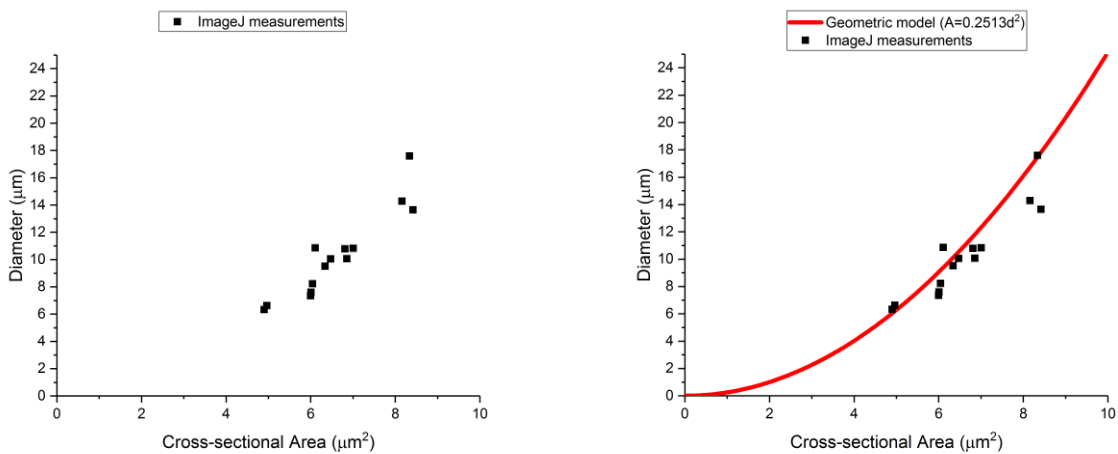


*Figure 3.12* A plot of diameter vs. cross-sectional area measurements, with the geometric model shown in red (right).

The diameter measurements were carried out on prepared tensile specimens, collected from each insect (G1 to G6), which were set aside and not used for tensile tests. Instead, the centre hole of the tensile card was cut out to keep the silk from being stretched or changed while being prepared for SEM. The card ring containing the silk was placed on a stub with carbon conductive tape and prepared as described in section 3.2.2 (see Figure 3.13).

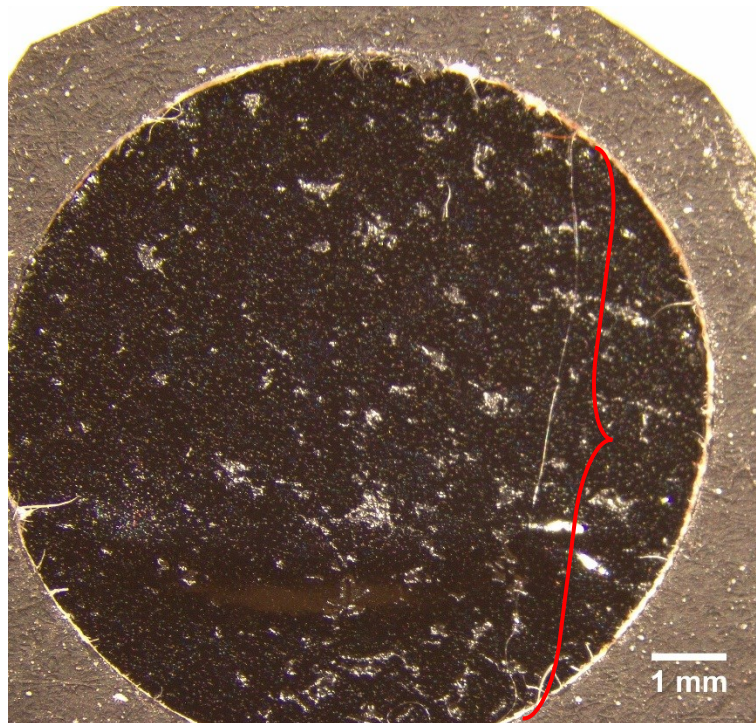


*Figure 3.13* The prepared silk sample mounted on the stub prior to applying the sputter coat. The silk's location is to the left of the red bracket (the single white strand extending vertically).

Images were taken at 3000x magnification along the length of each prepared specimen using a Zeiss Sigma 300 VP-FESEM microscope. Twenty-four diameter measurements were taken along the length of each specimen (ImageJ), one specimen per insect (see Figure 3.14). Care was taken to measure the diameter only where the bave was lying flat, and the medial line, indicating the point where the two brins come together, was centred as much as possible.

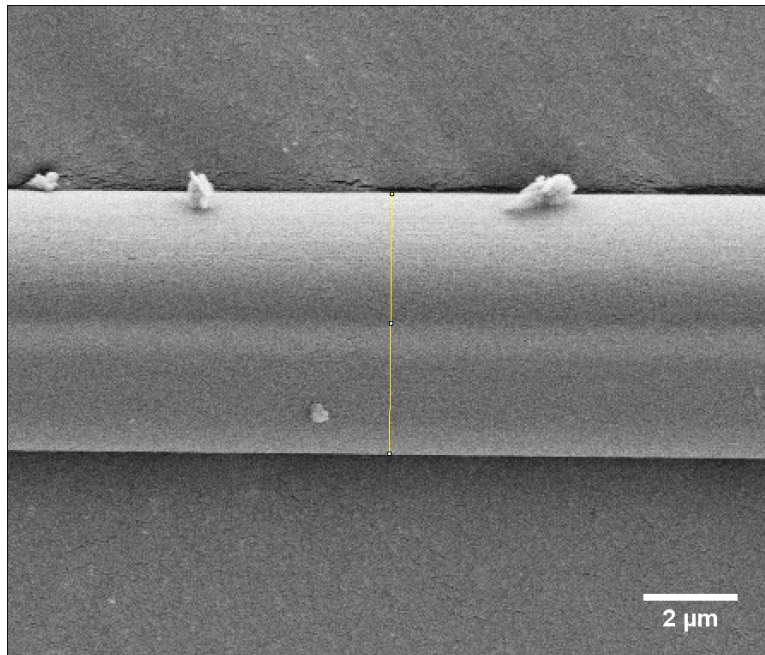


*Figure 3.14* An example of a bave diameter measurement (vertical yellow line) being taken with ImageJ software. The medial line is observable as the horizontal white- and dark-shaded region in the centre of the strand.

An average diameter measurement was calculated for each insect and was used to estimate the cross-sectional area (see Appendix C). This average value was then used to convert the measured force-extension tensile data into stress-strain curves. The measurement of the tensile properties is outlined in the next section.

### **3.3.3 Tensile properties**

Once the silk tensile specimens were collected and prepared as described in section 3.1.2, they were conditioned for  $24 \pm 4$  hours at  $65 \pm 2\%$  relative humidity and  $20 \pm 2^\circ\text{C}$  (CGSB Test Method CAN/CGSB-4.2 No. 2, 1988). The tensile test procedure was based on a standard test method (ASTM Test Method D3822, 2014) with the following modifications: a rectangular paper tab was used measuring 1" x 2" (25.4 x 50.8 mm), cyanoacrylate adhesive secured the

fibre, and a 3/8" (9.5 mm) hole punch (ek tools) was used to set the gauge length (see Figure 3.15).

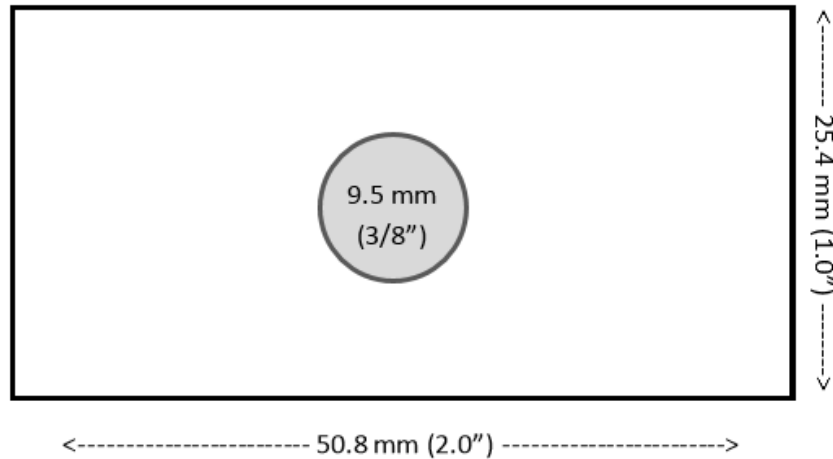


*Figure 3.15* A schematic of the paper tab used for the tensile tests.

The tensile tests were conducted using an Instron 5505 Constant Rate of Extension (CRE) machine equipped with a  $\pm 2.5$  N load cell and its accompanying grips. Each paper tab containing one bave was first placed into the clamps, taking care to align the fibre parallel to the direction of force, and then the sides of the tabs were cut to ensure the only force measured was from the bave itself (see Figure 3.16). Tests were run at a rate of extension of 0.5715 mm/min, which equates to a strain rate of 0.10%/sec. This rate is one order of magnitude less than Hepburn et al. (1979), and approximately equal to Fedič, Žurovec, & Sehnal (2003), when calculating based on an assumed gauge length of 3-5 cm. The tests were run at the standard conditions of  $21 \pm 1^\circ\text{C}$  and  $65 \pm 5\%$  relative humidity (ASTM Test Method D1776, 2008).

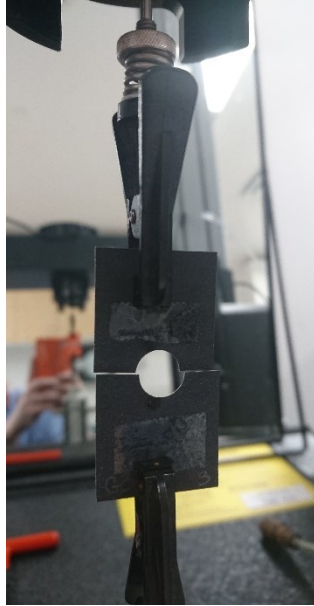


*Figure 3.16* The tensile test set-up showing the paper tab held in the clamps of the tensile tester with the sides cut, ready to be tested.

After measuring the diameter of one bave from each insect as described in the previous section, the calculated cross-sectional area was used to convert the force-extension curves to stress-strain curves. The following equation was used, where  $\sigma$  = engineering stress in MPa,  $F$  = force in mN, and  $A$  = cross-sectional area in  $\text{mm}^2$ .

$$\sigma = \frac{F/1000}{A} \quad (3.3)$$

Young's modulus of elasticity ( $E$ ) was calculated by running a linear regression analysis on the linear portion of each tensile curve (see Appendix D). The slope of the line generated was taken as Young's modulus in GPa. The stress and strain at the elastic limit ( $\sigma_e$  and  $\epsilon_e$ , respectively) were found by determining those values at the elastic limit on the tensile curve. The ultimate tensile strength (UTS) and strain at break ( $\epsilon_f$ ) were found by determining those values at the highest tensile force sustained by the silk fibre prior to break. The specific stress ( $\sigma_s$ ) was

calculated by using Equation 3.4, where  $\sigma_s$  = specific strain (mN/tex),  $UTS$  = ultimate tensile strength (MPa). The exact density of *Galleria* silk is not known, so the assumption was made that it would be similar to that of *B. mori* silk; the denominator is the density of *B. mori* silk as calculated from its specific gravity (Collier & Epps, 1999). Finally, toughness was calculated by finding the area under the engineering stress-strain curve (Origin 2017), resulting in a measurement of J/m<sup>3</sup>.

$$\sigma_s = \frac{UTS}{1.33598} \quad (3.4)$$

### **3.4 Data Analysis**

#### **3.4.1 Degumming**

A one-way ANOVA was used to determine if there was a statistically significant difference between the various degumming treatments and the control. A post-hoc Tukey test was used to determine how each treatment compared to the mean, and to each other.

#### **3.4.2 Tensile tests**

A one-way ANOVA was used to determine if there was a statistically significant difference between insects for the elastic modulus and strain at break. Levene's test for homogeneity of variance was violated for the fibre diameter, UTS, and specific stress, so a series of paired Welch's t-tests were completed to determine how each insect compared to the other for each property.

## 4 Results & Discussion

### 4.1 Silk Collection

#### 4.1.1 Cocoon collection

As discussed in Chapter 3, it was found that the insects tended to construct their cocoons against the glass of the collection jars, making the cocoons difficult to remove without inadvertently crushing the insect (Bronskill, 1961). It was found that cocoons which were attached to the mesh lid of the jar were easily removed clean and intact, which inspired the use of mesh to line the sides and bottom of each collection jar.

##### 4.1.1.1 Inclusion of diet

When a small quantity of artificial diet was added to the pupation jars along with the insects, the larvae created their cocoons within the diet and their frass, rendering the cocoons unusable (see Figure 4.1). As a result, the following silk collection experiments were conducted in mesh-lined jars without diet.



*Figure 4.1* Cocoons formed by the insects within the diet (left, indicated with black arrows); cocoons covered with frass and diet (right).

#### 4.1.1.2 Mesh size

After pupation, differences were observed between the cocoons formed in jars lined with coarse window screen mesh versus fine nylon mesh, regardless of the jar size used. The cocoons formed on the fine mesh tended to have frass and other debris attached to them, while the cocoons formed on the coarse mesh overall had little to no frass or debris attached (see Figure 4.2).



*Figure 4.2* A cocoon formed on fine mesh with frass and debris (left); cocoons, a pupa (indicated with an arrow), and feeding tunnel silk formed on coarse mesh with noticeably less frass and debris (right).

The pieces of frass are larger than the interstices or gaps between the yarns of the fine mesh, making it easier for the frass to be tangled up in the cocoon during formation. The larger interstices of the coarse mesh allowed for the frass to fall through (Bronskill, 1961), limiting the amount that was incorporated into the cocoons. Additionally, cocoon collection was easier with the coarse window screen, as the cocoons were more easily removed due to less surface area contact between the cocoon and mesh as compared to the fine white nylon mesh (Bronskill, 1961).

#### 4.1.1.3 Jar size

When comparing the 250 mL and 530 mL mason jars, no appreciable differences were observed in the cocoons produced. One possibility for this could be due to the narrowing of the top of the 250 mL jars; when lining the jars with mesh, this narrowing did not allow for the mesh to be pressed up against the wall of the jar, as was possible in the 250 mL jars. Because of this, the difference in volume within the mesh enclosure between the small and large jars was less than it would have been otherwise (see Figure 4.3).



*Figure 4.3* The mesh flush with the sides of the small jar (left), and the mesh not flush with the sides of the large jar (right) due to the narrowing at the mouth of the jar.

#### 4.1.1.4 Additional observations

As observed in these trials and when the silk was collected for the degumming experiments, an insect would sometimes pupate without constructing a cocoon (see Figure 4.2 above). One possible explanation is that these insects had already constructed a cocoon or similar structure before being removed from the main colony, and without additional diet, may have depleted the amount of silk they were able to produce and simply pupated without constructing another. In

many cases, it was also observed that the insects continued to produce feeding tunnel silk prior to pupation (see Figure 4.2 above); this silk was gently removed from the cocoons during collection to keep the two types of silk separate.

#### 4.1.1.4.1 Sewing the mesh

Regardless of the size of the mesh or jar used, though it was more common in the larger jars due to the extra space, the insects tended to move in between the mesh and the wall of the jar, pupating against the glass (see Figure 4.4).



*Figure 4.4* The insects moving between the mesh and side of jar after being added (left); cocoons formed up against the glass as a result (right).

To prevent this from happening, the circular and rectangular pieces used to line the glass jars were sewn together to form a single-piece lining for the jar. The top of the lining was then attached to the mouth of the jar using masking tape, so that the insects could not move between the mesh and the side of the jar. Initially this was done with polyester sewing thread (Gütermann Sew-All Thread); it was found that the insects chewed through that thread (see Figure 4.5), so the

end result was the use of coated craft wire which the insects were unable to chew through (see Figure 4.6).

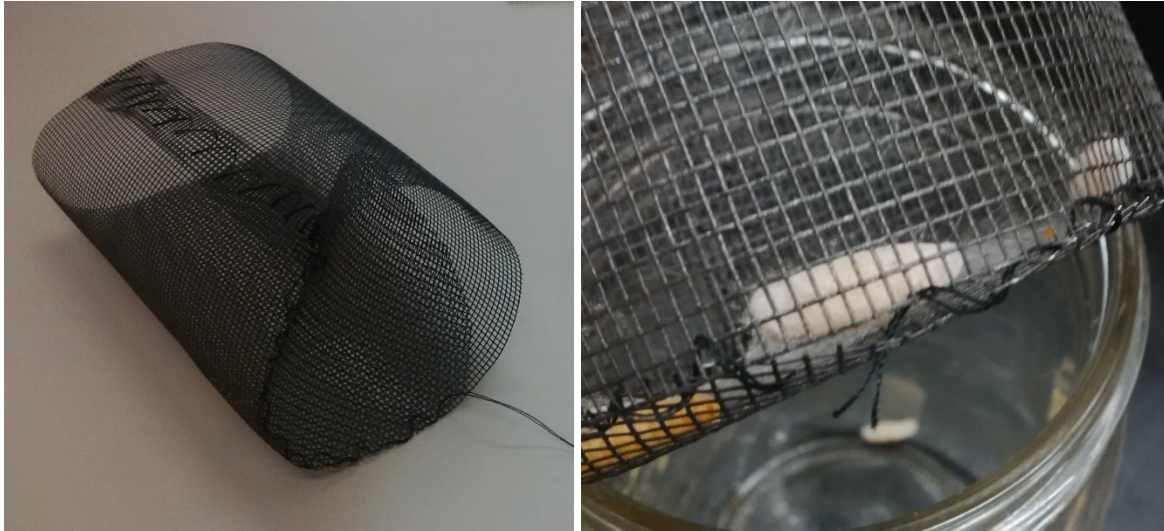


*Figure 4.5* The mesh sewn together with polyester thread (left); the thread chewed through, with a cocoon formed against the glass in the background (right).



*Figure 4.6* The mesh sewn together with craft wire(left); the insects contained within the mesh shortly after being transferred to the pupation jar (right).

#### **4.1.1.5 Final cocoon collection method**

After these experiments, the cocoon collection method used for the degumming experiments was as follows: ten insects were taken from one cohort in the main colony. The insects were then transferred to a 250 mL, window screen mesh-lined jar which was sewn together with craft wire and adhered to the mouth of the jar with masking tape. The cocoons were left to pupate for five days or until the cocoons had darkened (indicating pupation), at which point the cocoons were collected, and the pupae were removed and euthanized. This process was repeated every five days until the required mass of cocoon silk had been collected.

#### **4.1.2 Tensile specimen collection**

Initial collection work was done to determine the most effective use of light, physical stimulus, and warming of the insects to facilitate silk production and collection (see preface). The early collection of tensile specimens was done on cards with a one-inch gauge length; difficulties were encountered with the insects stopping part way through, and with aligning the silk strand on the centre of the card, so the gauge length was reduced to 3/8" (0.95 cm). This reduced gauge length allowed for greater consistency in fibre collection, as the insects were often able to walk over the distance without stopping, which also made it easier to guide the insect so that the fibre was centred on the card. Any specimens which were not centred were labelled and set aside for SEM, where the diameter was measured for cross-sectional area calculations.

During silk collection, in some specimens, the silk appeared to flatten out against the acrylic holder. Upon closer inspection with SEM, it was found that thin sheets of what appeared to be sericin were visible underneath the bave (see Figure 4.7). Visually, it does not appear to have had an effect on the diameter of the remaining bave, and the assumption was made that it did not impact the tensile strength tests due to sericin not contributing significantly to the tensile

capacity in other lepidopteran silks such as *B. mori* (Perez-Rigueiro et al., 2001). Future experiments could investigate the use of a material such as a mesh or pile fabric in between the tensile card and the acrylic holder to perhaps mitigate this occurrence.

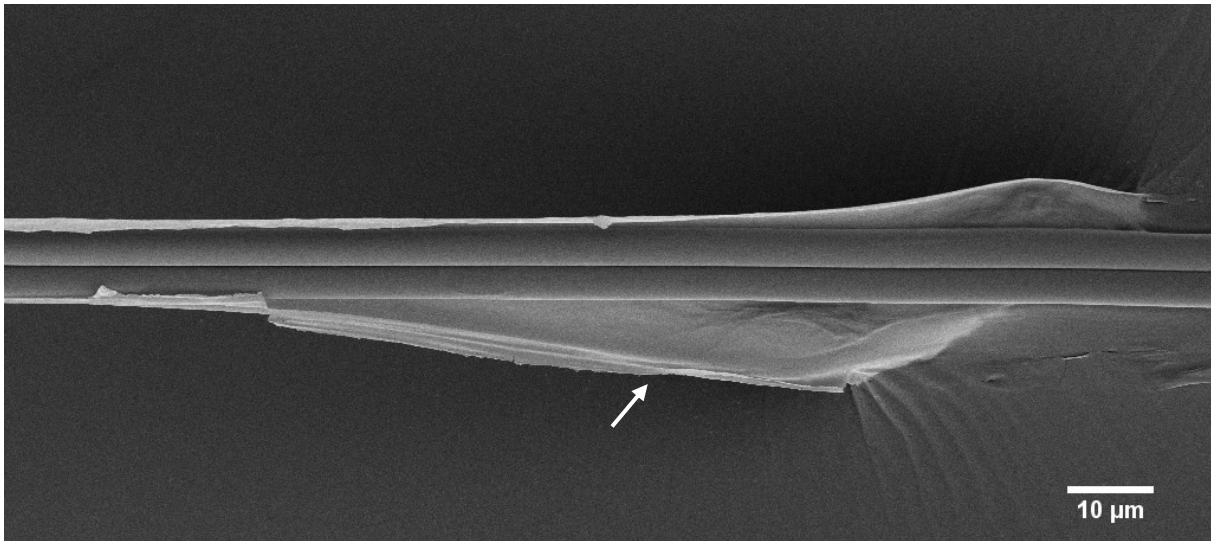


Figure 4.7 A bave with what appears to be a flattened sheet of sericin beneath it (see arrow).

## 4.2 Imaging

To obtain a well-rounded visual characterization of *Galleria* silk and the structures it is made from, macro photography, optical microscopy, and scanning electron microscopy were used.

### 4.2.1 Photography

Initial observations of *Galleria* silk specimens taken from cocoons and feeding tunnel silk were done with high resolution macrophotography. The cocoon, when collected as described earlier in this chapter, was bright white with little debris, and had a dimpled appearance (see Figure 4.8). The cocoon is more torpedo-shaped and translucent than that of *B. mori* (Ganga, 2003), which is usually more rounded and an opaque shade of white (Chen et al., 2012a); this translucency could be a result of the finer silk fibres (Fedič et al., 2003), a reduced quantity of silk in the cocoon

(Jindra & Sehnal, 1989), or both. The length of the continuous filament *Galleria* uses to make the cocoon is not known, but *B. mori*, which has been selectively bred for silk production over thousands of years, are known to produce between 400 and 1500 m cocoon filaments (Rheinberg, 1991). The *Galleria* cocoon also had an opening on one end with four “flaps”, as spun by the insect so that it may exit the cocoon after eclosion (Williams, 1997); this opening would render the cocoon unreelable in commercial silk production (Rheinberg, 1991). Some loose silk fibres, or floss, were visible on the outer surface of the cocoon. Initial observations of *Galleria* silk specimens taken from cocoons and feeding tunnel silk were done with high resolution macro photography. The cocoon, when collected as described earlier in this chapter, was bright white with little debris, and had a dimpled appearance (see Figure 4.8). The cocoon is more torpedo-shaped and translucent than that of *B. mori* (Ganga, 2003), which is usually more rounded and an opaque shade of white (Chen et al., 2012a); this translucency could be a result of the finer silk fibres (Fedič et al., 2003), a reduced quantity of silk in the cocoon (Jindra & Sehnal, 1989), or both. The length of the continuous filament *Galleria* uses to make the cocoon is not known, but *Bombyx mori*, which has been selectively bred for silk production over thousands of years, are known to produce 400-1500 m cocoon filaments (Rheinberg, 1991). The *Galleria* cocoon also had an opening on one end with four “flaps”, as spun by the insect so that it may exit the cocoon after eclosion (Williams, 1997); this opening would render the cocoon unreelable in commercial silk production (Rheinberg, 1991). Some loose silk fibres, or floss, were visible on the outer surface of the cocoon.



Figure 4.8 A photograph of a *Galleria* cocoon, with the dimpled appearance, loose silk fibres on the outside, and the eclosion opening on the end (indicated with an arrow).



Figure 4.9 A photograph of *Galleria* feeding tunnel silk, as collected from the main colony.

The feeding tunnel silk, removed from one jar in the main colony, was also bright white in colour. There was some debris tangled up in the fibres—mainly frass, pieces of diet, and exuviae (see Figure 4.9). Because the larvae are housed in mason jars and not in a bee colony, the silk has a random, cotton candy-like appearance to it, rather than a structured tube or tunnel appearance, as it would have in its natural habitat (Williams, 1997). Due to the random, unreliable structure of the feeding tunnel silk, it would be ideal for spun yarns or nonwoven textiles.

#### 4.2.2 Optical microscopy

Initial observations of the individual silk fibres were made with an optical microscope at 400x magnification. While this level of magnification is adequate to view *B. mori* or tussah silk specimens, *Galleria* silk was too fine to view in any great detail using this technique (see Figure 4.10); indeed, other researchers have found *Galleria* silk to be an order of magnitude finer than *B. mori* silk (Fedič et al., 2003). At this magnification, the structures of the baves are somewhat visible; one can see an outline of the two brins bound together to form the silk strand.

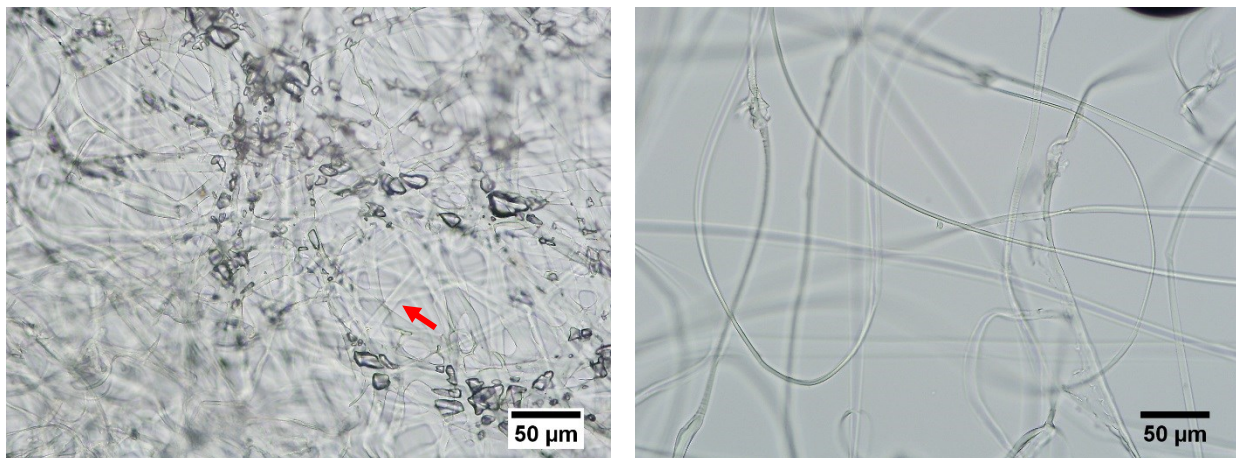
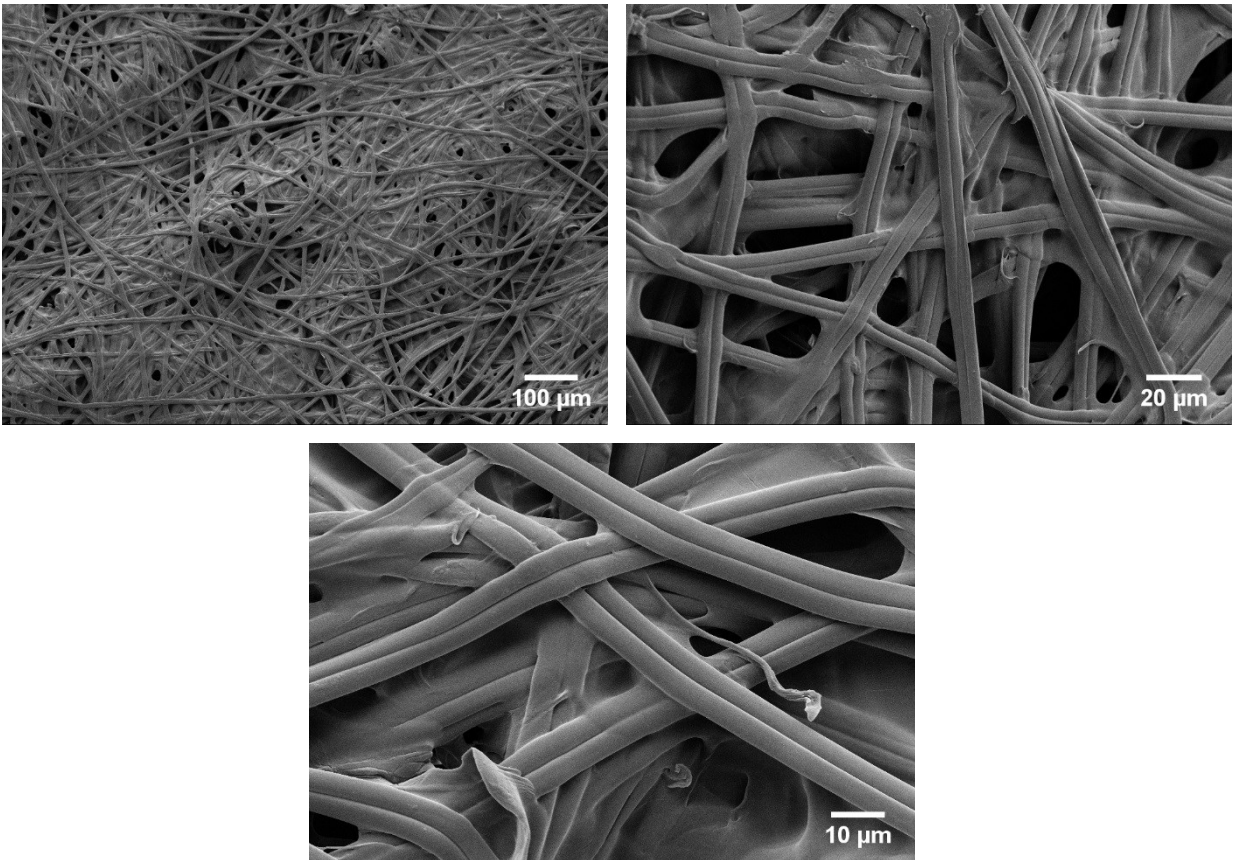


Figure 4.10 Images of cocoon silk (left) with the red arrow indicating a bave, and feeding tunnel silk (right) when viewed with an optical microscope at high magnification.

While the cocoon silk sample had the appearance of a nonwoven fibre web with baves crossing and overlapping each other, the feeding tunnel silk appears randomly tangled and somewhat irregular.

#### **4.2.3 Scanning electron microscopy**

Viewing the cocoon and feeding tunnel silk samples under scanning electron microscopy (SEM) showed much more detail. First, the inside and outside surfaces of the cocoon were viewed. The inside of the cocoon (see Figure 4.11) resembles what was observed with optical microscopy; the baves are seen crossing and overlapping each other (Borujeni et al., 2017; Chen et al., 2012a). The individual brins are more visible, and the sericin is seen, in some areas, as a thin adhesive sheet holding the fibres together, which has also been observed in other lepidopteran cocoons such as *B. mori* (Chen et al., 2012a).



*Figure 4.11* Images of the inside surface of a cocoon viewed under SEM at three different levels of magnification.

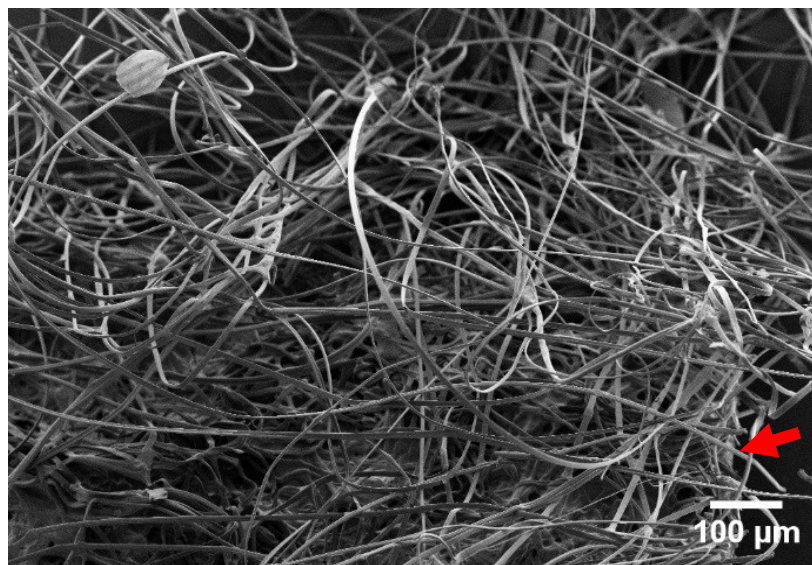


*Figure 4.12* Image of the outside of a cocoon viewed under SEM, with a small portion of the underlying cocoon visible (indicated by an arrow).

The outside of the cocoon appears to be a random tangled web of irregular silk fibres and debris (see Figure 4.12), which would be referred to as the floss in commercial silk production (Babu, 2012); a small portion of the underlying cocoon is visible underneath the floss.

The feeding tunnel silk also resembles what was seen when the silk was viewed under optical microscopy; a random tangle of fibres is visible, where some appear to be discrete, individual strands, and some appear to be adhered together, presumably with sericin (see Figure 4.13). It should be noted that this sample was taken from captive-reared insects, and not from feeding tunnel silk in an infested beehive; it is likely that if feeding tunnel structures were collected and viewed at high magnification, it would appear more ordered than the samples taken from this colony.

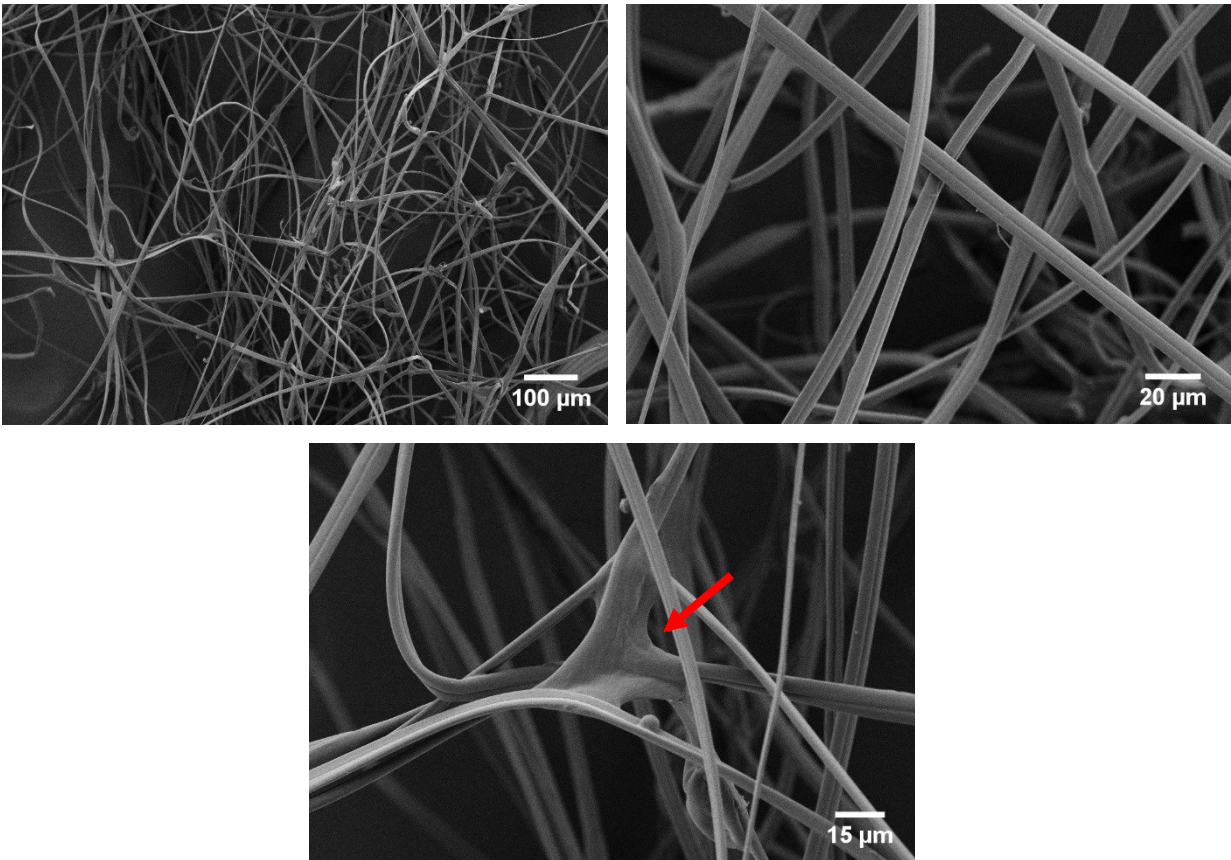


*Figure 4.13* Images of the feeding tunnel silk viewed under SEM at three different levels of magnification; the bottom image shows several silk strands adhered together (see arrow).

When the cocoon was viewed in cross-section, the various crisscrossing layers of silk adhered together by the sericin were more visible (see Figure 4.14). The inside of the cocoon (top of images) shows the same uniform, sericin-coated appearance as the longitudinal views, and the outside of the cocoon (bottom of images) shows the floss fibres not fully incorporated into the cocoon structure. At higher magnification, the outline of the brins can be seen embedded in the sericin matrix. This observation indicates that the sericin is still somewhat liquid after extrusion, and results in adhesion of freshly spun strands as layering progresses. There appears to be more sericin present in the *Galleria* cocoon than has been observed in *B. mori* cocoons (which is supported by quantitative degumming data in section 4.3.1), where the silk fibres are more

loosely held together and can be seen individually in cross-section (Chen et al., 2012a; see Figure 4.15). This loose intra-layer bonding is much weaker than the inter-layer bonding in *B. mori* cocoons (Chen et al., 2012a), which would potentially fall into the “brittle” cocoon category, characterized by strong inter-layer bonding and low porosity, but higher tensile strength (Chen, Porter, & Vollrath, 2012b).

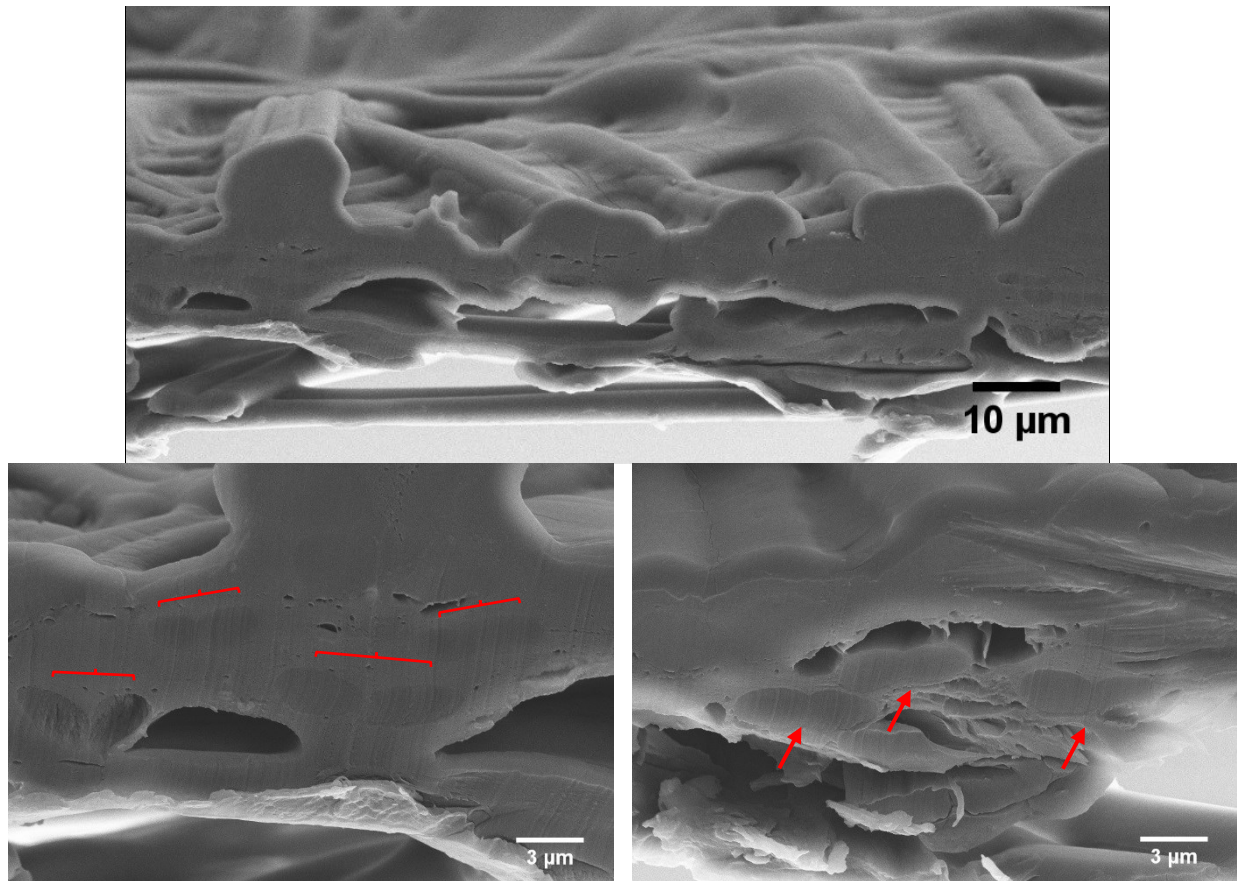


*Figure 4.14* Images of the cocoon in cross-section viewed under SEM at two different levels of magnification (all images: inside = top, outside = bottom). The outlines of the individual brins can be seen (indicated by brackets and arrows) embedded in the sericin adhesive.

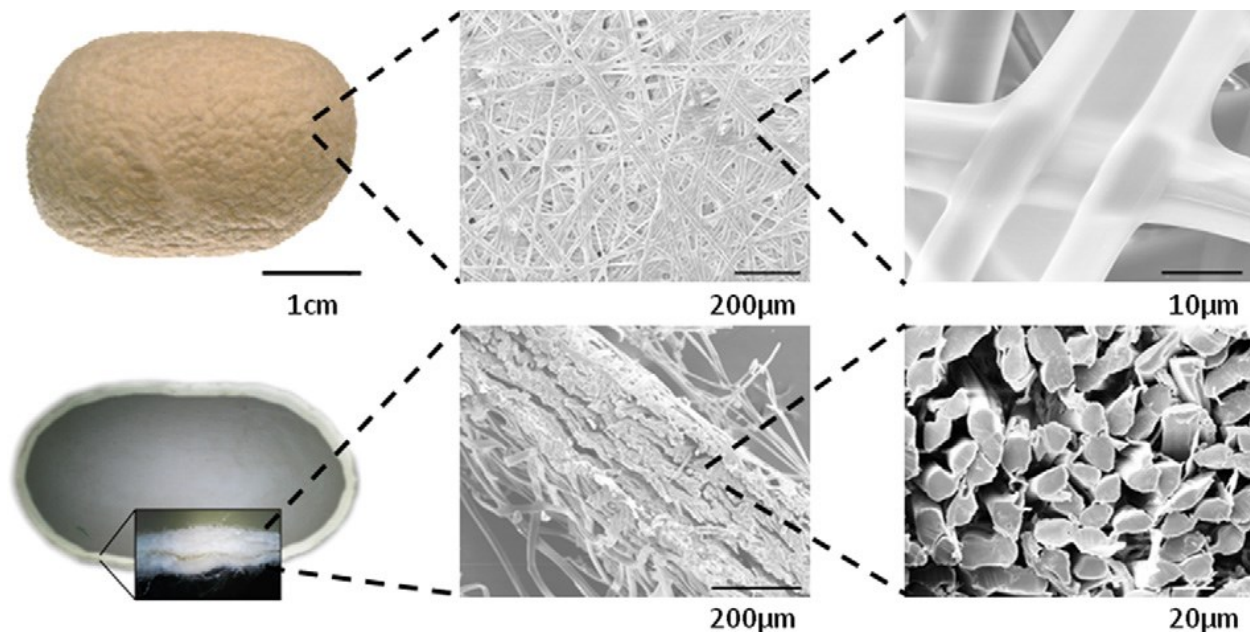


Figure 4.15 Images of a *B. mori* cocoon shown from the outside (top), and in cross-section (bottom). Note the fibres seen individually in cross-section, and not embedded in a sericin layer as seen in Figure 4.41. Reprinted with permission from Elsevier (Chen et al., 2012a, fig. 1).

### 4.3 Degumming

#### 4.3.1 Quantitative evaluation

The quantitative results for each of the degumming conditions are reported below. While the control condition showed a modest increase in weight ( $5.5 \pm 0.85\%$ ), each of the other conditions showed weight loss, indicating that some degree of degumming had occurred (see Table 4.1 and Figure 4.16). As outlined in Appendix B, there was a statistically significant difference between the treatments as determined by one-way ANOVA ( $F(4,10) = 119.606$ ,  $p = 2.12 \times 10^{-8}$ ). A Tukey post-hoc test revealed that when compared to the control, the two most effective degumming treatments were  $\text{Na}_2\text{CO}_3$  only ( $-45.9 \pm 3.12\%$ ,  $p = 0.0$ ) and  $\text{Na}_2\text{CO}_3 + \text{SLS}$  ( $-43.6 \pm 4.4\%$ ,  $p = 0.0$ ), which were found to not be statistically different from each other ( $p = 0.908$ ). The post-hoc test also showed that the water only ( $-22.5 \pm 4.42$ ,  $p = 7.98 \times 10^{-6}$ ) and SLS only ( $-29.7 \pm 2.10$ ,  $p =$

1.44 x10<sup>-6</sup>) treatments were statistically significantly different from the control treatment (albeit less so than the treatments containing Na<sub>2</sub>CO<sub>3</sub>) and were not statistically significantly different from each other (p = 0.128).

Table 4.1 Replication and average weight change results for each degumming treatment.

Replication	Control	Water only	Na <sub>2</sub> CO <sub>3</sub> only	SLS only	Na <sub>2</sub> CO <sub>3</sub> + SLS
1	6.06	-26.68	-45.13	-32.13	-42.26
2	5.99	-17.89	-49.29	-28.32	-48.51
3	4.55	-23.05	-43.20	-28.69	-40.00
<b>Mean (%)</b>	<b>5.5</b>	<b>-22.5</b>	<b>-45.9</b>	<b>-29.7</b>	<b>-43.6</b>
±std.dev.	±0.85	±4.42	±3.12	±2.10	±4.41

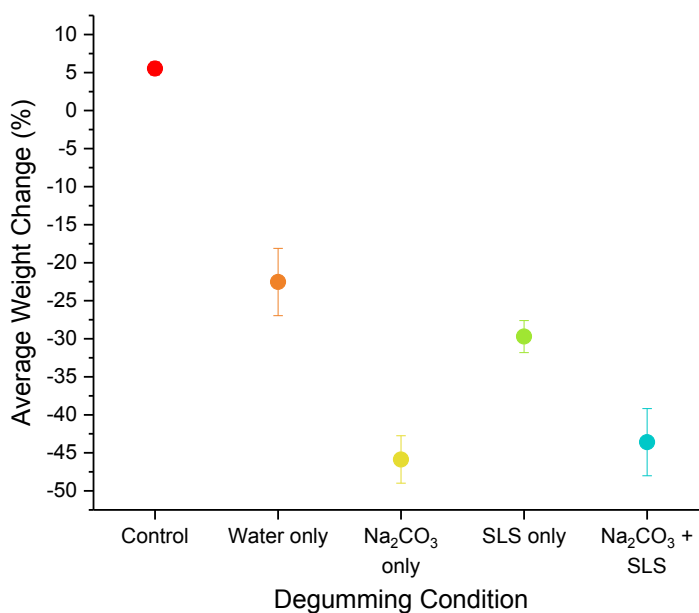


Figure 4.16 The average weight loss of each condition. Error bars represent standard deviation; n=3 for all conditions.

### **4.3.2 Qualitative evaluation**

While the quantitative evaluation gives an idea of the most effective degumming method based on weight change alone, it doesn't show the "quality" or evenness of the degumming treatments. To determine the quality of degumming, each treatment was stained as described in Chapter 3 and observed for the presence and distribution of sericin, and consistency of colour. All of the images shown in this section have been used to produce the comparative image Tables 4.2 and 4.3 in section 4.3.3 for an easier visual comparison between experiment replications and degumming treatments.

#### **4.3.2.1 Control**

After the control treatment (rinse only), the cocoons remained intact and looked no different than how they appeared prior to the treatment. After staining, the cocoons had a largely uniform darker pink appearance, with some darker red areas, indicating that a larger amount of sericin was still present (Nakpathom et al., 2009). When viewed at a higher magnification using an optical microscope, the stained sericin was present throughout. When viewed at an even higher magnification under SEM, the sericin coating can easily be seen where the baves overlap, and the fibres appear to be adhered to one another (see Figure 4.17).

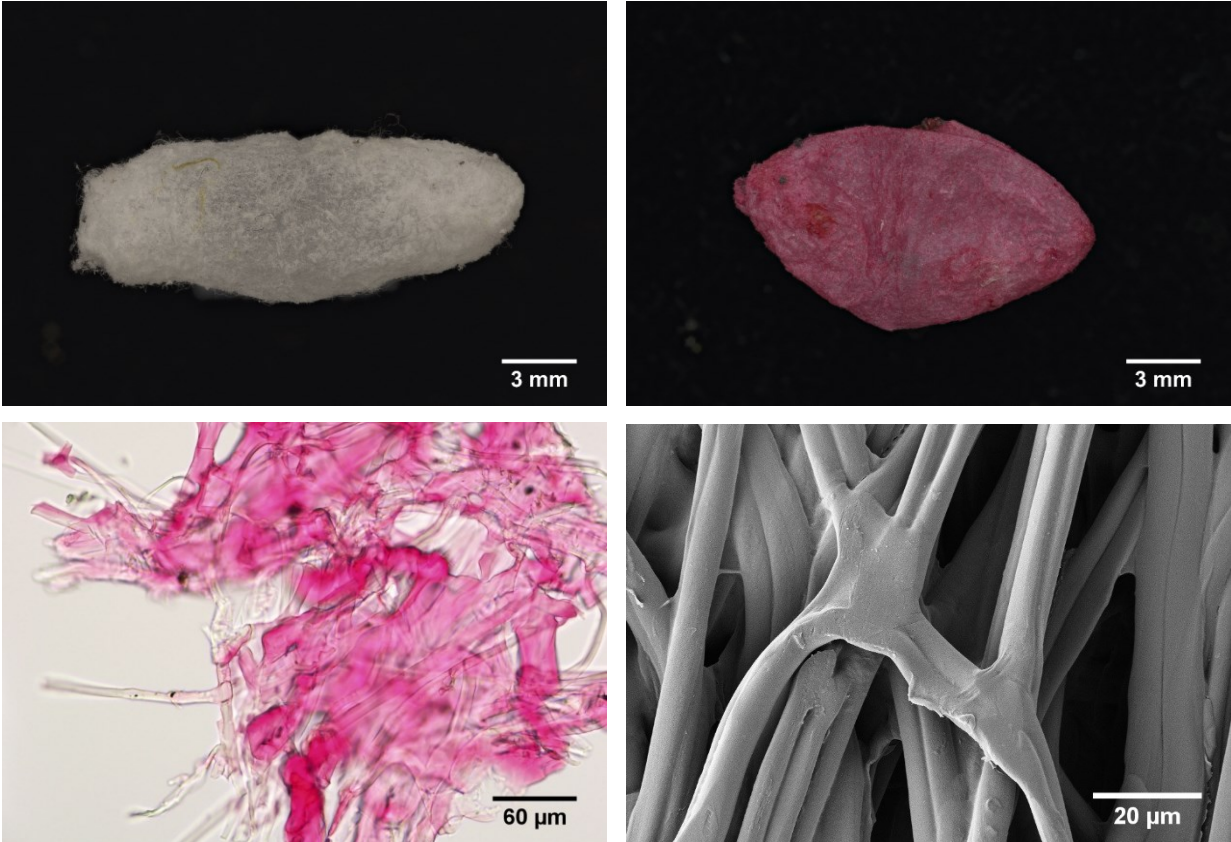


*Figure 4.17* A sample taken from the control group before staining (top left), after staining (top right), a stained sample under the optical microscope (bottom left), and under secondary electron SEM (bottom right).

#### 4.3.2.2 Water only

After the water only treatment, the cocoons remained intact, and had a very similar appearance to the control cocoons. After staining, the cocoons were noticeably more uneven and a somewhat splotchy pale pink, an indication that more sericin had been removed than in the control group (Nakpathom et al., 2009). When viewed with the optical microscope, the overlapping fibres were still visible (as if they were still in the cocoon's structure), but there appeared to be less sericin present; what was present was a paler shade of pink. When viewed under SEM, a tangle of fibres was visible, and appeared to be somewhat less adhered together than the control sample. A bave

was observed to have started separating, and no sericin was visible on overlapping silk fibres (see Figure 4.18).

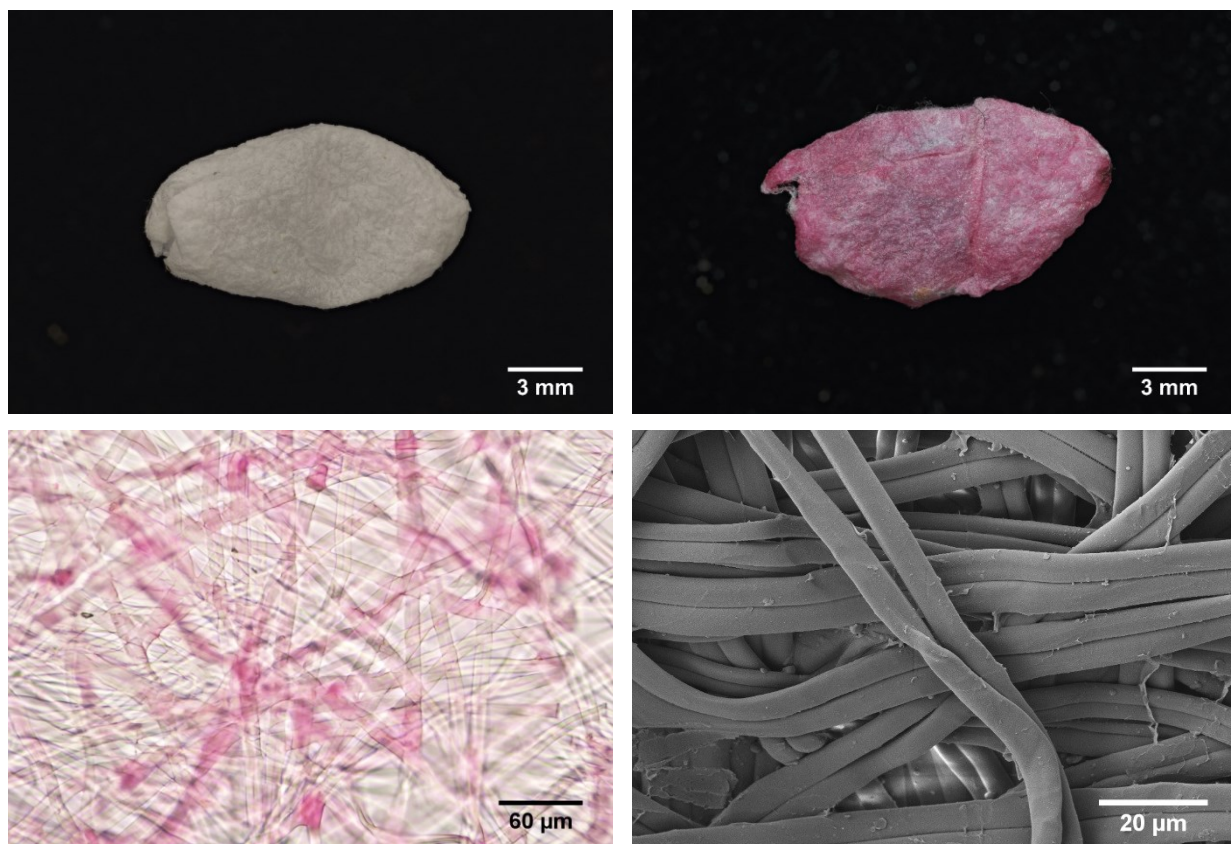


*Figure 4.18* A sample taken from the water only group before staining (top left), after staining (top right), a stained sample viewed under the optical microscope (bottom left), and under secondary electron SEM (bottom right).

#### 4.3.2.3 $\text{Na}_2\text{CO}_3$ only

After completing the  $\text{Na}_2\text{CO}_3$  only treatment, the cocoons had lost their structure (an indication of degumming effectiveness) and a soft tangle of fibres with pieces of frass and exoskeleton remained. When stained, the silk remained mostly pale white with some hints of pink, and some darker pink spots remained visible. When viewed at higher magnification, the darker pink spots resembled the appearance of the control cocoon, while the pale white/pink areas show loose

fibres with much less sericin attached to them. Under SEM, the dark pink area appears as a thick sheet of sericin, whereas the pale area shows looser fibres with no sericin at the fibre overlaps, and brins separating from one another (see Figure 4.19).

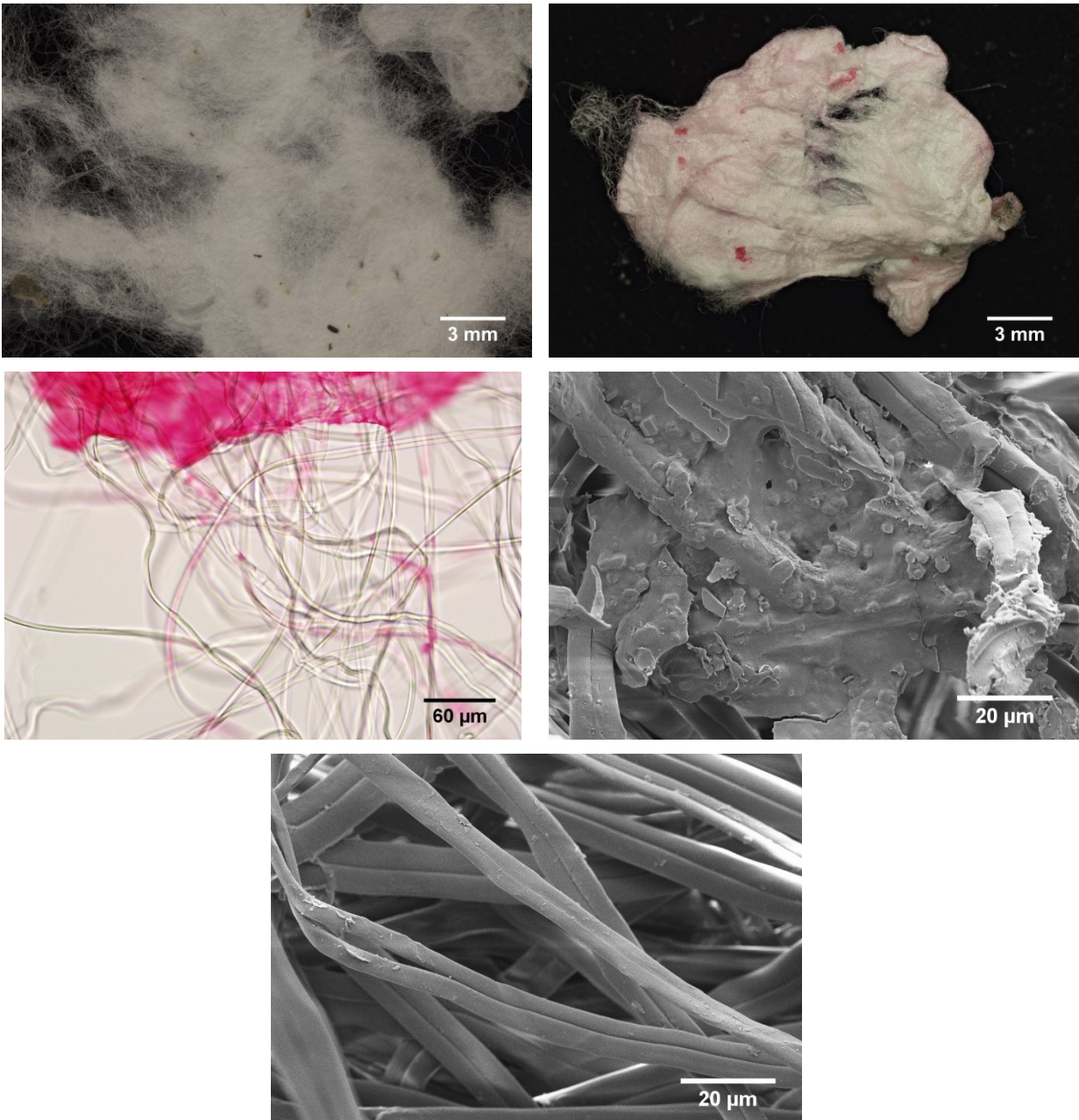


*Figure 4.19* A sample taken from the  $\text{Na}_2\text{CO}_3$  only group before staining (top left), after staining (top right), a stained sample viewed under the optical microscope (middle left), and under secondary electron SEM (thick sheet of sericin: middle right and separating brins: bottom).

#### 4.3.2.4 SLS only

After the SLS only treatment, the cocoons remained intact and looked very similar to the control cocoons. After staining, the cocoons had a largely uniform pink/red appearance, with some uneven areas of white. When viewed with an optical microscope, the pink/red staining was present throughout, with some isolated areas of white where the sericin was no longer present. Under SEM, a substance or coating was visible in the background (presumably sericin) which was holding the baves together; no separated brins were observed (see Figure 4.20).

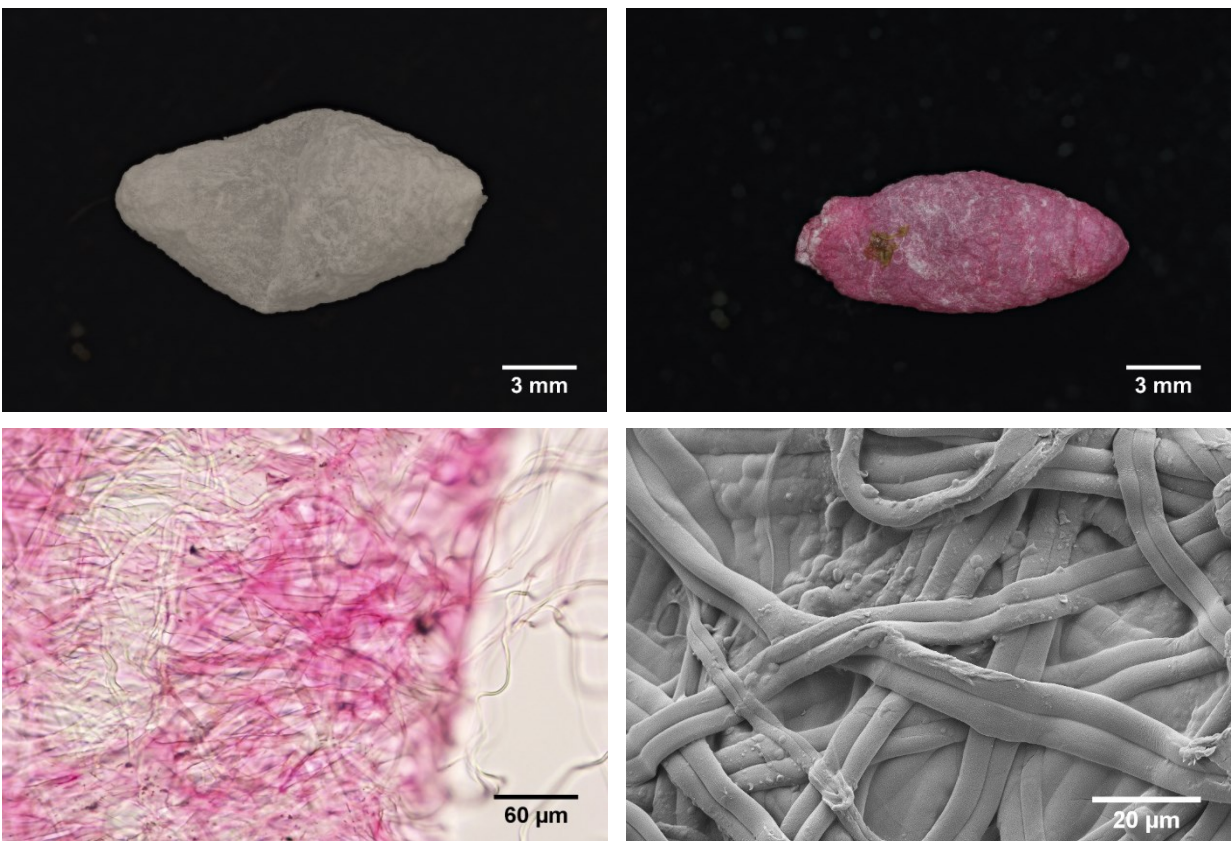


*Figure 4.20* A sample taken from the SLS only group before staining (top left), after staining (top right), a stained sample viewed under the optical microscope (bottom left), and under secondary electron SEM (bottom right).

#### 4.3.2.5 $\text{Na}_2\text{CO}_3$ + SLS

Following the  $\text{Na}_2\text{CO}_3$  + SLS treatment, the cocoons lost their shape and became a tangle of fibres with some pieces of frass and exoskeleton tangled within, which is an indication of degumming effectiveness. After staining, the silk was mostly pale white with some hints of pink, and the darker pink spots observed in the  $\text{Na}_2\text{CO}_3$  only treatment were not present. Under optical microscopy, the fibres were separated and largely white or pale pink, with one or two darker red spots. Under SEM the fibres appear to be separated, not adhered together, with the brins separating from each other (see Figure 4.21).

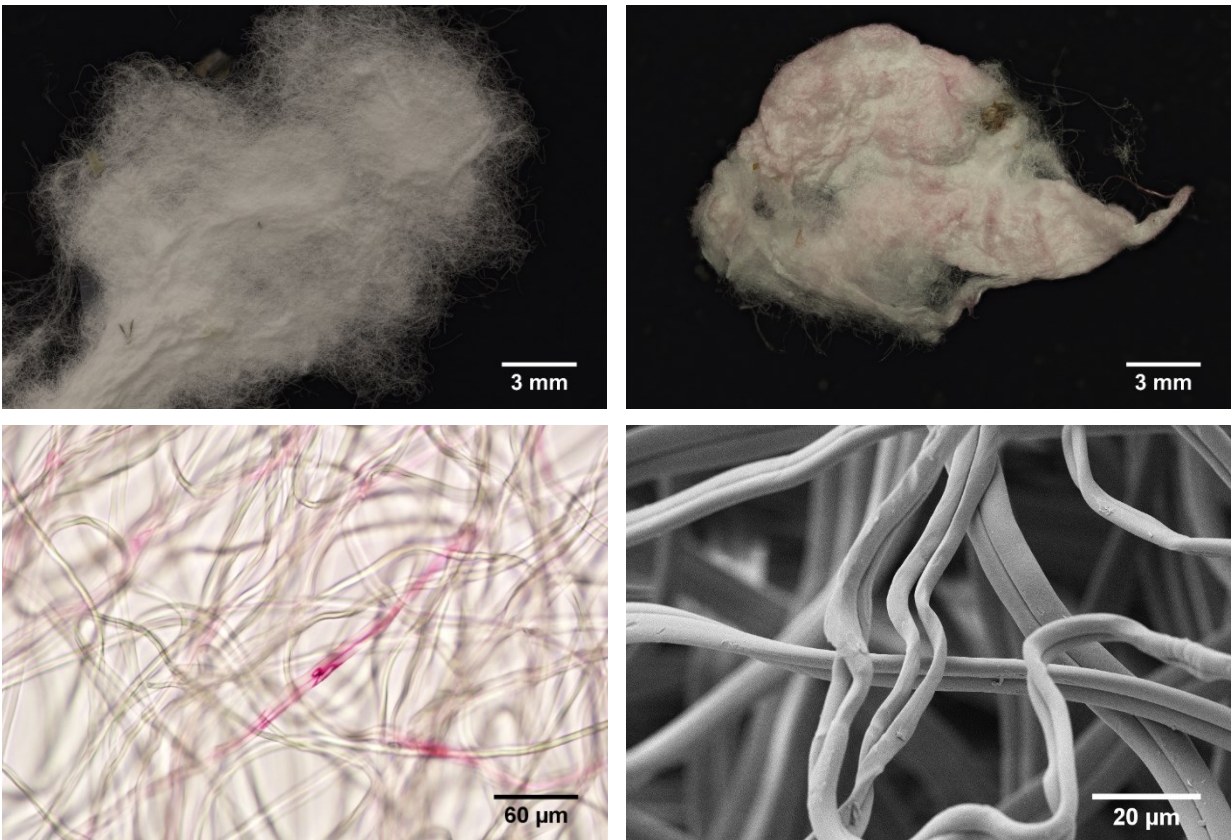


*Figure 4.21* A sample taken from the  $\text{Na}_2\text{CO}_3$  + SLS group before staining (top left), after staining (top right), a stained sample viewed under the optical microscope (bottom left), and under secondary electron SEM (bottom right).

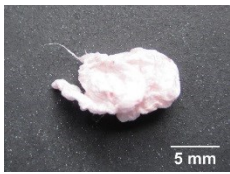
### 4.3.3 Comparative evaluations

It is not known with certainty why the control treatment showed an average weight increase of  $5.5 \pm 0.85\%$ ; one possible explanation is supercontraction, which is a phenomenon that has been observed in another silk that has been compared to spider dragline silk, from *A. pernyi* (Fu et al., 2011). Supercontraction occurs when silk has been exposed to water (which as described earlier in this thesis, can act as a plasticizing agent), and contracts as the inherent residual internal stress within the silk, as a result of being spun or extruded, is released (Bell, 2001). It is possible that this phenomenon also occurs in *Galleria* silk and may have caused the internal secondary structure of the silk to relax slightly, allowing for water to enter the amorphous regions of the fibre more readily, thus increasing the silk's moisture regain. More work is needed to determine whether this phenomenon does occur in *Galleria* silk. Regardless of the reason for the weight gain in the control treatment group, it is assumed that this is a factor in the weight change results for the other groups as well, and as such can still be compared to each other equally.

Water on its own, while a popular degumming method for researchers (Pérez-Rigueiro et al., 2000b), was not an effective degumming method in this study; it is possible that boiling the cocoons for a longer period of time may increase the amount of sericin removed from the silk, but this study identified more effective methods to use within the same amount of time. The SLS only treatment was similarly ineffective; while soaps or surfactants are a common additive to degumming solutions, they are always used in conjunction with an alkaline agent to maintain an effective pH of 9.5-10.5 (Gulrajani, 1992). The pH of the water and SLS degumming solutions were not individually recorded for each experiment but were measured to be approximately 7 during preliminary work.

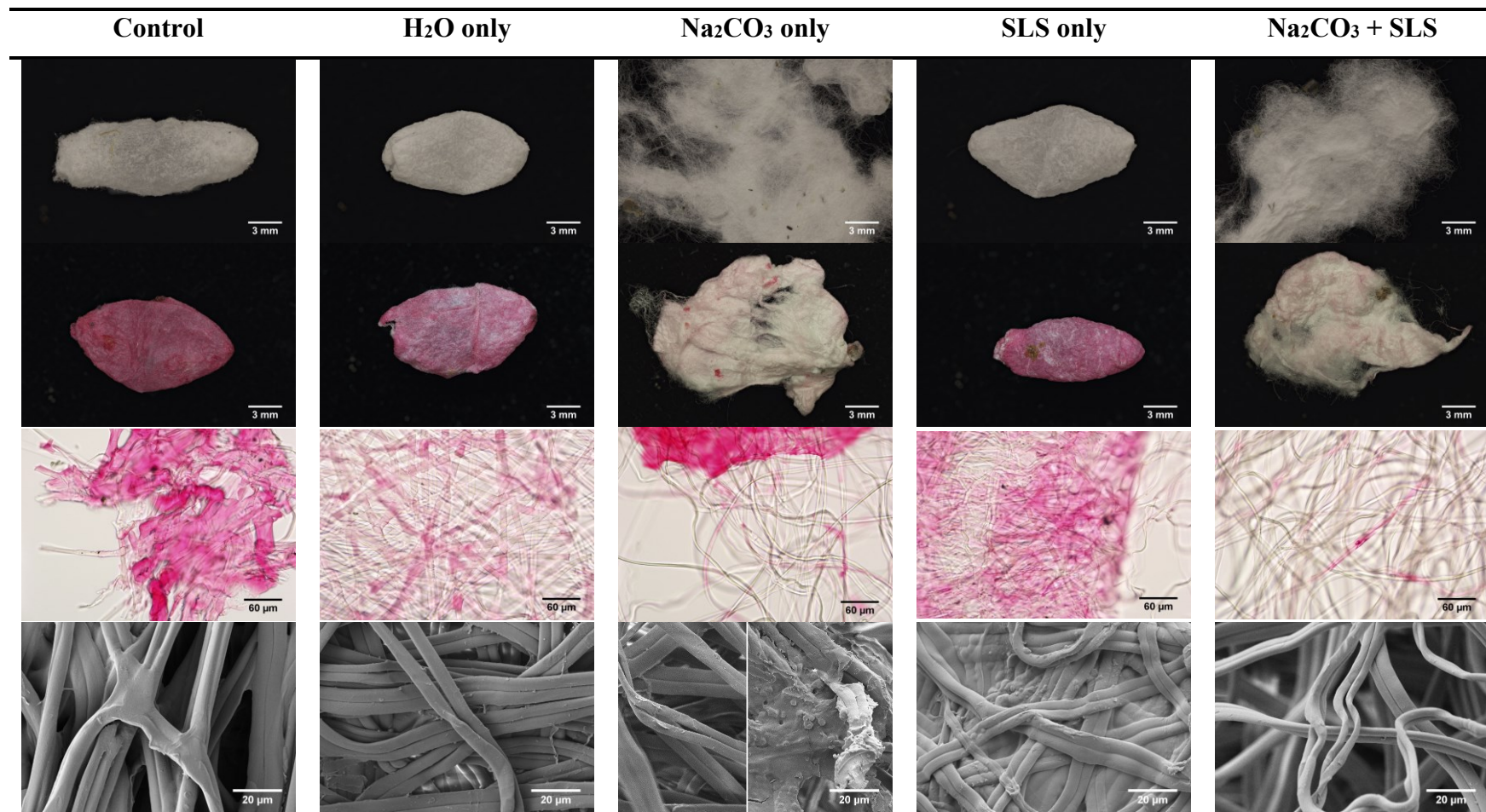
Overall, the two most effective degumming methods, both quantitatively and qualitatively, were  $\text{Na}_2\text{CO}_3$  only and  $\text{Na}_2\text{CO}_3 + \text{SLS}$ . Both degumming solutions were measured to be at a pH of 9, which is slightly below the recommended range, but was evidently still effective. While degumming becomes more effective at higher pH levels, it is well documented that strong alkaline agents can have an adverse effect on the structural integrity of the silk (Gulrajani, 1992; Mahall, 1993). These two treatments removed 42-49% of the overall weight of the cocoons, which is twice as much as the typical *B. mori* sericin content of 20-25% (Mahall, 1993), and three times as much as the typical *A. pernyi* sericin content of <8% (Fu et al., 2009). This is supported visually as well, when one compares photos of *Bombyx* and *Galleria* cocoons in cross-section, as described in section 4.2.3. While statistically the two treatments are not significantly different, the visual comparison shows the quality of the degumming treatment. The  $\text{Na}_2\text{CO}_3$  only treatments left visible regions of sericin still intact, while the addition of SLS seems to have made the degumming more even overall. As SLS is a surfactant, it is possible that its presence allowed for those areas to be wetted out, allowing degumming to occur. More work is needed to optimize the degumming conditions to find the most effective combination of time, temperature, and concentrations of degumming chemicals. Additional experiments could also be done to determine the best degumming method for feeding tunnel silk and its sericin content relative to cocoon silk. Finally it will also be important to determine how degumming treatments affect the tensile strength of *Galleria* silk.

Table 4.2 Photographs of each replication of each treatment after staining.

Rep	Control	H <sub>2</sub> O only	Na <sub>2</sub> CO <sub>3</sub> only	SLS only	Na <sub>2</sub> CO <sub>3</sub> + SLS
1					
2					
3					

All scale bars represent 5mm

Table 4.3 Comparison of all degumming methods. Top row: before staining; second row: after staining; third row: optical microscope; bottom row: secondary electron SEM.



#### 4.4 Tensile tests

While it is relatively common practice to report only the highest, most consistent results in tensile studies (Hepburn et al., 1979), the purpose of this section is to show trends for an entire population of insects to understand the range of values for different tensile properties of *Galleria* silk. This is especially important to understand in a production setting, where knowing the upper and lower limits of fibres' mechanical properties must be known to run production properly.

##### 4.4.1 Diameter and cross-sectional area

The results of the diameter measurements and cross-sectional area calculations for the specimens from each insect are reported in Table 4.4 below. The average diameters of the silk fibres from each insect ranged from 3.1-8.5  $\mu\text{m}$ , resulting in calculated cross-sectional areas of 2.4-18.1  $\mu\text{m}^2$ . When statistically analyzing the diameter measurements, the assumption of homogeneity of variance was violated; a series of paired Welch's t-tests were conducted to assess the statistical significance of any difference in values between insects. The only two pairings which were not statistically significantly different from each other were G3-G4 (G3 =  $3.2 \pm 0.3 \mu\text{m}$ , G4 =  $3.1 \pm 0.5 \mu\text{m}$ ,  $p=0.394$ ) and G5-G6 (G5 =  $3.8 \pm 0.5 \mu\text{m}$ , G6 =  $3.8 \pm 0.8 \mu\text{m}$ ,  $p=0.905$ ); all other pairings had p-values  $<0.001$ .

Table 4.4 Average diameter measurements and cross-sectional area calculations for each insect.

Insect	D ( $\mu\text{m}$ )	A ( $\mu\text{m}^2$ )
G1	$8.5 \pm 0.5$	$18.1 \pm 0.06$
G2	$5.1 \pm 0.4$	$6.5 \pm 0.05$
G3	$3.2 \pm 0.3$	$2.5 \pm 0.02$
G4	$3.1 \pm 0.5$	$2.4 \pm 0.05$
G5	$3.8 \pm 0.5$	$3.6 \pm 0.07$
G6	$3.8 \pm 0.8$	$3.7 \pm 0.18$

D, diameter; A, cross-sectional area.  $\pm$  is standard deviation;  $n=24$  for all conditions.

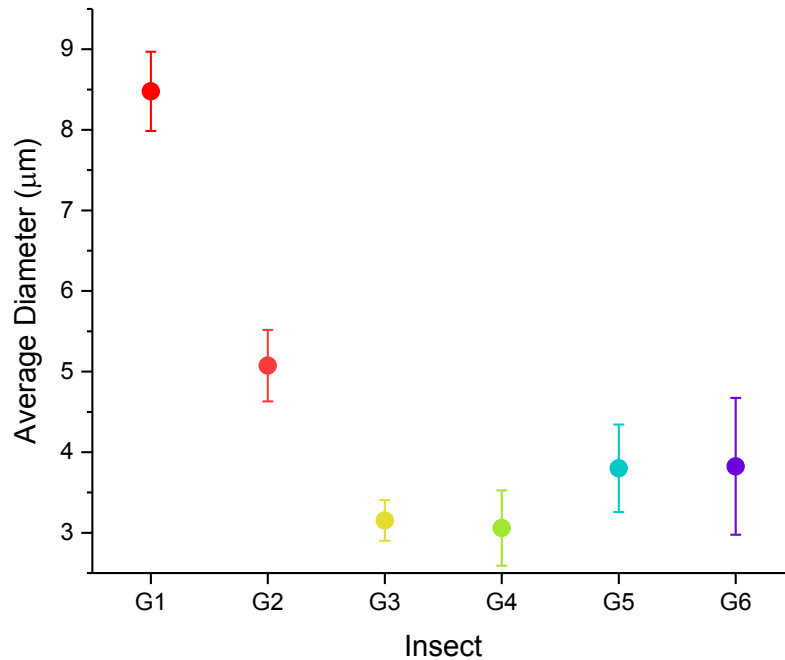


*Figure 4.22* The average diameter measurement for each insect. Error bars represent standard deviation; G1 n=3, G2 n=5, G3 n=4, G4 n=6, G5 n=7, G6 n=3.

While G3-G6 may not all be statistically significantly similar to each other, it is clear that they are more similar to each other than they are to G1 or G2 (see Figure 4.22). One explanation for this could be that, due to experimental timing, G1 and G2 were from different cohorts and G3-G4 were all from the same cohort. This variability could be due to the potential age differences between the three cohorts at the time of collection, or it could simply be differences between the cohorts themselves; more work would be needed to determine the cause.

#### 4.4.2 Tensile properties

A number of tensile properties were measured, calculated, and analyzed, including Young's modulus of elasticity ( $E$ ), stress and strain at the elastic limit ( $\sigma_e$ ,  $\epsilon_e$ ), ultimate tensile strength (mN and MPa), strain at break ( $\epsilon_f$ ), and specific stress ( $\sigma_s$ ). The results of the tensile testing and

analysis for the specimens from each insect are reported below (see Table 4.5); all of the statistical analyses discussed in this section are in Appendix D.

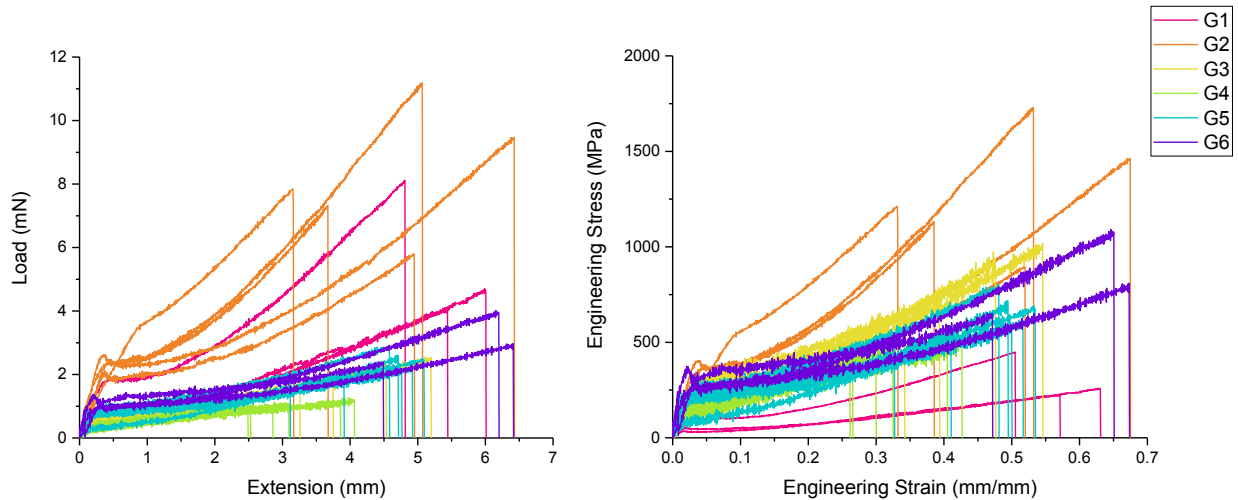


*Figure 4.23* Force-extension curves in mN and mm (left); stress-strain in MPa and mm/mm (right) for the various insects’ silk. G1 n=3, G2 n=5, G3 n=4, G4 n=6, G5 n=7, G6 n=3.

Figure 4.23 shows how force-extension curves change once converted to stress-strain curves by dividing the force by the fibre’s cross-sectional area, as described in Chapter 3. The tensile strengths of some curves increase relative to the others (e.g. G3), others decrease (e.g. G1), and some remain mostly the same (e.g. G2). It is difficult to discern individual curves from one another when they are all super-imposed as they are above, but when they are all separated, while the magnitudes may differ, the shapes of the curves are all largely the same (see Figure 4.24).

On first glance, the shapes are reminiscent of low-carbon steel, where “after the initial stress maxima, the deformation occurs within a narrow band, which propagates along the entire length of the ga[u]ge section before the stress rises again” (Davis, 2004, p. 6).

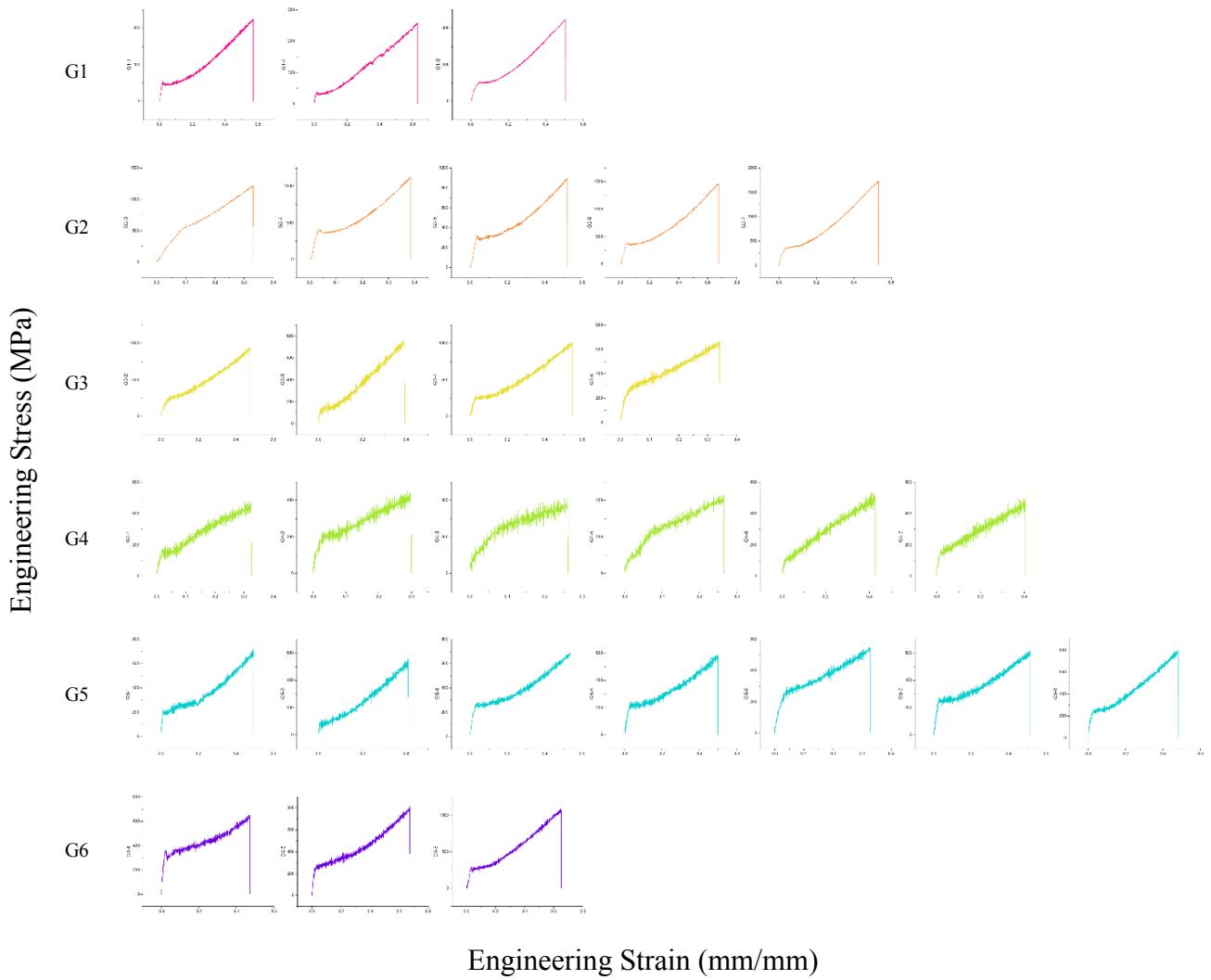


*Figure 4.24* Stress-strain curves for each insect: Engineering stress-strain in MPa and mm/mm. All curves have been scaled to fit their area and are to be compared for shape only. G1 n=3, G2 n=5, G3 n=4, G4 n=6, G5 n=7, G6 n=3.

The initial stress can be seen more easily when looking closer at a selection of representative curves, as in Figure 4.25; here it can be seen that the linear portions of the curves, from which Young’s Elastic Modulus is calculated, vary in slope but share commonalities in terms of shape.

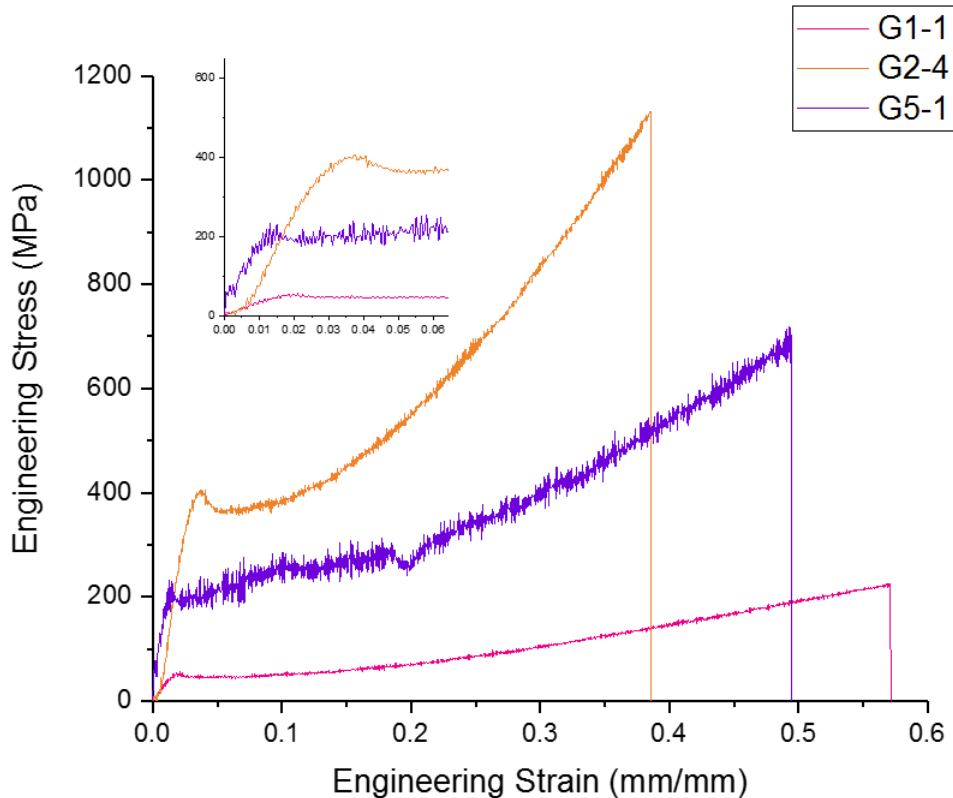


*Figure 4.25* Representative engineering stress-strain curves from three different insects, with a closer view of the linear region of elastic deformation inset upper left; these are the portions of the curves from which Young's Elastic Modulus was calculated.

The values calculated for Young's modulus of elasticity ranged from 3.2-12.6 GPa (see Figure 4.26 and Table 4.5). One feature of note in these and the following tensile results is that the standard deviations for each insect vary widely; the following results show not only inter-individual variability, but intra-individual variability as well. There was a statistically significant difference in elastic moduli between insects as determined by one-way ANOVA ( $F(5,22) = 5.696, p = 0.002$ ). A Tukey post-hoc test revealed that the most significantly different pair was G1-G6 ( $G1 = 3.12 \pm 0.70$  GPa,  $G6 = 12.76 \pm 4.83$  GPa,  $p = 0.006$ ). The next most significantly different pairs were G1-G5 ( $p = 0.011$ ) and G4-G6 ( $p = 0.021$ ). Three most similar to each other

were G2 ( $9.80 \pm 2.99$  GPa), G3 ( $9.67 \pm 3.24$  GPa), and G5 ( $10.70 \pm 2.94$  GPa), with p-values  $>0.99$  for each pairing.

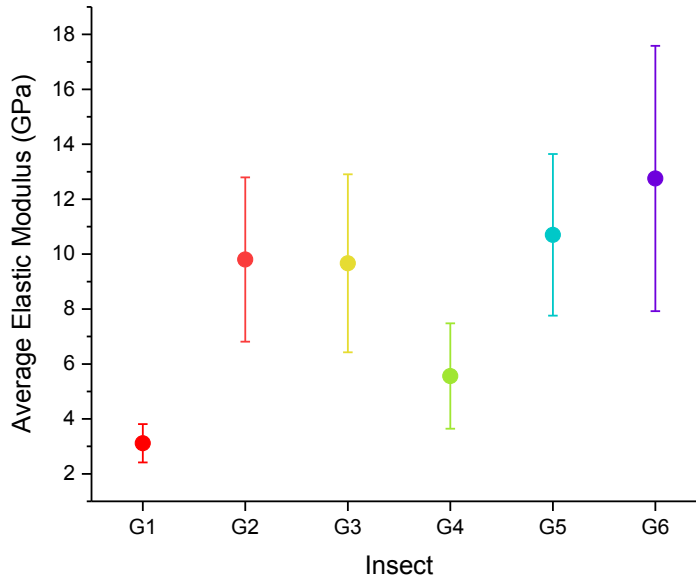


*Figure 4.26* The average Young's modulus of elasticity for each insect. Error bars represent standard deviation; G1 n=3, G2 n=5, G3 n=4, G4 n=6, G5 n=7, G6 n=3.

The values calculated for stress at the elastic limit ( $\sigma_e$ ) ranged from 48.9-364.9 MPa (see Table 4.5). There was a statistically significant difference in  $\sigma_e$  between insects as determined by one-way ANOVA ( $F(5,22) = 11.888$ ,  $p = 1.18 \times 10^{-5}$ ). A Tukey post-hoc test revealed that overall, G2 ( $364.9 \pm 79.1$  MPa) was the most statistically significantly different from all other insects, with p-values  $<0.034$  for each pairing. G1 and G2 were the most significantly different from each other ( $p = 5.86 \times 10^{-6}$ ). The values calculated for strain at the elastic limit ( $\epsilon_e$ ) ranged from 0.014-0.044 mm/mm. There was no statistically significant difference found in  $\epsilon_e$  between the insects as determined by one-way ANOVA ( $F(5,22) = 1.805$ ,  $p = 0.153$ ). Since the values for  $\epsilon_e$  were not

significantly different from each other, this shows that the differences in elastic modulus were attributable to the strength of the fibre.

Table 4.5 Average tensile properties of *Galleria* silk.

<b>Insect</b>	<b>E (GPa)</b>	<b><math>\sigma_e</math> (MPa)</b>	<b><math>\epsilon_e</math> (mm/mm)</b>	<b>UTS (MPa)</b>	<b><math>\epsilon_f</math> (mm/mm)</b>	<b><math>\sigma_s</math> (mN/tex)</b>	<b>Toughness (MJ/m<sup>3</sup>)</b>
G1 (n=3)	3.12 ±0.70	48.9 ±17.1	0.015 ±0.004	308.8 ±120.7	0.57 ±0.06	231.1 ±90.4	83.4 ±23.9
G2 (n=5)	9.80 ±2.99	364.9 ±79.1	0.044 ±0.022	1270.4 ±326.5	0.49 ±0.13	950.9 ±244.4	328.3 ±126.9
G3 (n=4)	9.67 ±3.24	194.0 ±60.7	0.023 ±0.013	835.9 ±166.8	0.44 ±0.09	625.7 ±124.8	203.6 ±67.7
G4 (n=6)	5.56 ±1.92	146.1 ±33.9	0.030 ±0.028	438.1 ±32.1	0.33 ±0.07	327.9 ±24.0	93.5 ±24.3
G5 (n=7)	10.70 ±2.94	188.0 ±57.3	0.018 ±0.010	629.5 ±89.5	0.47 ±0.07	465.1 ±67.0	170.8 ±43.3
G6 (n=3)	12.76 ±4.83	200.7 ±100.8	0.014 ±0.006	822.1 ±229.6	0.60 ±0.11	615.3 ±171.9	292.0 ±79.6

E, Young's modulus of elasticity;  $\sigma_e$ , stress at elastic limit;  $\epsilon_e$ , strain at elastic limit; UTS, ultimate tensile strength;  $\epsilon_f$ , strain at break;  $\sigma_s$ , specific stress. ± is standard deviation.

The values calculated for UTS (mN) ranged from 1.03-8.21 mN. The assumption of homogeneity of variance was violated, so a series of paired Welch's t-tests were conducted to assess the statistical significance of any difference in values between insects. The most significantly different pairing was G4-G5 (G4 = 1.03 ±0.08 mN, G5 = 2.28 ±0.33 mN, p = 3.19 x10<sup>-5</sup>). G2 (8.22 ±2.11 mN) was significantly different from G3, G4, G5, and G6, with p-values <0.004.

The values calculated for UTS (MPa) ranged from 308.8-1270.4 MPa (see Figure 4.27). The assumption of homogeneity of variance was violated, so a series of paired Welch's t-tests were conducted to assess the statistical significance of any difference in values between insects. The

most significantly different pairings were G4-G5 ( $G4 = 438.1 \pm 32.1$  MPa,  $G5 = 629.5 \pm 89.5$  MPa,  $p = 0.00109$ ) and G1-G2 ( $G1 = 308.8 \pm 120.7$  MPa,  $G2 = 1270.4 \pm 326.5$  MPa,  $p = 0.00142$ ), while G3-G6 were the most similar ( $G3 = 835.9$  MPa  $\pm 166.8$ ,  $G6 = 822.1$  MPa  $\pm 229.6$ ,  $p = 0.935$ ).

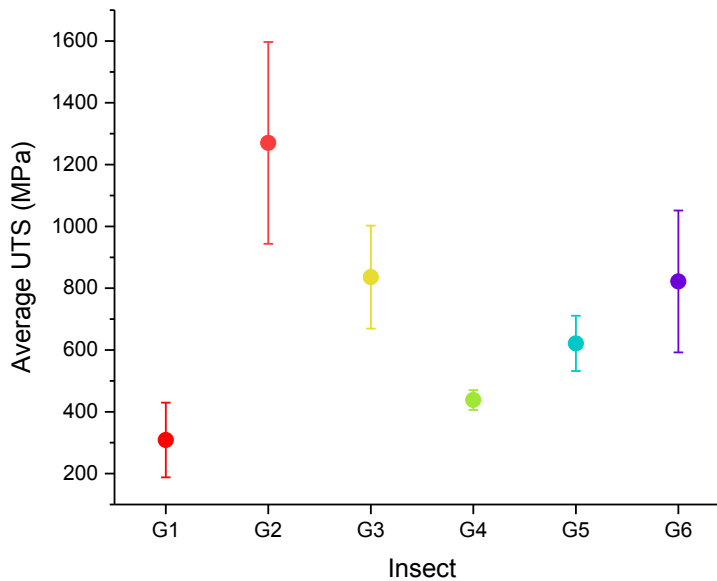


*Figure 4.27* The average ultimate tensile strength (UTS) for each insect in MPa. Error bars represent standard deviation; G1 n=3, G2 n=5, G3 n=4, G4 n=6, G5 n=7, G6 n=3.

The values calculated for specific stress ( $\sigma_s$ ) ranged from 231.1-950.9 mN/tex. The assumption of homogeneity of variance was violated, so a series of paired Welch's t-tests were conducted to assess the statistical significance of any difference in values between insects. The p-values obtained were the same as those for UTS (MPa) above. This result is to be expected, as the values for  $\sigma_s$  were calculated from UTS (MPa).

The values calculated for strain at break ( $\epsilon_f$ ) ranged from 0.33-0.6 mm/mm. There was a statistically significant difference in  $\epsilon_f$  between insects as determined by one-way ANOVA

( $F(5,22) = 1.131$ ,  $p = 0.373$ ). A Tukey post-hoc test revealed that G4 ( $0.33 \pm 0.07$  mm/mm) was the most significantly different from G6 ( $0.598 \pm 0.11$  mm/mm,  $p = 0.005$ ) and G1 ( $0.57 \pm 0.06$  mm/mm,  $p = 0.015$ ), with G1 and G6 being the most similar to each other ( $p = 0.999$ ).

The values calculated for toughness ranged from 83.4-328.3 MJ/m<sup>3</sup> (see Figure 4.28). The assumption of homogeneity of variance was violated, so a series of paired Welch's t-tests were conducted to assess the statistical significance of any difference in values between insects. The most significantly similar pairings were G2-G6 (G2 =  $328.3 \pm 126.9$  MJ/m<sup>3</sup>, G6 =  $292.0 \pm 79.6$  MJ/m<sup>3</sup>,  $p = 0.637$ ), and G1-G4 (G1 =  $83.4 \pm 23.9$  MJ/m<sup>3</sup>, G4 =  $203.6 \pm 67.7$  MJ/m<sup>3</sup>,  $p = 0.582$ ). These pairings show that their toughness was similar, even though the silk came from insects in different cohorts; the diameters may have been more similar between insects G3-6, but interindividual variability is apparent in their tensile properties.

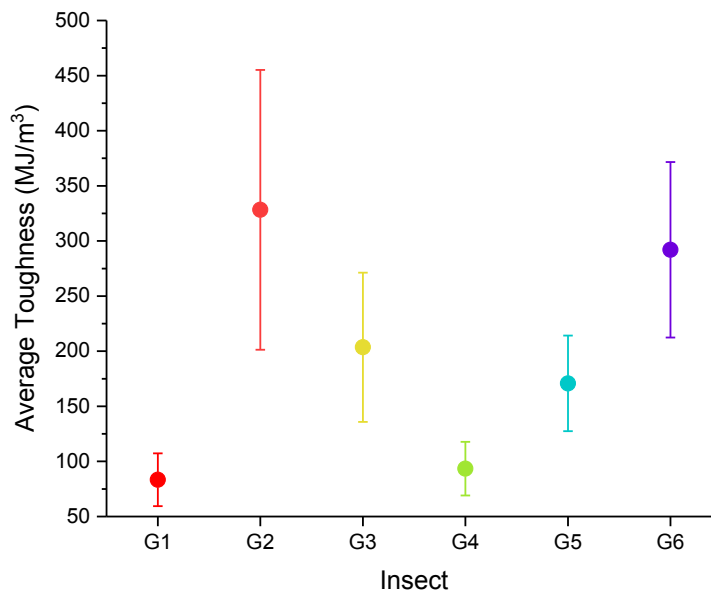


*Figure 4.28* The toughness for each insect in MJ/m<sup>3</sup>. Error bars represent standard deviation; G1 n=3, G2 n=5, G3 n=4, G4 n=6, G5 n=7, G6 n=3.

#### 4.4.2.1 Interpretation of tensile data

While the shape of the tensile curves were the same for each specimen collected, showing a stiff initial elastic region followed by a yield region, followed by further stiffening until failure (Swanson et al., 2006), it is particularly noteworthy that aside from the values obtained for strain at the elastic limit ( $\epsilon_e$ ), the results between insects are highly variable, in some cases even within specimens taken from the same insect. This intraindividual variability can be the result of varying volume fractions of sericin and fibroin from one length of fibre to the next (Madsen et al., 1999), but it is also an artifact of naturally spun silk (Pérez-Rigueiro et al., 2002). During cocoon formation, a silkworm moves its head in a figure-eight or -S motion, bending and stretching its body, and the speed of silk extrusion is often inconsistent (Zhao, Feng, & Shi, 2007). The faster the silk is extruded the narrower the silk diameter can be; in studies of forced-silking, faster reeling yields stronger and more brittle fibres, while slower reeling yields weaker and more extensible fibres (Shao & Vollrath, 2002). This phenomenon is well-understood and used to advantage in the production of synthetic polymers such as nylon 66, where increasing the drawing speed increases the orientation of the polymer chains within the fibre, which in turn increases the strength and stiffness of the fibre (Hearle & Morton, 2008). It was observed during silk collection that not all of the insects moved at the same speed every time they laid silk down on the fibre testing card; because the silk was not being forcibly collected from the insect, the speed of extrusion could not be controlled and was entirely dependent on the speed of the insect. Through rearing and collection, it was observed that *Galleria* larvae moved fastest shortly after being removed from their growth chamber, and slowed down within a few minutes as they cooled to room temperature; every effort was made to keep the insects warm between specimens collected, but it is possible that the repeated temperature fluctuations caused differences in the

speed at which the larvae laid silk down as they walked across the card. Differences may also have stemmed from the amount of silk the insect had already produced prior to being removed from the main colony; if the volume of raw material contained in the larva's body differed from one insect to another (Zhao et al., 2007), this could have affected the silk's properties, such as diameter and crystallinity.

#### 4.4.2.2 Comparisons to other *Galleria* studies

When comparing results between studies, it is important to proceed with caution, as the test protocol impacts the results obtained from those studies, making a like-for-like comparison difficult. While there is a wealth of literature surrounding traditional apparel and spider silks, very little work has been done on the tensile properties of *Galleria* silk; a comparison of the results from this study and two others can be found in Table 4.6. The UTS measured by Hepburn et al. (1979) from force-silked specimens falls right in the middle of the range measured in this study, but showed greater strain at break; these results are most comparable to those measured from G6, which had an average UTS and strain at break of  $822.1 \pm 229.6$  MPa and  $0.60 \pm 0.11$  mm/mm, respectively.

Table 4.6 Average tensile properties of *Galleria* silk compared to results from other studies.

Species	UTS (MPa)	$\epsilon_f$ (mm/mm)	Source
<i>G. mellonella</i> (measured)	308.8 – 1270.4	0.33 – 0.60	This study
<i>G. mellonella</i> (reported)*	750	0.70 – 1.01	(Hepburn et al., 1979)
<i>G. mellonella</i> (reported)*	110	-	(Fedič et al., 2003)

\* force-silked; UTS, ultimate tensile strength;  $\epsilon_f$ , strain at break.

While the reeling speed used by Hepburn et al. (1979) to collect their specimens wasn't specified, from these data it may have been somewhere between the fastest and slowest speeds of the *Galleria* larvae laying down their silk in this study.

When compared to the results of Fedič et al. (2003), their results are substantially lower than what was measured in this study. It is hard to say exactly why this may have occurred, as the tensile test method employed was not described in detail (parameters such as reeling speed, diameter, gauge length, and rate of extension were not provided). It is likely that the method used to measure the force imparted on the silk was at least in part responsible for this difference. Future work would be needed to try their collection method with a more widely used method of measuring fibre strength to determine if that was the cause.

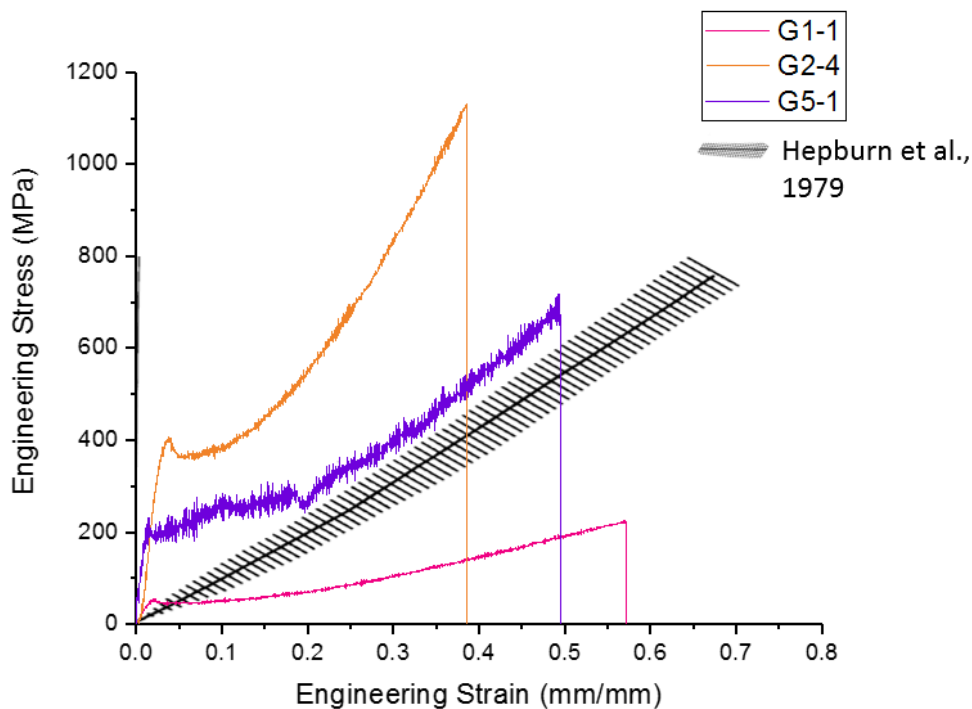


Figure 4.29 The generalized stress-strain curve of *Galleria* silk superimposed upon the tensile curves from Figure 4.25. Reprinted with permission from Elsevier (Hepburn et al., 1979, fig. 1).

Qualitatively, the shapes of the curves between this study and the Hepburn study look quite different (no curves were provided by Fedič et al.), though Hepburn et al. (1979) only provided generalized stress-strain curves (see Figure 4.29). Based on the shape of the Hepburn et al. curve, the silk may have been stretched during collection, inadvertently causing the elastic deformation and yield area of the curve (as seen in this study) to be drawn out (Pérez-Rigueiro et al., 2002). The cross-hatching, which presumably represents the variability between specimens, suggests that the tests were more repeatable than the naturally spun silks of the current study, which is also an artifact of forced-silking (Pérez-Rigueiro et al., 2002). The researchers noted, however, that the data presented were an average of “at least twelve reproducible curves” which gave the highest values of stiffness (Hepburn et al., 1979, p. 70). It should also be noted that the gauge lengths and rates of extension between this study and Hepburn et al. (1979) were different (1 mm vs 9.5 mm, and 1%/sec vs 0.1%/sec, respectively), which could also have contributed to differences in results between the two studies; the smaller gauge length in the Hepburn study may have reduced the quantity of defects present in a given specimen, for example. As with the UTS values, the balance between strength and elasticity for the samples of the Hepburn study seem to be in the middle of the range seen in the test specimens of this study.

#### **4.4.2.3 Comparisons to other species**

In contrast to the available literature surrounding the tensile strength of *Galleria* silk, there are numerous academic articles related to the mechanical properties of silkworm and spider silks. A comparison of the results from this study with the properties of silk produced by a selection of species can be found in Table 4.7; *B. mori* and *A. pernyi* were selected based on their common use in apparel textiles, and *Araneus diadematus* and *Nephila clavipes* were selected due to their prevalence in silk research, which is largely due to their mechanically strong fibers (Swanson et

al., 2006). When comparing elastic modulus, UTS, and strain at break, the results from this study have a large enough range that comparisons could be drawn to any of the materials listed in the table.

Table 4.7 Average tensile properties of *Galleria* silk from the present study compared to silks collected from other lepidopterans and spiders (separated by a line).

Species	E (GPa)	UTS (MPa)	$\epsilon_f$ (mm/mm)	Toughness (MJ/m <sup>3</sup> )	Source
<i>G. mellonella</i> (measured)	3.12 – 12.76	308.8 – 1270.4	0.33 – 0.60	83.4 – 328.3	This study
(average)	8.6	714.4	0.5	195.2	
<i>B. mori</i> (reported)*	12.4 – 17.9	360 – 530	0.18 – 0.23	100.0	(Mortimer et al., 2015; Perez-Rigueiro et al., 2001)
<i>B. mori</i> (reported)†	6.10	208.45	0.20	71 – 103	(Cheung et al., 2009; Malay et al., 2016)
<i>A. pernyi</i> (reported)*	10.2 – 10.9	444 – 649	0.34 – 0.63	60 – 79	(Fu et al., 2011; Malay et al., 2016)
<i>A. diadematus</i> (reported)*	6.90	1080	0.28	160	(Gosline et al., 1999; Madsen et al., 1999)
<i>N. clavipes</i> (reported)*	13.8	1000	0.2	111.2	(Swanson et al., 2006)

\*force-silked; † reeled; E, Young's modulus of elasticity; UTS, ultimate tensile strength;  $\epsilon_f$ , strain at break.

On average, the elastic modulus of *Galleria* silk is in between that of *B. mori* (reeled) and *A. diadematus* on the low end, and *B. mori* (force-silked), *A. pernyi*, and *N. clavipes* on the high end. The average tensile strength of *Galleria* silk is most comparable to that of *A. pernyi*, though on the high end, is even greater than the values reported for some spider dragline silks. The average strain at break (and range, for that matter) is also most comparable to the silk produced by *A. pernyi* and is more extensible than the spider dragline silks reported here. This combination of high strength and extensibility in *Galleria* silk is why the material has such high toughness relative to the other silks, the spider silks most surprisingly.

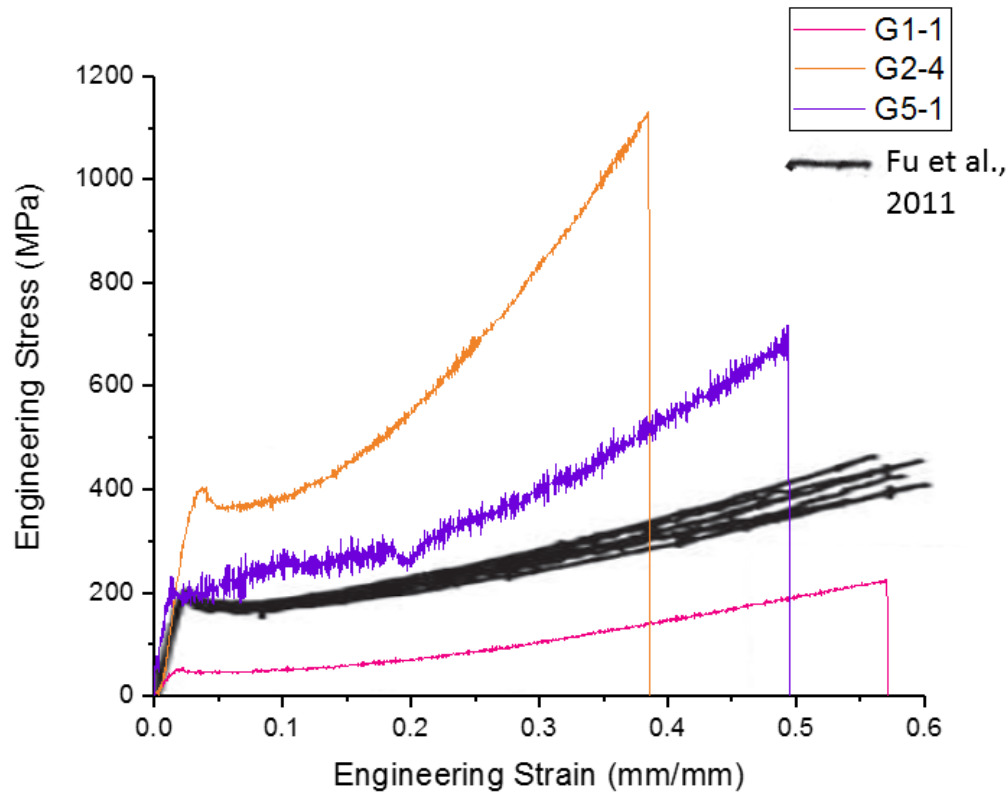


Figure 4.30 The *A. pernyi* stress-strain curves in black, superimposed upon the tensile curves from Figure 4.25. Reprinted with permission from John Wiley and Sons (Fu et al., 2011, fig. 3a).

When comparing the shapes of *Galleria* and *A. pernyi* tensile curves (see Figure 4.30), it is clear that the two silks have similarly shaped stress-strain curves. Qualitatively, the shape of the curves resembles that of Muga silk as well, produced by *Antheraea assamensis* (Rajkhowa, Kaur, Wang, & Batchelor, 2015).

As discussed in Chapter 2, what sets *Galleria* silk apart from other silk materials is its high-molecular-weight and “exceptionally homogenous” H-fibroin structure when compared to the weight and relative variability of *Bombyx* and *Antheraea* H-fibroins (Žurovec & Sehnal, 2002). While *Bombyx* and *Antheraea* silks both possess larger crystalline repeat units which get their strength from overlapping and interacting, *Galleria* silk gets its strength from the precise

matching of its shorter crystalline sections separated by short peptide strands (Fedič et al., 2003; Žurovec & Sehnal, 2002). The crystalline regions within the fibre impart strength and stiffness, while the frequently repeating short peptide strands impart flexibility and extensibility; this unique structure gives *Galleria* silk unique fibre properties when compared to other lepidopterans. This combined requirement of strength (cocoon durability) and elasticity (silk feeding tubes) has likely driven the evolution of the silk in *Galleria*, where one silk fibre is used for more than one purpose (Žurovec & Sehnal, 2002). It is possible that the increased amount of sericin observed in the *Galleria* cocoons earlier in this study is present to help maintain the rigidity of the cocoon while the insect is pupating, because the silk would be less able to perform that need on its own when compared to other lepidopteran silks.

Spider silks are among the strongest polymeric biomaterials known, and have protein structures which must allow a lot of movement in order to exhibit their high toughness and energy dissipation (Gosline et al., 1999). Unlike lepidopteran silks, large amorphous domains are the dominant feature of *A. diadematus* dragline silk, which are primarily responsible for the phenomenon of supercontraction; the crystalline regions present within the fibre are comparatively very short. This network of short crystalline areas separated by long amorphous chains is what is likely responsible for the toughness and viscoelasticity of spider dragline silks. While the base compositions of spider silks are similar to those produced by lepidopterans, they differ in the proportion of amino acids with bulky residues, such as proline. It has been found that silks with lower proline contents tend to be stiffer, likely because of more proline-free and glycine-rich ordered structures. Conversely, silks with higher proline contents tend to be more extensible, which could be a result of the proline interfering with the formation of more highly-ordered structures (Gosline et al., 1999).

Table 4.8 Average tensile properties of *Galleria* silk from the present study compared to silks collected from other lepidopterans and spiders (separated by a line), with proline content.

Species	E (GPa)	Toughness (MJ/m <sup>3</sup> )	Volume fraction proline (%)	Source
<i>G. mellonella</i> (measured)	3.12 – 12.76	83.4 – 328.3	3.2	This study, 1.
(average)	8.6	195.2		
<i>B. mori</i> (reported)*	12.4 – 17.9	100.0	0.3	1, 2, 3.
<i>B. mori</i> (reported)†	6.10	71 – 103		
<i>A. pernyi</i> (reported)*	10.2 – 10.9	60 – 79	0.2	1, 5, 6.
<i>A. diadematus</i> (reported)*	6.90	160	16	7, 8.
<i>N. clavipes</i> (reported)*	13.8	111.2	3	7, 9.

\*force-silked; † reeled; E, Young's modulus of elasticity; UTS, ultimate tensile strength;  $\epsilon_f$ , strain at break. 1: (Žurovec & Sehnal, 2002); 2: (Mortimer et al., 2015); 3: (Perez-Rigueiro et al., 2001); 4: (Cheung et al., 2009); 5: (Malay et al., 2016); 6: (Fu et al., 2011); 7: (Gosline et al., 1999); 8: (Madsen et al., 1999); 9: (Swanson et al., 2006)

When comparing proline contents and mechanical properties as seen in Table 4.8, this general trend can be seen, at least when comparing lepidopteran silks and spider silks to each other. Though proline content may impact silk structure and performance within closely related groups, it is not the single most important factor in determining where protein structure and performance differences originate. As discussed earlier in this chapter, it would be interesting to see if the phenomenon of supercontraction is present in *Galleria* silk, as the presence of proline has been shown to affect supercontraction in other lepidopteran silks such as *A. pernyi* (Fu et al., 2009); if this phenomenon is observed in a silk with 0.2% proline, it would be interesting to compare how

*Galleria* silk would compare to that of a spider silk with a similar proline content, such as *N. clavipes* dragline silk.

#### 4.4.2.4 Comparisons to other man-made materials

When discussing the extraordinary mechanical properties of silks, comparisons are often made to steel and other man-made materials (see Table 4.9). There is certainly no contest in stiffness and UTS between a viscoelastic protein material like silk when compared to highly crystalline materials such as Kevlar 49 and high-tensile steel; silk really shines, however, when one takes a closer look at its specific stress and toughness.

Table 4.9 Average tensile properties of *Galleria* silk from the present study compared to the mechanical properties of other man-made materials.

Material	E (GPa)	UTS (MPa)	$\epsilon_f$ (mm/mm)	$\sigma_s$ (mN/tex)	Toughness (MJ/m <sup>3</sup> )	Source
<i>G. mellonella</i> silk (measured) (average)	3.12 – 12.76 8.6	308.8 – 1270.4 714.4	0.33 – 0.60 0.5	231.1 – 950.9 195.2	83.4 – 328.3 195.2	This study
Nylon fibre	5	950	0.18	290	80	(Gosline et al., 1999; Hearle & Morton, 2008)
Kevlar 49 fibre	130	3600	0.027	2100	50	
High-tensile steel	200	1500	0.008	260	6	

E, Young's modulus of elasticity; UTS, ultimate tensile strength;  $\epsilon_f$ , strain at break;  $\sigma_s$ , specific stress.

While one may not choose to make a load-bearing structure such as a building frame from silk, its toughness makes it very desirable for other applications such as ballistic protection (Drodge, Mortimer, Holland, & Siviour, 2012), and in biomedical textiles such as wound dressings, soft-tissue and gastro-intestinal implants, and stents (Li et al., 2015). Silk is considered an excellent biomedical textile due to its tensile strength, knot strength, elasticity, biodegradability, and biocompatible properties (Altman et al., 2003).

## 5 Conclusions and Future Work

### 5.1 Summary

The purpose of this research was to investigate the potential use of *Galleria mellonella* silk as a textile fibre, by determining how to collect the silk for degumming and tensile tests, describing the silk's morphology, identifying an effective degumming method, and measuring its tensile properties for the purposes of comparison to other silks and textile fibres.

A method to collect clean cocoons free from frass and debris was developed, and those cocoons were used to assess how effective conventional degumming methods were in removing the sericin coating from *Galleria* silk. A novel method was developed for collecting naturally spun silk threads directly from the insect, so that the samples were handled as minimally as possible and the results would more closely represent the properties of *Galleria* silk as extruded by the insect. The results from the tensile tests were compared and contrasted to other studies where mechanical properties of *Galleria* silk were tested; the results were similarly compared and contrasted to known values of other lepidopteran and spider silks, and to other man-made materials such as high tenacity textile fibres and steel.

### 5.2 Conclusions

The conclusions based on this study are as follows:

1. *Galleria* can be reared to collect frass- and debris-free cocoons, by removing 6<sup>th</sup> to 7<sup>th</sup> instars from the main colony when close to pupation and allowing them to construct cocoons on an open mesh substrate.

2. The most effective degumming method used in this study was boiling the silk for 30 minutes in a combined solution of  $\text{Na}_2\text{CO}_3$  (to maintain an effective pH of ~9) and sodium lauryl sulfate (to facilitate wetting and evenness of degumming).
3. Visual observations of *Galleria* cocoons support claims by other researchers that the selective pressures of the beehive have caused the evolution of *Galleria* silk to be both strong and elastic. While spiders have multiple different types of silk and silk glands depending on the function of the silk (e.g. dragline, adhesive, and egg sacs), lepidopterans are capable of producing only one type of silk. To construct a strong and stiff cocoon with silk that is more extensible than other lepidopterans, it appears as though *Galleria* uses approximately twice the amount of sericin to hold their cocoons together than *Bombyx mori*.
4. Tensile specimens can be collected in such a way that the insect lays down the fibre as it walks, limiting the amount of handling necessary; this method allows for the measuring of tensile properties of the silk as-produced by the insect and limits any inadvertent changes to the silk's material properties as a result of handling.
5. The tensile results have a larger spread than those reported previously by (Hepburn et al., 1979), but are in-line with those results despite differences in collection procedures and tensile test parameters.
6. *Galleria* silk has unique mechanical properties for a lepidopteran silk and is comparable to the properties of commonly studied spider silks.

### 5.3 Future work

*Galleria* are easy to rear and produce large quantities of silk whose mechanical properties and biological compatibility could be used effectively in biomedical textiles and soft implants.

*Galleria* silk could be a viable alternative to synthetic or transgenically produced spider silks currently being researched and utilized.

Recommendations for future work include:

1. The optimization of the  $\text{Na}_2\text{CO}_3$  + SLS degumming procedure to determine the concentrations, time, and temperature of maximum effectiveness with the least amount of damage done to the silk fibres. Work should also be done to explore other methods of degumming, such as enzymatic degumming (for energy efficiency and reduced damage potential), and autoclaving (which is especially relevant if the silk is to be used in biomedical textile applications).
2. Run degumming experiments on feeding tunnel silk to see how the quantity of sericin may differ from cocoon silk. It is predicted that there will be less sericin present on feeding tunnel silk, as it is more important for those structures to be elastic to accommodate larval movement.
3. Evaluate the tensile properties of silk collected from cocoons and feeding tunnels, to see how they compare to the naturally extruded fibres of this study. It would also be worth investigating the average speed at which larvae lay down the silk in their feeding tubes and try to replicate that reeling speed in forced-silk collection tests.
4. Investigate how changing different components of *Galleria* diet impacts the properties of both cocoon and feeding tunnel silk. The insects used in this study were reared on a diet

specifically developed for robust immune systems, as is needed in pathology research. A diet developed to optimize silk properties would be important for larger scale production.

5. Start to explore the use of this fibre as a biomedical textile. Does *Galleria* silk support tissue growth? How does *Galleria* silk compare to other materials currently used for tissue scaffolds and soft implants? Initial studies could include the creation of either nonwoven structures or yarns from degummed feeding tunnel and cocoon silks.

## References

- AATCC Test Method 20. (2013). *Fiber Analysis: Qualitative*. Research Triangle Park, NC: American Association of Textile Chemists and Colorists.
- Ahumada, O., Cocca, M., Gentile, G., Martuscelli, E., & D’Orazio, L. (2004). Uniaxial Tensile Properties of Yarns: Effects of Moisture Level on the Shape of Stress-Strain Curves. *Textile Research Journal*, 74(11), 1001–1006.  
<https://doi.org/10.1177/004051750407401111>
- Altman, G. H., Diaz, F., Jakuba, C., Calabro, T., Horan, R. L., Chen, J., ... Kaplan, D. L. (2003). Silk-based biomaterials. *Biomaterials*, 24(3), 401–416.
- Andersen, S. O. (1970). Amino acid composition of spider silks. *Comparative Biochemistry and Physiology*, 35(3), 705–711. [https://doi.org/10.1016/0010-406X\(70\)90988-6](https://doi.org/10.1016/0010-406X(70)90988-6)
- Andersson, M., Jia, Q., Abella, A., Lee, X.-Y., Landreh, M., Purhonen, P., ... Rising, A. (2017). Biomimetic spinning of artificial spider silk from a chimeric minispidroin. *Nature Chemical Biology*, 13(3), 262–264. <https://doi.org/10.1038/nchembio.2269>
- Anghileri, A., Freddi, G., Mossotti, R., & Innocenti, R. (2007). Mechanical Properties of Silk Yarn Degummed with Several Proteases. *Journal of Natural Fibers*, 4(1), 13–23.  
[https://doi.org/10.1300/J395v04n01\\_02](https://doi.org/10.1300/J395v04n01_02)
- Asakura, T., Umemura, K., Nakazawa, Y., Hirose, H., Higham, J., & Knight, D. (2007). Some Observations on the Structure and Function of the Spinning Apparatus in the Silkworm *Bombyx mori*. *Biomacromolecules*, 8(1), 175–181. <https://doi.org/10.1021/bm060874z>
- Ashby, M. F., Gibson, L. J., Wegst, U., & Olive, R. (1995). The Mechanical Properties of Natural Materials. I. Material Property Charts. *Proceedings of the Royal Society of*

- London A: Mathematical, Physical and Engineering Sciences*, 450(1938), 123–140.  
<https://doi.org/10.1098/rspa.1995.0075>
- ASTM Standard D4848. (1998). *Standard Terminology Related to Force, Deformation and Related Properties of Textiles*. ASTM International.
- ASTM Test Method D1776. (2008). *Standard Practice for Conditioning and Testing Textiles*. West Conshohocken, PA: ASTM International.
- ASTM Test Method D3822. (2014). *Test Method for Tensile Properties of Single Textile Fibers*. ASTM International.
- Babu, K. M. (2012). Silk fibres. In R. Kozłowski (Ed.), *Handbook of natural fibres*. Oxford; Philadelphia, PA: Woodhead Pub.
- Babu, K. M. (2013). *Silk: processing, properties and applications*. Cambridge, UK: Woodhead Publishing in association with the Textile Institute.
- Bell, S. (2001). Measurement good practice guide no. 11 (issue 2). *A Beginner's Guide to Uncertainty of Measurement*. National Physical Laboratory Teddington, Middlesex, United Kingdom.
- Bolt Threads. (n.d.). Microsilk. Retrieved September 24, 2018, from <http://boltthreads.com/technology/microsilk/>
- Bombelli, P., Howe, C. J., & Bertocchini, F. (2017). Polyethylene bio-degradation by caterpillars of the wax moth *Galleria mellonella*. *Current Biology*, 27(8), R292–R293.

- Borujeni, E. K., Najar, S. S., & Dolatabadi, M. K. (2017). The study on structural properties and tensile strength of reared silkworm cocoon. *The Journal of The Textile Institute*, 0(0), 1–7. <https://doi.org/10.1080/00405000.2017.1335378>
- Bronskill, J. (1961). A cage to simplify the rearing of the greater wax moth, *Galleria mellonella* (Pyralidae). *J. Lep. Soc*, 15(2), 102–104.
- CGSB Test Method CAN/CGSB-4.2 No. 2. (1988). *Conditioning Textile Materials for Testing*. Ottawa, ON: Canadian General Standards Board.
- Chakraborty, A., Mahato, N., Rajak, P., & Ghosh, J. (2014). Effect of Enzymatic Degumming on the Properties of Silk Fabric. *Journal of the Textile Association*, 75(4), 265–273.
- Chen, F., Porter, D., & Vollrath, F. (2012a). Silk cocoon (*Bombyx mori*): Multi-layer structure and mechanical properties. *Acta Biomaterialia*, 8(7), 2620–2627. <https://doi.org/10.1016/j.actbio.2012.03.043>
- Chen, F., Porter, D., & Vollrath, F. (2012b). Structure and physical properties of silkworm cocoons. *Journal of The Royal Society Interface*, 9(74), 2299–2308. <https://doi.org/10.1098/rsif.2011.0887>
- Cheng, Y., Koh, L.-D., Li, D., Ji, B., Han, M.-Y., & Zhang, Y.-W. (2014). On the strength of  $\beta$ -sheet crystallites of *Bombyx mori* silk fibroin. *Journal of The Royal Society Interface*, 11(96), 20140305. <https://doi.org/10.1098/rsif.2014.0305>
- Cheung, H.-Y., Lau, K.-T., Ho, M.-P., & Mosallam, A. (2009). Study on the Mechanical Properties of Different Silkworm Silk Fibers. *Journal of Composite Materials*, 43(22), 2521–2531. <https://doi.org/10.1177/0021998309345347>

- Collier, B. J., & Epps, H. H. (1999). *Textile Testing and Analysis*. Upper Saddle River, NJ: Prentice Hall.
- Craig, C. L. (2003). *Spiderwebs and silk: tracing evolution from molecules to genes to phenotypes*. Oxford; New York: Oxford University Press.
- Dadd, R. H. (1964). A study of carbohydrate and lipid nutrition in the wax moth, *Galleria mellonella* (L.), using partially synthetic diets. *Journal of Insect Physiology*, *10*(2), 161–178.
- Dadd, R. H. (1966). Beeswax in the nutrition of the wax moth, *Galleria mellonella* (L.). *Journal of Insect Physiology*, *12*(12), 1479–1492. [https://doi.org/10.1016/0022-1910\(66\)90038-2](https://doi.org/10.1016/0022-1910(66)90038-2)
- Datta, A., Ghosh, A. K., & C. Kundu, S. (2001). Purification and characterization of fibroin from the tropical Saturniid silkworm, *Antheraea mylitta*. *Insect Biochemistry and Molecular Biology*, *31*(10), 1013–1018. [https://doi.org/10.1016/S0965-1748\(01\)00049-2](https://doi.org/10.1016/S0965-1748(01)00049-2)
- Davis, J. R. (2004). *Tensile testing, second edition* (2nd ed.). Materials Park, Ohio: ASM International.
- Denny, M. W. (1980). Silks - their properties and functions. In J. F. V. Vincent & J. D. Currey (Eds.), *The mechanical properties of biological materials* (pp. 247–272). Cambridge, UK: Cambridge University Press.
- Drodge, D. R., Mortimer, B., Holland, C., & Siviour, C. R. (2012). Ballistic impact to access the high-rate behaviour of individual silk fibres. *Journal of the Mechanics and Physics of Solids*, *60*(10), 1710–1721. <https://doi.org/10.1016/j.jmps.2012.06.007>

- Dunaway, D. L., Thiel, B. L., Srinivasan, S. G., & Viney, C. (1995). Characterizing the cross-sectional geometry of thin, non-cylindrical, twisted fibres (spider silk). *Journal of Materials Science*, 30(16), 4161–4170. <https://doi.org/10.1007/BF00360725>
- Dunaway, D. L., Thiel, B. L., & Viney, C. (1995). Tensile mechanical property evaluation of natural and epoxide-treated silk fibers. *Journal of Applied Polymer Science*, 58(3), 675–683. <https://doi.org/10.1002/app.1995.070580322>
- Eischen, F. A., & Dietz, A. (1990). Improved Culture Techniques for Mass Rearing *Galleria mellonella*. *Entomological News*, 101, 123–128.
- Eisoldt, L., Smith, A., & Scheibel, T. (2011). Decoding the secrets of spider silk. *Materials Today*, 14(3), 80–86. [https://doi.org/10.1016/S1369-7021\(11\)70057-8](https://doi.org/10.1016/S1369-7021(11)70057-8)
- Fahnestock, S. R., & Irwin, S. L. (1997). Synthetic spider dragline silk proteins and their production in *Escherichia coli*. *Applied Microbiology and Biotechnology*, 47(1), 23–32. <https://doi.org/10.1007/s002530050883>
- Fan, Q. (2005). *Chemical testing of textiles*. Boca Raton : CRC Press ; Cambridge : Woodhead Publishing.
- Fedič, R., Žurovec, M., & Sehnal, F. (2003). Correlation between Fibroin Amino Acid Sequence and Physical Silk Properties. *Journal of Biological Chemistry*, 278(37), 35255–35264. <https://doi.org/10.1074/jbc.M305304200>
- Fu, C., Porter, D., Chen, X., Vollrath, F., & Shao, Z. (2011). Understanding the Mechanical Properties of *Antheraea pernyi* Silk-From Primary Structure to Condensed Structure of the Protein. *Advanced Functional Materials*, 21(4), 729–737. <https://doi.org/10.1002/adfm.201001046>

- Fu, C., Porter, D., & Shao, Z. (2009). Moisture Effects on *Antheraea pernyi* Silk's Mechanical Property. *Macromolecules*, 42(20), 7877–7880. <https://doi.org/10.1021/ma901321k>
- Ganga, G. (2003). *Comprehensive Sericulture Volume 2: Silkworm Rearing and Silk Reeling*. Enfield, NH: Science Publishers, Inc.
- Geddes, A. J., Parker, K. D., Atkins, E. D. T., & Beighton, E. (1968). “Cross- $\beta$ ” conformation in proteins. *Journal of Molecular Biology*, 32(2), 343–358. [https://doi.org/10.1016/0022-2836\(68\)90014-4](https://doi.org/10.1016/0022-2836(68)90014-4)
- Gohl, E. P. G., & Vilensky, L. D. (1983). *Textile Science: An explanation of fibre properties* (2nd ed.). Melbourne: Longman Cheshire.
- Good, M. E., Morrison, F. O., & Mankiewicz, E. (1953). Lipolytic Enzymes Extracted from *Galleria mellonella* L. (Lepidoptera: Pyralidae) Reared on Natural and Artificial Media. *The Canadian Entomologist*, 85(07), 252–253. <https://doi.org/10.4039/Ent85252-7>
- Gosline, J. M., Guerette, P. A., Ortlepp, C. S., & Savage, K. N. (1999). The mechanical design of spider silks: From fibroin sequence to mechanical function. *Journal of Experimental Biology*, 202(23), 3295–3303.
- Grzelak, K., Couble, P., Garel, A., Kludkiewicz, B., & Alrouz, H. (1988). Low molecular weight silk proteins in *Galleria mellonella*. *Insect Biochemistry*, 18(3), 223–228. [https://doi.org/10.1016/0020-1790\(88\)90086-8](https://doi.org/10.1016/0020-1790(88)90086-8)
- Guerette, P. A., Ginzinger, D. G., Weber, B. H. F., & Gosline, J. M. (1996). Silk Properties Determined by Gland-Specific Expression of a Spider Fibroin Gene Family. *Science*, 272(5258), 112–115. <https://doi.org/10.1126/science.272.5258.112>

- Gulrajani, M. L. (1992). Degumming of silk. *Review of Progress in Coloration and Related Topics*, 22(1), 79–89. <https://doi.org/10.1111/j.1478-4408.1992.tb00091.x>
- Haydak, M. H. (1936). Is Wax a Necessary Constituent of the Diet of Wax Moth Larvae? *Annals of the Entomological Society of America*, 29(4), 581–588.  
<https://doi.org/10.1093/aesa/29.4.581>
- Hearle, J. W. S., & Morton, W. E. (2008). *Physical Properties of Textile Fibres*. Elsevier.
- Hepburn, H. R., Chandler, H. D., & Davidoff, M. R. (1979). Extensometric properties of insect fibroins: The green lacewing cross- $\beta$ , honeybee  $\alpha$ -helical and greater waxmoth parallel- $\beta$  conformations. *Insect Biochemistry*, 9(1), 69–77. [https://doi.org/10.1016/0020-1790\(79\)90028-3](https://doi.org/10.1016/0020-1790(79)90028-3)
- Hinman, M. B., & Lewis, R. V. (1992). Isolation of a clone encoding a second dragline silk fibroin. *Nephila clavipes* dragline silk is a two-protein fiber. *Journal of Biological Chemistry*, 267(27), 19320–19324.
- Holland, C., Vollrath, F., Ryan, A. J., & Mykhaylyk, O. O. (2012). Silk and Synthetic Polymers: Reconciling 100 Degrees of Separation. *Advanced Materials*, 24(1), 105–109.  
<https://doi.org/10.1002/adma.201103664>
- Hudspeth, M., Nie, X., Chen, W., & Lewis, R. (2012). Effect of Loading Rate on Mechanical Properties and Fracture Morphology of Spider Silk. *Biomacromolecules*, 13(8), 2240–2246. <https://doi.org/10.1021/bm3003732>
- Humphries, M. (2009). *Fabric Reference*. Pearson Prentice Hall.
- Inoue, S., Tanaka, K., Arisaka, F., Kimura, S., Ohtomo, K., & Mizuno, S. (2000). Silk Fibroin of *Bombyx mori* Is Secreted, Assembling a High Molecular Mass Elementary Unit

- Consisting of H-chain, L-chain, and P25, with a 6:6:1 Molar Ratio. *Journal of Biological Chemistry*, 275(51), 40517–40528. <https://doi.org/10.1074/jbc.M006897200>
- Jindra, M., & Sehnal, F. (1989). Larval growth, food consumption, and utilization of dietary protein and energy in *Galleria mellonella*. *Journal of Insect Physiology*, 35(9), 719–724. [https://doi.org/10.1016/0022-1910\(89\)90091-7](https://doi.org/10.1016/0022-1910(89)90091-7)
- Jones, J. A., Harris, T. I., Tucker, C. L., Berg, K. R., Christy, S. Y., Day, B. A., ... Lewis, R. V. (2015). More Than Just Fibers: An Aqueous Method for the Production of Innovative Recombinant Spider Silk Protein Materials. *Biomacromolecules*, 16(4), 1418–1425. <https://doi.org/10.1021/acs.biomac.5b00226>
- Knott, J., Freddi, G., & Belly, M. (1983). Analytical investigations of degumming of silk (*Bombyx mori* L.). *Melliand Textilberichte*, 64(No.7), 481–483.
- Leedy, P. D., & Ormrod, J. E. (2009). *Practical Research: Planning and Design* (9 edition). Upper Saddle River, NJ: Pearson.
- Li, G., Li, Y., Chen, G., He, J., Han, Y., Wang, X., & Kaplan, D. L. (2015). Silk-Based Biomaterials in Biomedical Textiles and Fiber-Based Implants. *Advanced Healthcare Materials*, 4(8), 1134–1151. <https://doi.org/10.1002/adhm.201500002>
- Liljas, A., Liljas, L., Piskur, J., Lindblom, G., Nissen, P., & Kjeldgaard, M. (2009). *Textbook of structural biology*. Hackensack, NJ: World Scientific.
- Lucas, F., & Rudall, K. M. (1968). Extracellular Fibrous Proteins: The Silks. In M. Florkin & E. H. Stota (Eds.), *Comprehensive Biochemistry: Extracellular and Supporting Structures* (Vol. 26B).

- Lucas, F., Shaw, J. T. B., & Smith, S. G. (1955). The Chemical Constitution of some Silk Fibroins and its Bearing on their Physical Properties. *Journal of the Textile Institute Transactions*, 46(6), T440–T452. <https://doi.org/10.1080/19447027.1955.10750333>
- Lucas, F., Shaw, J. T. B., & Smith, S. G. (1960). Comparative studies of fibroins: I. The amino acid composition of various fibroins and its significance in relation to their crystal structure and taxonomy. *Journal of Molecular Biology*, 2(6), 339–349. [https://doi.org/10.1016/S0022-2836\(60\)80045-9](https://doi.org/10.1016/S0022-2836(60)80045-9)
- Madsen, B., Shao, Z. Z., & Vollrath, F. (1999). Variability in the mechanical properties of spider silks on three levels: interspecific, intraspecific and intraindividual. *International Journal of Biological Macromolecules*, 24(2), 301–306. [https://doi.org/10.1016/S0141-8130\(98\)00094-4](https://doi.org/10.1016/S0141-8130(98)00094-4)
- Magoshi, J., Magoshi, Y., & Nakamura, S. (1993). Mechanism of Fiber Formation of Silkworm. In D. L. Kaplan, W. W. Adams, B. Farmer, & C. Viney (Eds.), *Silk Polymers* (Vol. 544, pp. 292–310). American Chemical Society. Retrieved from <http://dx.doi.org/10.1021/bk-1994-0544.ch025>
- Mahall, K. (1993). *Quality Assessment of Textiles: Damage Detection by Microscopy*. Berlin; New York: Springer-Verlag.
- Malay, A. D., Sato, R., Yazawa, K., Watanabe, H., Ifuku, N., Masunaga, H., ... Numata, K. (2016). Relationships between physical properties and sequence in silkworm silks. *Scientific Reports*, 6, 27573. <https://doi.org/10.1038/srep27573>

- Marsh, R. E., Corey, R. B., & Pauling, L. (1955a). An investigation of the structure of silk fibroin. *Biochimica et Biophysica Acta*, *16*, 1–34. [https://doi.org/10.1016/0006-3002\(55\)90178-5](https://doi.org/10.1016/0006-3002(55)90178-5)
- Marsh, R. E., Corey, R. B., & Pauling, L. (1955b). The structure of tussah silk fibroin. *Acta Crystallographica*, *8*(11), 710–715. <https://doi.org/10.1107/S0365110X5500217X>
- Marston, N. L., Campbell, B., & Boldt, P. E. (1975). *Mass producing eggs of the greater wax moth, Galleria mellonella (L.)*. Agricultural Research Service, US Dept. of Agriculture.
- Matsumoto, A., Kim, H. J., Tsai, I. Y., Wang, X., Cebe, P., & Kaplan, D. L. (2007). Chapter 6. Silk. In M. Lewin (Ed.), *Handbook of fiber chemistry*. Boca Raton: CRC/Taylor & Francis.
- Mortimer, B., Drodge, D., Siviour, C., & Holland, C. (2012). Shooting Silk: Stress Strain Properties of Single Fibres at High Rate. *Journal of Biomechanics*, *45*, Supplement 1, S86. [https://doi.org/10.1016/S0021-9290\(12\)70087-8](https://doi.org/10.1016/S0021-9290(12)70087-8)
- Mortimer, B., Guan, J., Holland, C., Porter, D., & Vollrath, F. (2015). Linking naturally and unnaturally spun silks through the forced reeling of Bombyx mori. *Acta Biomaterialia*, *11*, 247–255. <https://doi.org/10.1016/j.actbio.2014.09.021>
- Mukherjee, K., Domann, E., & Hain, T. (2011). The Greater Wax Moth *Galleria mellonella* as an Alternative Model Host for Human Pathogens. In A. Vilcinskas (Ed.), *Insect Biotechnology*. Dordrecht: Springer Netherlands. Retrieved from <http://link.springer.com/10.1007/978-90-481-9641-8>
- Nakpathom, M., Somboon, B., & Narumol, N. (2009). Papain enzymatic degumming of Thai Bombyx mori silk fibers. *Journal of Microscopy Society of Thailand*, *23*(1), 142–146.

- Nayak, R. K., Padhye, R., & Fergusson, S. (2012). Identification of natural textile fibres. In R. Kozłowski (Ed.), *Handbook of natural fibres*. Oxford; Philadelphia, Pa.: Woodhead Publishing.
- Needles, H. L. (1981). *Handbook of textile fibers, dyes, and finishes*. New York: Garland STPM Press.
- Nirmala, X., Kodrik, D., Žurovec, M., & Sehnal, F. (2001). Insect silk contains both a Kunitz-type and a unique Kazal-type proteinase inhibitor. *European Journal of Biochemistry*, 268(7), 2064–2073. <https://doi.org/10.1046/j.1432-1327.2001.02084.x>
- Ortlepp, C. S., & Gosline, J. M. (2004). Consequences of Forced Silking. *Biomacromolecules*, 5(3), 727–731. <https://doi.org/10.1021/bm034269x>
- Pauling, L., & Corey, R. B. (1953). Two Rippled-Sheet Configurations of Polypeptide Chains, and a Note about the Pleated Sheets. *Proceedings of the National Academy of Sciences of the United States of America*, 39(4), 253–256.
- Perez-Rigueiro, J., Elices, M., Llorca, J., & Viney, C. (2001). Tensile properties of silkworm silk obtained by forced silking. *Journal of Applied Polymer Science*, 82(8), 1928–1935. <https://doi.org/10.1002/app.2038>
- Pérez-Rigueiro, J., Elices, M., Llorca, J., & Viney, C. (2002). Effect of degumming on the tensile properties of silkworm (*Bombyx mori*) silk fiber. *Journal of Applied Polymer Science*, 84(7), 1431–1437. <https://doi.org/10.1002/app.10366>
- Pérez-Rigueiro, J., Elices, M., Plaza, G. R., Real, J. I., & Guinea, G. V. (2006). The influence of anaesthesia on the tensile properties of spider silk. *Journal of Experimental Biology*, 209(2), 320–326. <https://doi.org/10.1242/jeb.02009>

- Pérez-Rigueiro, J., Viney, C., Llorca, J., & Elices, M. (1998). Silkworm silk as an engineering material. *Journal of Applied Polymer Science*, 70(12), 2439–2447.  
[https://doi.org/10.1002/\(SICI\)1097-4628\(19981219\)70:12<2439::AID-APP16>3.0.CO;2-J](https://doi.org/10.1002/(SICI)1097-4628(19981219)70:12<2439::AID-APP16>3.0.CO;2-J)
- Pérez-Rigueiro, J., Viney, C., Llorca, J., & Elices, M. (2000a). Mechanical properties of silkworm silk in liquid media. *Polymer*, 41(23), 8433–8439.  
[https://doi.org/10.1016/S0032-3861\(00\)00179-8](https://doi.org/10.1016/S0032-3861(00)00179-8)
- Pérez-Rigueiro, J., Viney, C., Llorca, J., & Elices, M. (2000b). Mechanical properties of single-brin silkworm silk. *Journal of Applied Polymer Science*, 75(10), 1270–1277.  
[https://doi.org/10.1002/\(SICI\)1097-4628\(20000307\)75:10<1270::AID-APP8>3.0.CO;2-C](https://doi.org/10.1002/(SICI)1097-4628(20000307)75:10<1270::AID-APP8>3.0.CO;2-C)
- Powell, J. A. (2009). *Moths of Western North America*. Berkeley : University of California Press,.
- Rajkhowa, R., Kaur, J., Wang, X., & Batchelor, W. (2015). Intrinsic tensile properties of cocoon silk fibres can be estimated by removing flaws through repeated tensile tests. *Journal of The Royal Society Interface*, 12(107), 20150177. <https://doi.org/10.1098/rsif.2015.0177>
- Reed, E. J., Bianchini, L. L., & Viney, C. (2012). Sample selection, preparation methods, and the apparent tensile properties of silkworm (*B. mori*) cocoon silk. *Biopolymers*, 97(6), 397–407. <https://doi.org/10.1002/bip.22005>
- Rheinberg, L. (1991). THE ROMANCE OF SILK: A Review of Sericulture and the Silk Industry. *Textile Progress*, 21(4), 1–43. <https://doi.org/10.1080/00405169108688854>

- Roy, D. N. (1937). On the nutrition of larvae of bee-wax moth, *Galleria mellonella*. *Zeitschrift Für Vergleichende Physiologie*, 24(5), 638–643. <https://doi.org/10.1007/BF00592301>
- Rudall, K. M. (1962). CHAPTER 9: Silk and Other Cocoon Proteins. In M. Florkin (Ed.), *Comparative Biochemistry V4: A Comprehensive Treatise* (pp. 397–433).
- Rudall, K. M., & Kenchington, W. (1971). Arthropod Silks: The Problem of Fibrous Proteins in Animal Tissues. *Annual Review of Entomology*, 16(1), 73–96. <https://doi.org/10.1146/annurev.en.16.010171.000445>
- Sehnal, F. (1966). A critical study of the biome and biometry of the wax moth *Galleria mellonella* raised in varying conditions. *Zeitschrift für wissenschaftliche Zoologie*, 174, 53–82.
- Sehnal, F. (2011). Biotechnologies Based on Silk. In A. Vilcinskas (Ed.), *Insect Biotechnology*. Dordrecht: Springer Netherlands. Retrieved from <http://link.springer.com/10.1007/978-90-481-9641-8>
- Sehnal, F., & Akai, H. (1990). Insect silk glands: their types, development and function, and effects of environmental factors and morphogenetic hormones on them. *International Journal of Insect Morphology and Embryology*, 19(2), 79–132. [https://doi.org/10.1016/0020-7322\(90\)90022-H](https://doi.org/10.1016/0020-7322(90)90022-H)
- Sehnal, F., & Sutherland, T. (2008). Silks produced by insect labial glands. *Prion*, 2(4), 145–153. <https://doi.org/10.4161/pri.2.4.7489>
- Sezutsu, H., & Yukuhiro, K. (2000). Dynamic Rearrangement Within the *Antheraea pernyi* Silk Fibroin Gene Is Associated with Four Types of Repetitive Units. *Journal of Molecular Evolution*, 51(4), 329–338. <https://doi.org/10.1007/s002390010095>

- Sezutsu, H., & Yukuhiro, K. (2014). The complete nucleotide sequence of the Eri-silkworm (*Samia cynthia ricini*) fibroin gene. *Journal of Insect Biotechnology and Sericology*, 83(3), 3\_059-3\_070. [https://doi.org/10.11416/jibs.83.3\\_059](https://doi.org/10.11416/jibs.83.3_059)
- Shao, Z., & Vollrath, F. (2002). Materials: Surprising strength of silkworm silk. *Nature*, 418(6899), 741–741.
- Somerville, D. (2007). Wax moth. NSW Department of Primary Industries. Retrieved from [http://www.dpi.nsw.gov.au/\\_\\_data/assets/pdf\\_file/0010/176284/wax-moth.pdf](http://www.dpi.nsw.gov.au/__data/assets/pdf_file/0010/176284/wax-moth.pdf)
- Sprague, K. U. (1975). Bombyx mori silk proteins. Characterization of large polypeptides. *Biochemistry*, 14(5), 925–931. <https://doi.org/10.1021/bi00676a008>
- Suzuki, Y., & Brown, D. D. (1972). Isolation and Identification of the messenger RNA for silk fibroin from Bombyx mori. *Journal of Molecular Biology*, 63(3), 409–429. [https://doi.org/10.1016/0022-2836\(72\)90437-8](https://doi.org/10.1016/0022-2836(72)90437-8)
- Swanson, B. O., Blackledge, T. A., Beltrán, J., & Hayashi, C. Y. (2006). Variation in the material properties of spider dragline silk across species. *Applied Physics A*, 82(2), 213–218. <https://doi.org/10.1007/s00339-005-3427-6>
- Takahashi, Y. (1993). Crystal Structure of Silk of Bombyx mori. In *Silk Polymers* (Vol. 544, pp. 168–175). American Chemical Society. Retrieved from <http://dx.doi.org/10.1021/bk-1994-0544.ch015>
- Tamura, T., & Kubota, T. (1989). In H. Akai & M. Kiguchi (Eds.), *Wild Silkmoths '88: Proceedings of Workshop in XVIII International Congress of Entomology, Vancouver, Canada, July 3-9, 1988* (pp. 67–72). Tsukuba, Japan: International Society for Wild Silkmoths.

- Tanaka, K., & Mizuno, S. (2001). Homologues of fibroin L-chain and P25 of *Bombyx mori* are present in *Dendrolimus spectabilis* and *Papilio xuthus* but not detectable in *Antheraea yamamai*. *Insect Biochemistry and Molecular Biology*, 31(6–7), 665–677.  
[https://doi.org/10.1016/S0965-1748\(00\)00173-9](https://doi.org/10.1016/S0965-1748(00)00173-9)
- Tanaka, K., Mori, K., & Mizuno, S. (1993). Immunological Identification of the Major Disulfide-Linked Light Component of Silk Fibroin. *Journal of Biochemistry*, 114(1), 1–4.
- Vollrath, F., Porter, D., & Holland, C. (2011). There are many more lessons still to be learned from spider silks. *Soft Matter*, 7(20), 9595. <https://doi.org/10.1039/c1sm05812f>
- Walters, R. H., & Hougen, O. A. (1934). Silk Degumming: I. Degradation of Silk Sericin by Alkalies. *Textile Research*, 5(2), 92–104. <https://doi.org/10.1177/004051753400500213>
- Warwicker, J. O. (1960). Comparative studies of fibroins: II. The crystal structures of various fibroins. *Journal of Molecular Biology*, 2(6), 350-IN1. [https://doi.org/10.1016/S0022-2836\(60\)80046-0](https://doi.org/10.1016/S0022-2836(60)80046-0)
- Wen, H., Lan, X., Zhang, Y., Zhao, T., Wang, Y., Kajiura, Z., & Nakagaki, M. (2009). Transgenic silkworms (*Bombyx mori*) produce recombinant spider dragline silk in cocoons. *Molecular Biology Reports*, 37(4), 1815–1821. <https://doi.org/10.1007/s11033-009-9615-2>
- Williams, J. L. (1997). Insects: Lepidoptera (moths). In R. A. Morse & R. Nowogrodzki (Eds.), *Honey bee pests, predators, and diseases*. (pp. 121–141). Medina, OH, USA: AI Root Company. Retrieved from <https://www.cabdirect.org/cabdirect/abstract/19910229933>

- Work, R. W. (1976). The Force-Elongation Behavior of Web Fibers and Silks Forcibly Obtained from Orb-Web-Spinning Spiders. *Textile Research Journal*, 46(7), 485–492.  
<https://doi.org/10.1177/004051757604600704>
- Work, R. W. (1981). A Comparative Study of the Supercontraction of Major Ampullate Silk Fibers of Orb-Web-Building Spiders (Araneae). *The Journal of Arachnology*, 9(3), 299–308.
- Wray, L. S., Hu, X., Gallego, J., Georgakoudi, I., Omenetto, F. G., Schmidt, D., & Kaplan, D. L. (2011). Effect of processing on silk-based biomaterials: Reproducibility and biocompatibility. *Journal of Biomedical Materials Research Part B: Applied Biomaterials*, 99B(1), 89–101. <https://doi.org/10.1002/jbm.b.31875>
- Xu, J., Dong, Q., Yu, Y., Niu, B., Ji, D., Li, M., ... Tan, A. (2018). Mass spider silk production through targeted gene replacement in *Bombyx mori*. *Proceedings of the National Academy of Sciences*, 115(35), 8757–8762. <https://doi.org/10.1073/pnas.1806805115>
- Yang, C., Teng, X., Žurovec, M., Scheller, K., & Sehnal, F. (1998). Characterization of the P25 silk gene and associated insertion elements in *Galleria mellonella*. *Gene*, 209(1–2), 157–165. [https://doi.org/10.1016/S0378-1119\(98\)00029-8](https://doi.org/10.1016/S0378-1119(98)00029-8)
- Yazawa, K., Ishida, K., Masunaga, H., Hikima, T., & Numata, K. (2016). Influence of Water Content on the  $\beta$ -Sheet Formation, Thermal Stability, Water Removal, and Mechanical Properties of Silk Materials. *Biomacromolecules*, 17(3), 1057–1066.  
<https://doi.org/10.1021/acs.biomac.5b01685>
- Zemlin, J. C. (1968). *A Study of the Mechanical Behavior of Spider Silks*.

Zhao, H.-P., Feng, X.-Q., & Shi, H.-J. (2007). Variability in mechanical properties of Bombyx mori silk. *Materials Science and Engineering: C*, 27(4), 675–683.

<https://doi.org/10.1016/j.msec.2006.06.031>

Žurovec, M., Kodrík, D., Yang, C., Sehnal, F., & Scheller, K. (1998). The P25 component of Galleria silk. *Molecular and General Genetics MGG*, 257(3), 264–270.

<https://doi.org/10.1007/s004380050647>

Žurovec, M., & Sehnal, F. (2002). Unique Molecular Architecture of Silk Fibroin in the Waxmoth, Galleria mellonella. *Journal of Biological Chemistry*, 277(25), 22639–22647.

<https://doi.org/10.1074/jbc.M201622200>

Žurovec, M., Sehnal, F., Scheller, K., & Kumaran, A. K. (1992). Silk gland specific cDNAs from Galleria mellonella L. *Insect Biochemistry and Molecular Biology*, 22(1), 55–67.

Žurovec, M., Vašková, M., Kodrík, D., Sehnal, F., & Kumaran, A. K. (1995). Light-chain fibroin of Galleria mellonella L. *Molecular and General Genetics MGG*, 247(1), 1–6.

<https://doi.org/10.1007/BF00425815>

## Appendix A: Diet Recipe

Ingredient	Quantity (g)
Wheatgerm (Planet Organic)	264
Brewer's Yeast (Planet Organic)	134
Beeswax (locally sourced)	205
Glycerol (Sigma-Aldrich)	134
Honey (locally sourced)	132
Deionized Ultra-Filtered (DIUF) Water	67

### Directions:

1. Place the wheatgerm, yeast, and beeswax into a large bowl, and stir until combined.
2. Weigh the glycerol, honey, and water in a large Erlenmeyer flask with magnetic stirring rod, and warm on a hotplate at medium-low temperature until the honey starts to liquify.
3. Begin stirring and remove from heat once the honey has completely liquified.
4. Pour the glycerol/honey/water mixture into the dry ingredients slowly, while mixing. Stir until well incorporated, and the mixture has a soft granola appearance and consistency.
5. Feed insects as needed. May be stored in the refrigerator for up to two weeks.

## Appendix B: Degumming Experiments & Statistical Analysis

Group 1:

Date	Experiment	Cohort	Degumming conditions					Before weights (g)			
			Na2CO3 (g)	SLS (g)	Time (mins)	Temp (°C)	water (mL)	Temp (°C)	RH (%)	silk	paper
1-Jun-17	Degumming w/vacuum filter		0.024	-	30		100.00			0.0492	0.1473
3-Oct-17	control	7apr17 --> 24may17 21apr17 --> 24may17			30			19.3	63	0.0500	0.3877
3-Oct-17	water only	7apr17 --> 19may17			30	97	100.00	19.3	63	0.0506	0.3821
3-Oct-17	Na2CO3 only	7apr17 --> 19may17 7apr17 --> 24may17	0.020 (pH=9.0)		30	96	100.00	19.4	63	0.0503	0.3936
4-Oct-17	SLS only	21apr17 --> 24may17		1.008	30	96	100.00	19.3	63	0.0498	0.3843
4-Oct-17	Na2CO3 + SLS	25apr17 --> 30may17	0.019 (pH=9.0)	1.001	30	97	100.00	19.3	63	0.0504	0.3935
3-Oct-17	control paper only				30			19.4	63		0.4001

Experiment	After weights (g)					Observations
	Temp (°C)	RH (%)	Silk + paper	silk only, calculated (g)	weight change (%)	
Degumming w/vacuum filter			0.1733	0.0260	-47.15	
control	19.9	60	0.4367	0.0490	-2.00	weighed, removed from conditioning room, reconditioned & reweighed
water only	19.9	60	0.4192	0.0371	-26.68	rinsed 100mL room temp RO water, vacuumed 5 additional minutes. V. little separation
Na2CO3 only	19.9	60	0.4212	0.0276	-45.13	rinsed 100mL room temp RO water, vacuumed 5 additional minutes. Moderate separation
SLS only	19.9	60	0.4181	0.0338	-32.13	rinsed 100mL room temp RO water, vacuumed 5 additional minutes. V. little separation
Na2CO3 + SLS	19.9	60	0.4226	0.0291	-42.26	rinsed 100mL room temp RO water, vacuumed 5 additional minutes. Moderate "plus" separation
control paper only	19.9	60	0.4026		0.6248	paper only, wetted w/100mL room temp RO water, vacuumed 5 mins, dried overnight & reconditioned

Group 2:

Date	Experiment	Cohort	Degumming conditions					Before weights (g)			
			Na2CO3 (g)	SLS (g)	Time (mins)	Temp (°C)	water (mL)	Temp (°C)	RH (%)	silk	paper
1-Nov-17	water only	Apr 25 --> May 30/17			30	96	100.00	19.5	63	0.0492	0.3923
1-Nov-17	Na2CO3 only	Apr 25 --> May 30/17 July 27 --> Sep 7/17	0.020 (pH=9.0)		30	99	100.00	19.5	62	0.0495	0.3916
1-Nov-17	SLS only	July 27 --> Sep 7/17 Aug 3--> Sep 17/17		1.003	30	96	100.00	19.5	63	0.0505	0.3797
1-Nov-17	Na2CO3 + SLS	Aug 3--> Sep 17/17	0.021 (pH=9.0)	1.009	30	96	100.00	19.5	63	0.0505	0.3846
1-Nov-17	control (rinse only)	Aug 3--> Sep 17/17 Aug 3 --> Sep 24/17						19.5	62	0.0495	0.3850
1-Nov-17	control #2 (rinse only)	Aug 3 --> Sep 24/17						19.5	61	0.0501	0.3887

Experiment	After weights (g)					Observations
	Temp (°C)	RH (%)	Silk + paper	silk only, calculated (g)	weight change (%)	
water only	19.5	63	0.4327	0.0404	-17.89	rinsed 100mL room temp RO water, vacuumed 5 additional minutes. V. little separation
Na2CO3 only	19.5	63	0.4167	0.0251	-49.29	rinsed 100mL room temp RO water, vacuumed 5 additional minutes. Moderate separation
SLS only	19.5	62	0.4159	0.0362	-28.32	rinsed 100mL room temp RO water, vacuumed 5 additional minutes. V. little separation
Na2CO3 + SLS	19.5	62	0.4106	0.0260	-48.51	rinsed 100mL room temp RO water, vacuumed 5 additional minutes. Moderate "plus" separation
control (rinse only)	19.6	62	0.4375	0.0525	6.06	rinse only 100 mL RO water at room temp, vacuum 5 mins
control #2 (rinse only)	19.6	62	0.4418	0.0531	5.99	rinse only 100 mL RO water at room temp, vacuum 5 mins

Group 3:

Date	Experiment	Cohort	Degumming conditions					Before weights (g)			
			Na <sub>2</sub> CO <sub>3</sub> (g)	SLS (g)	Time (mins)	Temp (°C)	water (mL)	Temp (°C)	RH (%)	silk	paper
4-Dec-17	water only	Aug 3/17 --> Sep 24/17 Aug 17/17 --> Sep 30/17			30	96	100.00	19.4	64	0.0512	0.3868
4-Dec-17	Na <sub>2</sub> CO <sub>3</sub> only	Aug 17/17 --> Sep 30/17	0.020 (pH=9.0)		30	98	100.00	19.4	64	0.0507	0.3815
4-Dec-17	SLS only	Aug 17/17 --> Sep 30/17		0.999	30	96	100.00	19.4	64	0.0502	0.3954
4-Dec-17	Na <sub>2</sub> CO <sub>3</sub> + SLS	Aug 17/17 --> Sep 30/17 Aug 28/17 --> Oct 8/17	0.020 (pH=9.0)	1.004	30	96	100.00	19.4	64	0.0500	0.3891
4-Dec-17	control (rinse only)	Aug 28/17 --> Oct 8/17						19.4	64	0.0505	0.3842

Experiment	After weights (g)					Observations
	Temp (°C)	RH (%)	Silk + paper	silk only, calculated (g)	weight change (%)	
water only	19.3	64	0.4262	0.0394	-23.05	rinsed 100mL room temp RO water, vacuumed 5 additional minutes. V. little separation
Na <sub>2</sub> CO <sub>3</sub> only	19.3	64	0.4103	0.0288	-43.20	rinsed 100mL room temp RO water, vacuumed 5 additional minutes. Moderate separation
SLS only	19.3	64	0.4312	0.0358	-28.69	rinsed 100mL room temp RO water, vacuumed 5 additional minutes. V. little separation
Na <sub>2</sub> CO <sub>3</sub> + SLS	19.3	64	0.4191	0.0300	-40.00	rinsed 100mL room temp RO water, vacuumed 5 additional minutes. Moderate "plus" separation
control (rinse only)	19.3	64	0.4370	0.0528	4.55	rinse only 100 mL RO water at room temp, vacuum 5 mins

## Degumming Stain Boiling

Cocoons boiled for 1 minute in 0.5% solution of C.I. Direct Red 80 and rinsed twice in an ultrasonic bath (Knott et al., 1983). Cocoons are pale pink in the middle and darker red on the ends.



Sericin beads up (scale unknown, viewed at 400x magnification):



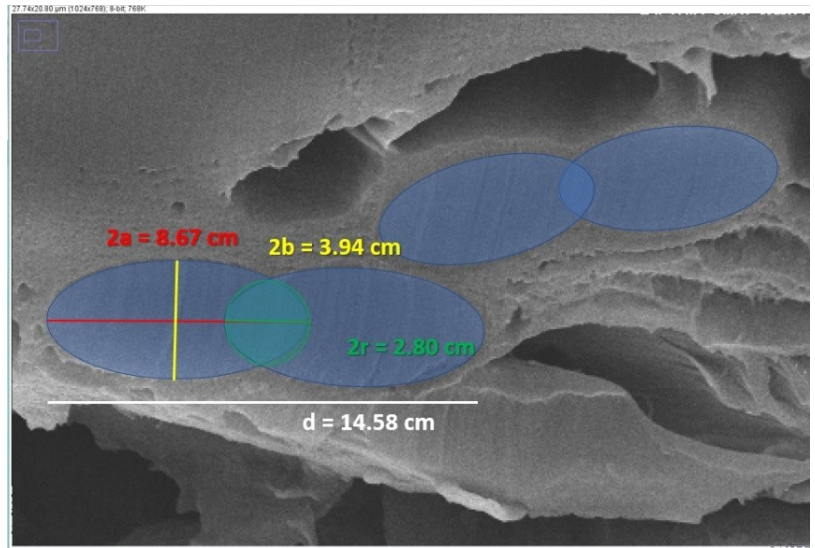
## Appendix C: Diameter & Cross-Sectional Area

### ImageJ Diameter Measurements

Measurement	Diameter ( $\mu\text{m}$ )					
	G1	G2	G3	G4	G5	G6
1	8.102	4.759	2.655	2.464	3.036	3.144
2	7.525	4.813	2.732	2.536	2.810	3.180
3	7.695	4.921	2.795	2.714	3.167	3.193
4	8.136	4.921	2.902	2.667	3.119	3.171
5	8.226	4.858	2.894	2.714	3.402	2.760
6	8.452	4.877	2.920	2.821	3.348	2.777
7	8.408	4.903	2.991	3.072	3.680	2.806
8	8.995	4.705	3.036	2.661	3.464	2.799
9	9.673	4.633	3.116	2.563	4.298	3.109
10	8.495	4.579	3.107	2.591	3.905	3.084
11	8.585	4.269	3.238	2.723	4.858	3.049
12	8.584	4.102	3.274	2.723	4.762	3.145
13	9.156	5.381	3.369	3.298	4.464	4.348
14	8.706	5.363	3.333	3.019	4.572	4.143
15	8.653	5.555	3.179	3.054	3.536	4.689
16	9.401	5.484	3.190	3.063	3.738	4.585
17	8.646	5.417	3.370	3.072	3.595	4.930
18	8.541	5.363	3.381	3.098	3.402	4.822
19	8.146	5.244	3.054	3.619	3.988	4.812
20	8.305	5.262	3.152	3.810	3.976	4.976
21	8.412	5.388	3.403	3.858	4.036	4.467
22	8.513	5.442	3.474	3.902	4.012	4.572
23	8.240	5.704	3.537	3.786	4.000	4.656
24	7.885	5.830	3.561	3.590	4.018	4.560
<b>Average:</b>	<b>8.478</b>	<b>5.074</b>	<b>3.153</b>	<b>3.059</b>	<b>3.799</b>	<b>3.824</b>
Std dev:	0.49	0.44	0.25	0.47	0.54	0.85
<b>Cross-sectional area (<math>\mu\text{m}^2</math>):</b>	<b>18.07</b>	<b>6.470</b>	<b>2.498</b>	<b>2.352</b>	<b>3.628</b>	<b>3.675</b>

## Cross-section Measurements and Geometric Model

x-sectional area ( $\mu\text{m}^2$ )	diameter ( $\mu\text{m}$ )
6.624	4.964
13.646	8.418
7.598	6.009
10.792	6.809
10.056	6.473
8.227	6.045
10.853	6.109
6.334	4.899
9.515	6.338
10.826	7.004
10.07	6.855
14.281	8.156
17.596	8.336
7.346	5.999

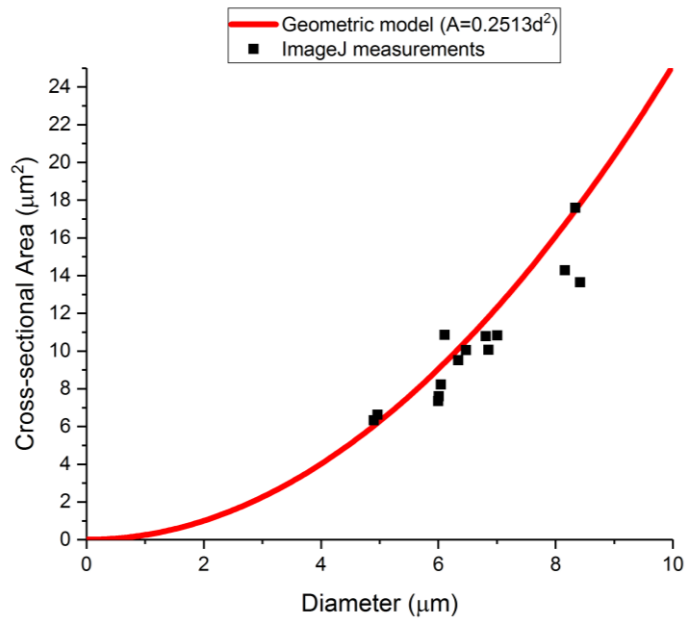


Assumptions and approximations:

- $d = 4a - 2r$
- $r = \frac{a}{3}$
- $b = \frac{a}{2}$
- $d = 3\frac{1}{3}a$
- $a = \frac{d}{3\frac{1}{3}}$

Model development:

1.  $A = 2\pi ab - \pi r^2$   
(area of two ellipses minus the area of their circular intersection)
2. Substitute b:  $b=a/2$
3.  $A = 2\pi a \frac{a}{2} - \pi r^2$
4.  $A = \pi a^2 - \pi r^2$
5. Substitute r:  $r=a/3$
6.  $A = \pi a^2 - \frac{\pi a^2}{9}$
7.  $A = \frac{8}{9}\pi a^2$
8. Substitute a:  $a = \frac{d}{3\frac{1}{3}}$
9.  $A = \frac{8}{9}\pi \times d^2 / 3\frac{1}{3}^2$
10.  $A = 0.251327d^2$



## ANOVA Degumming

ANOVAOneWay (09/09/2018 14:21:20)

### Notes

Description	Perform One-Way ANOVA
User Name	Mary
Operation Time	09/09/2018 14:21:20
Report Status	New Analysis Report
Data Filter	No

### Input Data

	Data	Range
Control	[Book1]Sheet2!A"Control"	[1:3]
Water only	[Book1]Sheet2!B"Water only"	[1:3]
Na\-(2)CO\-(3) only	[Book1]Sheet2!C"Na\-(2)CO\-(3) only"	[1:3]
SLS only	[Book1]Sheet2!D"SLS only"	[1:3]
Na\-(2)CO\-(3) + SLS	[Book1]Sheet2!E"Na\-(2)CO\-(3) + SLS"	[1:3]

### Descriptive Statistics

	N Analysis	N Missing	Mean	Standard Deviation	SE of Mean
Control	3	0	5.53436	0.8494	0.4904
Water only	3	0	-22.53763	4.41889	2.55125
Na\-(2)CO\-(3) only	3	0	-45.87247	3.11604	1.79904
SLS only	3	0	-29.7102	2.10241	1.21382
Na\-(2)CO\-(3) + SLS	3	0	-43.59225	4.41056	2.54644

### One Way ANOVA

#### Overall ANOVA

	DF	Sum of Squares	Mean Square	F Value	Prob>F
Model	4	5150.81422	1287.70355	119.60626	2.12172E-8
Error	10	107.66189	10.76619		
Total	14	5258.4761			

Null Hypothesis: The means of all levels are equal.

Alternative Hypothesis: The means of one or more levels are different.

At the 0.05 level, the population means are significantly different.

#### Fit Statistics

R-Square	Coeff Var	Root MSE	Data Mean
0.97953	-0.12047	3.28119	-27.23564

### Means Comparisons

#### Tukey Test

	MeanDiff	SEM	q Value	Prob	Alpha	Sig	LCL	UCL
Water only Control	-28.07199	2.67908	14.81845	7.97968E-6	0.05	1	-36.88906	-19.25493
Na\-(2)CO\-(3) only Control	-51.40684	2.67908	27.13629	0	0.05	1	-60.2239	-42.58977
Na\-(2)CO\-(3) only Water only	-23.33484	2.67908	12.31784	4.23913E-5	0.05	1	-32.15191	-14.51778
SLS only Control	-35.24456	2.67908	18.60466	1.44062E-6	0.05	1	-44.06163	-26.4275
SLS only Water only	-7.17257	2.67908	3.78621	0.12806	0.05	0	-15.98963	1.64449
SLS only Na\-(2)CO\-(3) only	16.16227	2.67908	8.53163	9.26688E-4	0.05	1	7.34521	24.97934
Na\-(2)CO\-(3) + SLS Control	-49.12661	2.67908	25.93262	0	0.05	1	-57.94368	-40.30955
Na\-(2)CO\-(3) + SLS Water only	-21.05462	2.67908	11.11417	1.04196E-4	0.05	1	-29.87168	-12.23756
Na\-(2)CO\-(3) + SLS Na\-(2)CO\-(3) only	2.28022	2.67908	1.20367	0.90814	0.05	0	-6.53684	11.09729
Na\-(2)CO\-(3) + SLS SLS only	-13.88205	2.67908	7.32796	0.00293	0.05	1	-22.69911	-5.06499

Sig equals 1 indicates that the difference of the means is significant at the 0.05 level.

Sig equals 0 indicates that the difference of the means is not significant at the 0.05 level.

#### Powers

Actual Power	Alpha	Sample Size	Power
	0.05	15	1

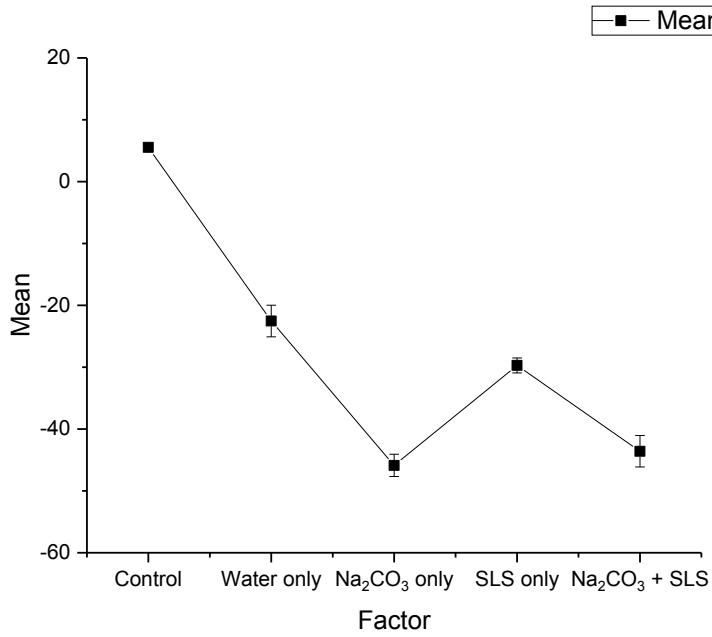
### Homogeneity of Variance Test

#### Levene's Test(Absolute Deviations)

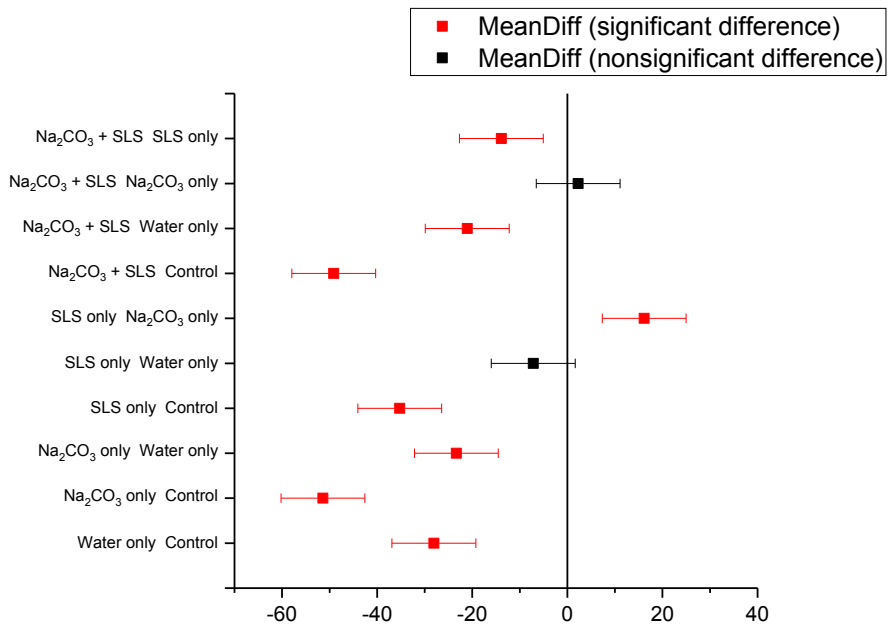
	DF	Sum of Squares	Mean Square	F Value	Prob>F
Model	4	14.17556	3.54389	1.62361	0.24315
Error	10	21.82726	2.18273		

At the 0.05 level, the population variances are not significantly different.

Means Plot (SE as Error)



Means Comparison Plot



## Appendix D: Tensile Data & Statistical Analysis

### *Tensile Data Compilation*

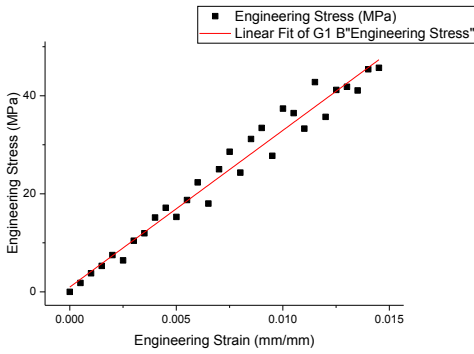
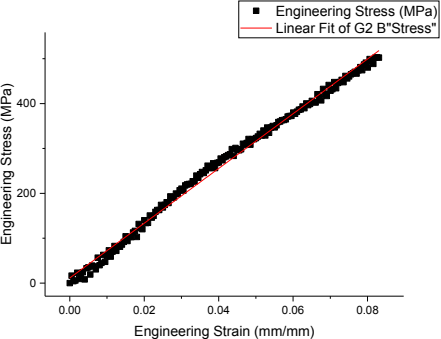
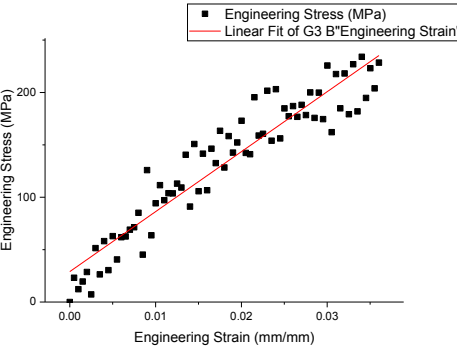
Property	<i>Galleria</i> silk*	<i>Galleria</i> silk <sup>†</sup>	G1	G2	G3	G4	G5	G6
Gauge length (mm)	1	30-50	9.525	9.525	9.525	9.525	9.525	9.525
Breaking strength (N)	0.012	0.0025	0.0056	0.0082	0.0021	0.0010	0.0023	0.0030
Breaking strength (mN)	11.78	2.52	5.5780	8.2197	2.0880	1.0303	2.2839	3.0213
Extension (mm)	0.7		5.42	4.65	4.18	3.15	4.44	5.70
Cross-sectional area (mm <sup>2</sup> )	1.57E-05	2.29E-02	1.807E-05	6.47E-06	2.5E-06	2.352E-06	3.628E-06	3.675E-06
Cross-sectional area (μm <sup>2</sup> )	15.7	22.9	18.1	6.5	2.5	2.4	3.6	3.7
Diameter (μm)		8.5	8.5	5.1	3.2	3.1	3.8	3.8
Density (g/cm <sup>3</sup> )	1.33598	1.33598	1.33598	1.33598	1.33598	1.33598	1.33598	1.33598
Linear density (tex, g/km)	0.021	0.031	0.024	0.009	0.003	0.003	0.005	0.005
Linear density (dtex, g/10km)	0.210	0.306	0.241	0.086	0.033	0.031	0.048	0.049
Specific stress (N/tex)	0.56	0.08	0.23	0.95	0.63	0.33	0.47	0.62
Specific stress (mN/tex)	561.4	82.3	<b>231.1</b>	<b>950.9</b>	<b>625.7</b>	<b>327.9</b>	<b>471.2</b>	<b>615.3</b>
Stress (MPa, N/mm <sup>2</sup> )	<b>750</b>	<b>110</b>	<b>308.76</b>	<b>1270.39</b>	<b>835.86</b>	<b>438.08</b>	<b>629.52</b>	<b>822.07</b>
Strain	0.7		0.569	0.489	0.439	0.330	0.466	0.598
Elongation (%)	<b>70.00</b>		<b>56.88</b>	<b>48.86</b>	<b>43.91</b>	<b>33.04</b>	<b>46.62</b>	<b>59.84</b>
Toughness (MJ/m <sup>3</sup> )			<b>83.35</b>	<b>328.27</b>	<b>203.59</b>	<b>93.49</b>	<b>170.80</b>	<b>291.99</b>
Rate of extension (mm/min)	0.64	2.22	0.57	0.57	0.57	0.57	0.57	0.57
Rate of extension (mm/sec)	0.0106	0.0370	0.0095	0.0095	0.0095	0.0095	0.0095	0.0095
Strain rate (%/sec)	1.06	0.07 - 0.12	0.10	0.10	0.10	0.10	0.10	0.10

\* (Hepburn et al., 1979); <sup>†</sup> (Fedič et al., 2003)

From literature:	reported value	est. from graph	est. from text	
Measured:	avg force to break	avg extension to break	x-sect used to convert to stress/strain	avg diameter

## Linear Regression Analyses for Young's Modulus of Elasticity

One example from each insect:

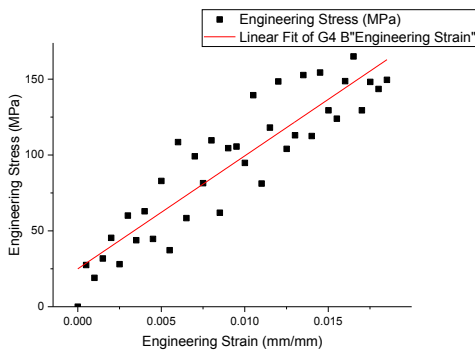
Specimen	Linear Fit Plot	Output of Analysis																		
<b>G1-1</b>		<table border="1" style="width: 100%; border-collapse: collapse;"> <tr> <td>Equation</td> <td><math>y = a + b \cdot x</math></td> </tr> <tr> <td>Plot</td> <td>Engineering Stress</td> </tr> <tr> <td>Weight</td> <td>No Weighting</td> </tr> <tr> <td>Intercept</td> <td><math>0.96713 \pm 0.88945</math></td> </tr> <tr> <td>Slope</td> <td><math>3196.33438 \pm 105.25003</math></td> </tr> <tr> <td>Residual Sum of Squares</td> <td>174.58292</td> </tr> <tr> <td>Pearson's r</td> <td>0.98516</td> </tr> <tr> <td>R-Square(COD)</td> <td>0.97053</td> </tr> <tr> <td>Adj. R-Square</td> <td>0.96948</td> </tr> </table>	Equation	$y = a + b \cdot x$	Plot	Engineering Stress	Weight	No Weighting	Intercept	$0.96713 \pm 0.88945$	Slope	$3196.33438 \pm 105.25003$	Residual Sum of Squares	174.58292	Pearson's r	0.98516	R-Square(COD)	0.97053	Adj. R-Square	0.96948
Equation	$y = a + b \cdot x$																			
Plot	Engineering Stress																			
Weight	No Weighting																			
Intercept	$0.96713 \pm 0.88945$																			
Slope	$3196.33438 \pm 105.25003$																			
Residual Sum of Squares	174.58292																			
Pearson's r	0.98516																			
R-Square(COD)	0.97053																			
Adj. R-Square	0.96948																			
<b>G2-3</b>		<table border="1" style="width: 100%; border-collapse: collapse;"> <tr> <td>Equation</td> <td><math>y = a + b \cdot x</math></td> </tr> <tr> <td>Plot</td> <td>Engineering Stress</td> </tr> <tr> <td>Weight</td> <td>No Weighting</td> </tr> <tr> <td>Intercept</td> <td><math>11.42393 \pm 1.76412</math></td> </tr> <tr> <td>Slope</td> <td><math>6100.58502 \pm 36.72628</math></td> </tr> <tr> <td>Residual Sum of Squares</td> <td>21631.66565</td> </tr> <tr> <td>Pearson's r</td> <td>0.99702</td> </tr> <tr> <td>R-Square(COD)</td> <td>0.99406</td> </tr> <tr> <td>Adj. R-Square</td> <td>0.99402</td> </tr> </table>	Equation	$y = a + b \cdot x$	Plot	Engineering Stress	Weight	No Weighting	Intercept	$11.42393 \pm 1.76412$	Slope	$6100.58502 \pm 36.72628$	Residual Sum of Squares	21631.66565	Pearson's r	0.99702	R-Square(COD)	0.99406	Adj. R-Square	0.99402
Equation	$y = a + b \cdot x$																			
Plot	Engineering Stress																			
Weight	No Weighting																			
Intercept	$11.42393 \pm 1.76412$																			
Slope	$6100.58502 \pm 36.72628$																			
Residual Sum of Squares	21631.66565																			
Pearson's r	0.99702																			
R-Square(COD)	0.99406																			
Adj. R-Square	0.99402																			
<b>G3-2</b>		<table border="1" style="width: 100%; border-collapse: collapse;"> <tr> <td>Equation</td> <td><math>y = a + b \cdot x</math></td> </tr> <tr> <td>Plot</td> <td>Engineering Stress</td> </tr> <tr> <td>Weight</td> <td>No Weighting</td> </tr> <tr> <td>Intercept</td> <td><math>29.0414 \pm 4.84404</math></td> </tr> <tr> <td>Slope</td> <td><math>5723.83283 \pm 232.05078</math></td> </tr> <tr> <td>Residual Sum of Squares</td> <td>31033.4332</td> </tr> <tr> <td>Pearson's r</td> <td>0.94631</td> </tr> <tr> <td>R-Square(COD)</td> <td>0.8955</td> </tr> <tr> <td>Adj. R-Square</td> <td>0.89403</td> </tr> </table>	Equation	$y = a + b \cdot x$	Plot	Engineering Stress	Weight	No Weighting	Intercept	$29.0414 \pm 4.84404$	Slope	$5723.83283 \pm 232.05078$	Residual Sum of Squares	31033.4332	Pearson's r	0.94631	R-Square(COD)	0.8955	Adj. R-Square	0.89403
Equation	$y = a + b \cdot x$																			
Plot	Engineering Stress																			
Weight	No Weighting																			
Intercept	$29.0414 \pm 4.84404$																			
Slope	$5723.83283 \pm 232.05078$																			
Residual Sum of Squares	31033.4332																			
Pearson's r	0.94631																			
R-Square(COD)	0.8955																			
Adj. R-Square	0.89403																			

(continued)

**Specimen Linear Fit Plot**

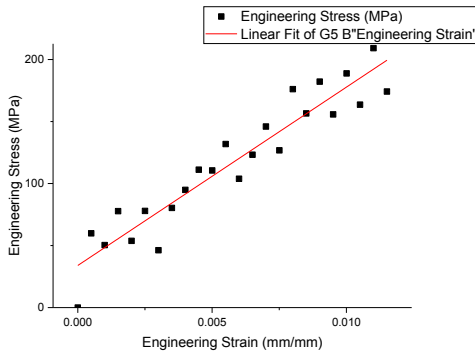
**Output of Analysis**

**G4-1**



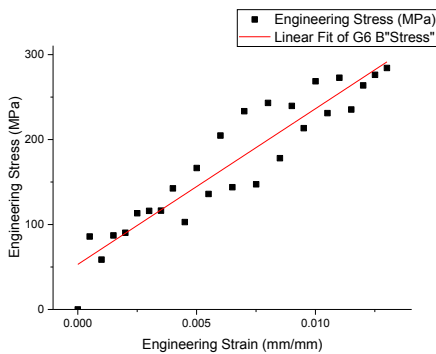
Equation	$y = a + b \cdot x$
Plot	Engineering Stress
Weight	No Weighting
Intercept	$24.97018 \pm 6.08643$
Slope	$7445.49208 \pm 565.53199$
Residual Sum of Squares	13176.04701
Pearson's r	0.90996
R-Square(COD)	0.82802
Adj. R-Square	0.82325

**G5-1**



Equation	$y = a + b \cdot x$
Plot	Engineering Stress
Weight	No Weighting
Intercept	$33.9537 \pm 7.11252$
Slope	$14377.09884 \pm 1058.85548$
Residual Sum of Squares	7103.84525
Pearson's r	0.94519
R-Square(COD)	0.89339
Adj. R-Square	0.88854

**G6-4**



Equation	$y = a + b \cdot x$
Plot	Engineering Stress
Weight	No Weighting
Intercept	$53.03583 \pm 10.35852$
Slope	$18326.03733 \pm 1365.83691$
Residual Sum of Squares	19131.59561
Pearson's r	0.93705
R-Square(COD)	0.87807
Adj. R-Square	0.87319

# ANOVA Young's Modulus of Elasticity

ANOVAOneWay (18/09/2018 17:17:17)

## Notes

Description	Perform One-Way ANOVA
User Name	Mary
Operation Time	18/09/2018 17:17:17
Report Status	New Analysis Report
Data Filter	No

## Descriptive Statistics

	N Analysis	N Missing	Mean	Standard Deviation	SE of Mean
G1	3	4	3.11517	0.69722	0.40254
G2	5	2	9.80328	2.99132	1.33776
G3	4	3	9.66568	3.24047	1.62023
G4	6	1	5.56095	1.91792	0.78299
G5	7	0	10.70188	2.94304	1.11237
G6	3	4	12.75503	4.83064	2.78897

## One Way ANOVA

### Overall ANOVA

	DF	Sum of Squares	Mean Square	F Value	Prob>F
Model	5	239.89127	47.97825	5.69637	0.00162
Error	22	185.29708	8.42259		
Total	27	425.18835			

Null Hypothesis: The means of all levels are equal.

Alternative Hypothesis: The means of one or more levels are different.

At the 0.05 level, the population means are significantly different.

### Fit Statistics

	R-Square	Coeff Var	Root MSE	Data Mean
	0.5642	0.33363	2.90217	8.69888

## Means Comparisons

### Tukey Test

		MeanDiff	SEM	q Value	Prob	Alpha	Sig	LCL	UCL	
G2	G1	6.68811	2.11945	4.46268	0.04591	0.05	1	0.08574	13.29047	
G3	G1	6.5505	2.21657	4.17934	0.06963	0.05	0	-0.35442	13.45542	
G3	G2	-0.1376	1.94684	0.09996		1	0.05	0	-6.20226	5.92706
G4	G1	2.44577	2.05214	1.68548	0.836	0.05	0	-3.94694	8.83849	
G4	G2	-4.24233	1.75735	3.41398	0.1944	0.05	0	-9.71672	1.23206	
G4	G3	-4.10473	1.87334	3.09872	0.28109	0.05	0	-9.94045	1.73099	
G5	G1	7.5867	2.00269	5.35741	0.01133	0.05	1	1.34805	13.82535	
G5	G2	0.8986	1.69934	0.74783	0.99436	0.05	0	-4.39507	6.19227	
G5	G3	1.0362	1.81903	0.8056	0.99205	0.05	0	-4.63033	6.70274	
G5	G4	5.14093	1.61462	4.50284	0.04322	0.05	1	0.11117	10.17069	
G6	G1	9.63985	2.36961	5.75318	0.00594	0.05	1	2.25819	17.02152	
G6	G2	2.95175	2.11945	1.96957	0.7308	0.05	0	-3.65062	9.55411	
G6	G3	3.08935	2.21657	1.97107	0.7302	0.05	0	-3.81556	9.99427	
G6	G4	7.19408	2.05214	4.95772	0.02144	0.05	1	0.80137	13.58679	
G6	G5	2.05315	2.00269	1.44985	0.90441	0.05	0	-4.1855	8.2918	

Sig equals 1 indicates that the difference of the means is significant at the 0.05 level.

Sig equals 0 indicates that the difference of the means is not significant at the 0.05 level.

## Homogeneity of Variance Test

### Levene's Test(Absolute Deviations)

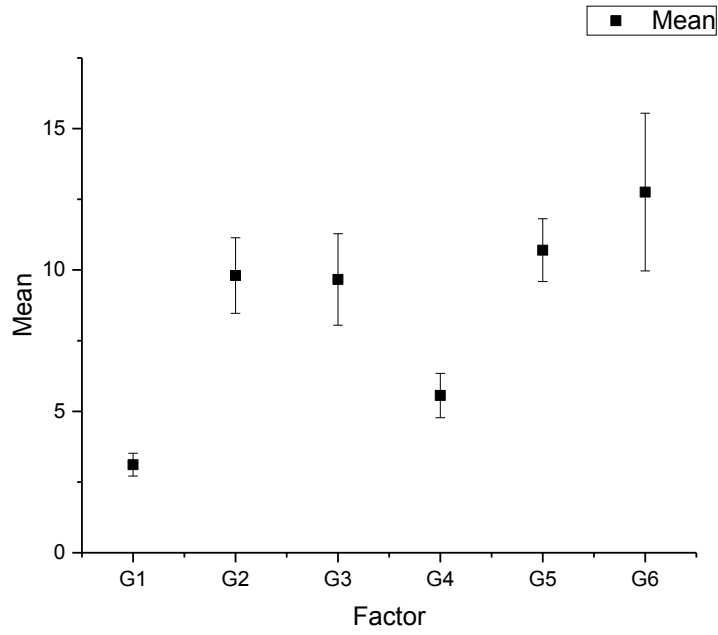
	DF	Sum of Squares	Mean Square	F Value	Prob>F
Model	5	19.55578	3.91116	1.90911	0.13362
Error	22	45.07107	2.04868		

At the 0.05 level, the population variances are not significantly different.

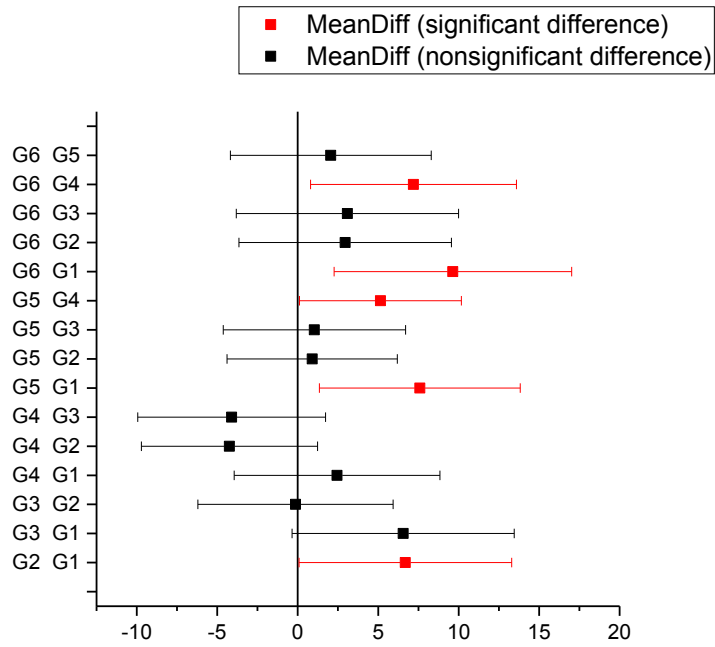
## Powers

	Alpha	Sample Size	Power
Actual Power	0.05	28	0.97052

Means Plot (SE as Error)



Means Comparison Plot



## Statistics Diameter

### Descriptive statistics:

Diameter	N total	Mean	Standard Deviation	Sum	Minimum	Median	Maximum
G1	24	8.47833	0.49111	203.48	7.525	8.4735	9.673
G2	24	5.07387	0.44441	121.773	4.102	5.0825	5.83
G3	24	3.15263	0.25302	75.663	2.655	3.1655	3.561
G4	24	3.05908	0.46732	73.418	2.464	3.0365	3.902
G5	24	3.79942	0.54324	91.186	2.81	3.8215	4.858
G6	24	3.82404	0.8488	91.777	2.76	3.668	4.976

### Levene's Homogeneity of Variance Test:

	DF	Sum of Squares	Mean Square	F Value	Prob>F
Model	5	4.87548	0.9751	15.1921	7.03E-12
Error	138	8.85745	0.06418		

At the 0.05 level, the population variances are significantly different.

### Welch's T-Tests:

	Diameter		
	P-value	95% CI	
	a=0.05	lower	upper
G1-G4	6.52E-37	5.1407	5.6978
G1-G3	7.10E-33	5.09871	5.5527
G1-G5	1.93E-32	4.37802	4.97981
G1-G2	2.25E-28	3.13232	3.6766
G1-G6	1.29E-23	4.25137	5.05722
G2-G3	4.69E-20	1.71113	2.13137
G2-G4	1.20E-19	1.74982	2.27977
G2-G5	2.06E-11	0.98608	1.56284
G2-G6	2.45E-07	0.85617	1.6435
G4-G5	7.50E-06	-1.03476	-0.4459
G3-G5	8.22E-06	-0.89302	-0.40056
G4-G6	4.46E-04	-1.16308	-0.36684
G3-G6	9.37E-04	-1.03534	-0.3075
G3-G4	0.39431	-0.12481	0.31189
G5-G6	0.90533	-0.43869	0.38944

significantly different

not significantly different

## Statistics UTS (mN)

### Descriptive statistics:

UTS mN	N total	Mean	Standard Deviation	Sum	Minimum	Median	Maximum
G1	3	5.57802	2.18096	16.73405	4.05396	4.6038	8.07629
G2	5	8.21973	2.11238	41.09867	5.78898	7.33058	11.18735
G3	4	2.08795	0.41662	8.35181	1.64753	2.07969	2.5449
G4	6	1.03033	0.07551	6.18196	0.91077	1.02872	1.1186
G5	7	2.28392	0.32899	15.98745	1.97048	2.22262	2.889
G6	3	3.02131	0.84398	9.06393	2.29967	2.81492	3.94934

### Levene's Homogeneity of Variance Test:

	DF	Sum of Squares	Mean Square	F Value	Prob>F
Model	5	12.00521	2.40104	9.8434	4.78E-05
Error	22	5.36633	0.24392		

At the 0.05 level, the population variances are significantly different.

### Welch's T-Tests:

	UTS mN		
	P-value	95% CI	
	a=0.05	lower	upper
G4-G5	3.19E-05	-1.55758	-0.94961
G2-G4	0.00159	5.25884	9.11998
G2-G3	0.00231	3.56218	8.70138
G2-G5	0.00302	4.16137	7.71025
G2-G6	0.00329	1.9957	8.40114
G3-G4	0.0137	0.66761	1.44764
G4-G6	0.05447	-2.75279	-1.22917
G1-G4	0.06876	2.59555	6.49983
G1-G3	0.10549	0.70881	6.27132
G1-G5	0.11893	1.50057	5.08762
G1-G2	0.16493	-6.45777	1.17434
G1-G6	0.16915	-1.19198	6.30539
G3-G6	0.18515	-2.15797	0.29126
G5-G6	0.26616	-1.54762	0.07285
G3-G5	0.45463	-0.70722	0.31528

significantly different

borderline but not significant

not significantly different

## Statistics UTS (MPa)

### Descriptive statistics:

UTS MPa	N total	Mean	Standard Deviation	Sum	Minimum	Median	Maximum
G1	3	308.7585	120.7224	926.2756	224.3978	254.833	447.0448
G2	5	1270.394	326.4772	6351.969	894.7108	1132.971	1729.051
G3	4	835.865	166.7844	3343.46	659.5517	832.5573	1018.794
G4	6	438.079	32.10629	2628.474	387.2454	437.3938	475.6115
G5	7	621.4355	89.51574	4350.049	536.1508	604.7559	786.0722
G6	3	822.0727	229.6395	2466.218	625.7206	765.9157	1074.582

### Levene's Homogeneity of Variance Test:

	DF	Sum of Squares	Mean Square	F Value	Prob>F
Model	5	181921	36384.2	5.97434	1.23E-03
Error	22	133981.8	6090.083		

At the 0.05 level, the population variances are significantly different.

### Welch's T-Tests:

	UTS MPa		
	P-value	95% CI	
	a=0.05	lower	upper
G4-G5	0.00109	-268.54	-98.1729
G1-G2	0.00142	-1454	-469.273
G2-G4	0.00452	532.3783	1132.251
G1-G3	0.00468	-821.733	-232.48
G2-G5	0.00984	364.7846	933.132
G3-G4	0.01622	241.1328	554.439
G1-G5	0.0274	-469.023	-156.331
G2-G3	0.04055	6.45425	862.6035
G1-G6	0.04106	-929.189	-97.4395
G2-G6	0.06615	-83.6934	980.3358
G3-G5	0.07553	43.02171	385.8372
G4-G6	0.09999	-594.188	-173.8
G1-G4	0.20131	-246.367	-12.2744
G5-G6	0.26616	-421.095	19.82097
G3-G6	0.9346	-367.838	395.4231

significantly different
borderline but significant
borderline but not significant
not significantly different

Statistics Specific Stress (mN/tex)

Descriptive statistics:

Specific stress	N total	Mean	Standard Deviation	Sum	Minimum	Median	Maximum
G1	3	231.1102	90.36243	693.3305	167.965	190.7461	334.6194
G2	5	950.9078	244.3728	4754.539	669.7037	848.0452	1294.219
G3	4	625.6568	124.8405	2502.627	493.6838	623.1809	762.5815
G4	6	327.9084	24.03202	1967.45	289.8587	327.3955	356.002
G5	7	465.1533	67.0038	3256.073	401.3165	452.6684	588.3862
G6	3	615.3331	171.8884	1845.999	468.3607	573.2988	804.3397

Levene's Homogeneity of Variance Test:

	DF	Sum of Squares	Mean Square	F Value	Prob>F
Model	5	101925.5	20385.1	5.97434	1.23E-03
Error	22	75066.46	3412.112		

At the 0.05 level, the population variances are significantly different.

Welch's T-Tests:

	UTS (spec stress) mN/tex		
	P-value	95% CI	
	a=0.05	lower	upper
G4-G5	0.00109	-201.006	-73.4838
G1-G2	0.00142	-1088.34	-351.257
G2-G4	0.00452	398.4927	847.5062
G1-G3	0.00468	-615.079	-174.015
G2-G5	0.00984	273.0465	698.4626
G3-G4	0.01622	180.4914	415.0055
G1-G5	0.0274	-351.071	-117.016
G2-G3	0.04055	4.8311	645.671
G1-G6	0.04106	-695.511	-72.9349
G2-G6	0.06615	-62.6457	733.7952
G3-G5	0.07553	32.20236	288.8046
G4-G6	0.09999	-444.758	-130.092
G1-G4	0.20131	-184.409	-9.18755
G5-G6	0.26616	-315.196	14.83627
G3-G6	0.9346	-275.332	295.9798

- significantly different
- borderline but significant
- borderline but not significant
- not significantly different

## ANOVA Strain at Break

ANOVAOneWay (23/09/2018 08:56:24)

### Notes

Description	Perform One-Way ANOVA
User Name	Mary
Operation Time	23/09/2018 08:56:24
Report Status	New Analysis Report
Data Filter	No

### Descriptive Statistics

	N Analysis	N Missing	Mean	Standard Deviation	SE of Mean
G1	3	4	0.56883	0.06283	0.03628
G2	5	2	0.48863	0.13479	0.06028
G3	4	3	0.43913	0.08988	0.04494
G4	6	1	0.33037	0.07036	0.02873
G5	7	0	0.46619	0.07291	0.02756
G6	3	4	0.59836	0.11051	0.0638

### One Way ANOVA

#### Overall ANOVA

	DF	Sum of Squares	Mean Square	F Value	Prob>F
Model	5	0.19973	0.03995	4.72781	0.0044
Error	22	0.18588	0.00845		
Total	27	0.38561			

Null Hypothesis: The means of all levels are equal.

Alternative Hypothesis: The means of one or more levels are different.

At the 0.05 level, the population means are significantly different.

#### Fit Statistics

R-Square	Coeff Var	Root MSE	Data Mean
0.51796	0.19879	0.09192	0.46239

### Means Comparisons

#### Tukey Test

	MeanDiff	SEM	q Value	Prob	Alpha	Sig	LCL	UCL
G2 G1	-0.0802	0.06713	1.68968	0.83461	0.05	0	-0.28932	0.12891
G3 G1	-0.1297	0.0702	2.61265	0.45811	0.05	0	-0.34839	0.089
G3 G2	-0.04949	0.06166	1.13514	0.964	0.05	0	-0.24158	0.14259
G4 G1	-0.23846	0.065	5.18845	0.01487	0.05	1	-0.44093	-0.03599
G4 G2	-0.15826	0.05566	4.02098	0.08722	0.05	0	-0.33164	0.01513
G4 G3	-0.10876	0.05933	2.59234	0.46644	0.05	0	-0.29359	0.07607
G5 G1	-0.10264	0.06343	2.28836	0.59594	0.05	0	-0.30023	0.09496
G5 G2	-0.02243	0.05382	0.58947	0.99816	0.05	0	-0.1901	0.14523
G5 G3	0.02706	0.05761	0.66422	0.99676	0.05	0	-0.15241	0.20653
G5 G4	0.13582	0.05114	3.75604	0.12538	0.05	0	-0.02348	0.29513
G6 G1	0.02953	0.07505	0.55636	0.9986	0.05	0	-0.20427	0.26332
G6 G2	0.10973	0.06713	2.31171	0.58583	0.05	0	-0.09938	0.31884
G6 G3	0.15922	0.0702	3.20742	0.24857	0.05	0	-0.05947	0.37792
G6 G4	0.26798	0.065	5.83088	0.00523	0.05	1	0.06551	0.47046
G6 G5	0.13216	0.06343	2.94666	0.33117	0.05	0	-0.06543	0.32976

Sig equals 1 indicates that the difference of the means is significant at the 0.05 level.

Sig equals 0 indicates that the difference of the means is not significant at the 0.05 level.

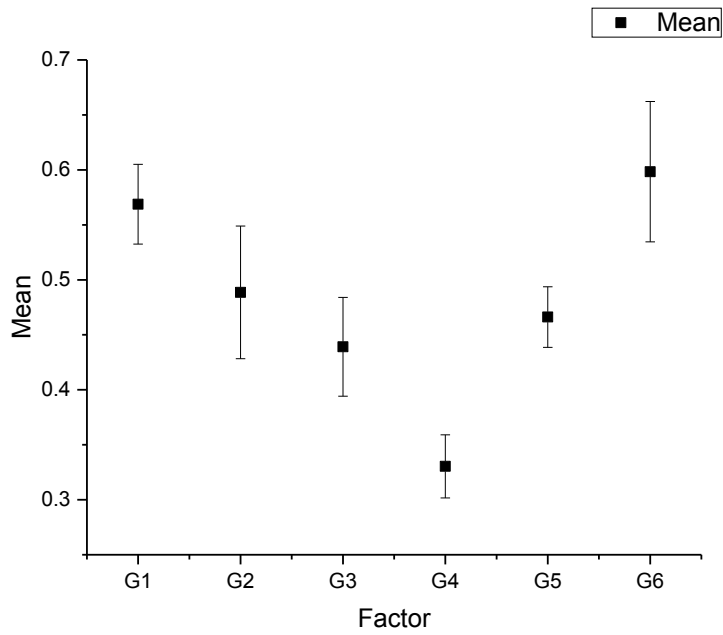
### Homogeneity of Variance Test

#### Levene's Test(Absolute Deviations)

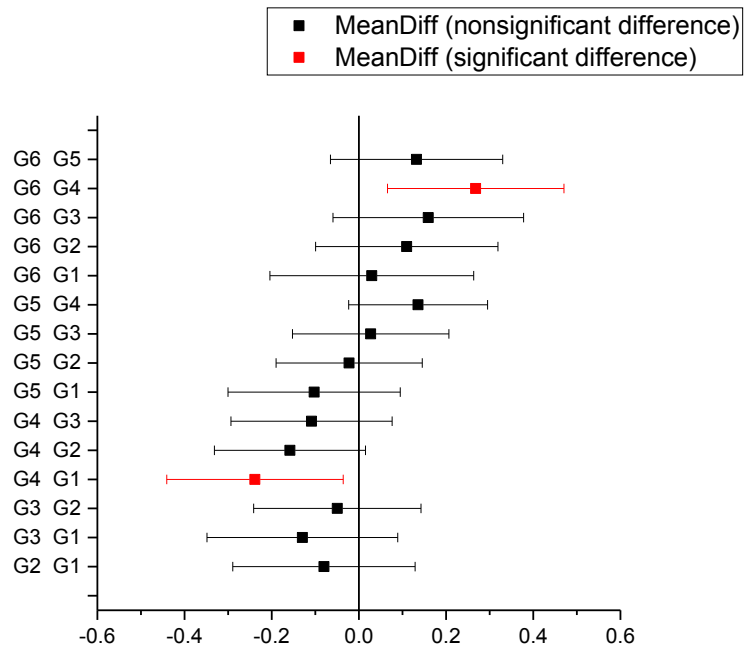
	DF	Sum of Squares	Mean Square	F Value	Prob>F
Model	5	0.0111	0.00222	1.13125	0.37332
Error	22	0.04317	0.00196		

At the 0.05 level, the population variances are not significantly different.

Means Plot (SE as Error)



Means Comparison Plot



## Statistics Toughness (MJ/m<sup>3</sup>)

### Descriptive statistics:

Toughness	N total	Mean	Standard Deviation	Sum	Minimum	Median	Maximum
G1	3	83.3548	23.92998	250.0644	63.05568	77.2685	109.7402
G2	5	328.2741	126.9435	1641.371	228.8177	249.4037	483.5916
G3	4	203.586	67.70965	814.3438	146.0404	192.2584	283.7866
G4	6	93.48524	24.32174	560.9115	68.80541	88.44625	126.3325
G5	7	170.8032	43.33429	1195.622	106.6956	185.4599	215.2222
G6	3	291.9856	79.57137	875.9568	206.7334	304.936	364.2875

### Levene's Homogeneity of Variance Test:

	DF	Sum of Squares	Mean Square	F Value	Prob>F
Model	5	28998.68	5799.737	11.15972	1.90E-05
Error	22	11433.46	519.7026		

At the 0.05 level, the population variances are significantly different.

### Welch's T-Tests:

	Toughness (MJ/m <sup>3</sup> )		
	P-value	95% CI	
	a=0.05	lower	upper
G4-G5	0.00255	-121.352	-33.2835
G1-G5	0.00471	-150.129	-24.7676
G1-G2	0.01096	-431.775	-58.0633
G2-G4	0.01345	116.2339	353.3439
G1-G3	0.03119	-227.404	-13.0584
G1-G6	0.03613	-341.825	-75.4362
G3-G4	0.0422	42.06804	178.1334
G4-G6	0.04409	-277.487	-119.514
G2-G5	0.04778	43.93829	271.0036
G5-G6	0.10473	-208.215	-34.1502
G2-G3	0.10594	-42.9826	292.3589
G3-G6	0.19666	-231.107	54.30775
G3-G5	0.42793	-41.9775	107.543
G1-G4	0.58247	-50.6113	30.35046
G2-G6	0.63724	-166.307	238.8845

significantly different

borderline but significant

not significantly different



**Mary J. Glasper and John A. Nychka**  
*Goodnight Galleria*, 2017  
Digital photography and collage